PB86-239787

Critical Review of Open Source Particulate Emission Measurements Field Comparison

Southern Research Inst., Birmingham, AL

Prepared for

Environmental Protection Agency
Research Triangle Park, NC

Aug 86

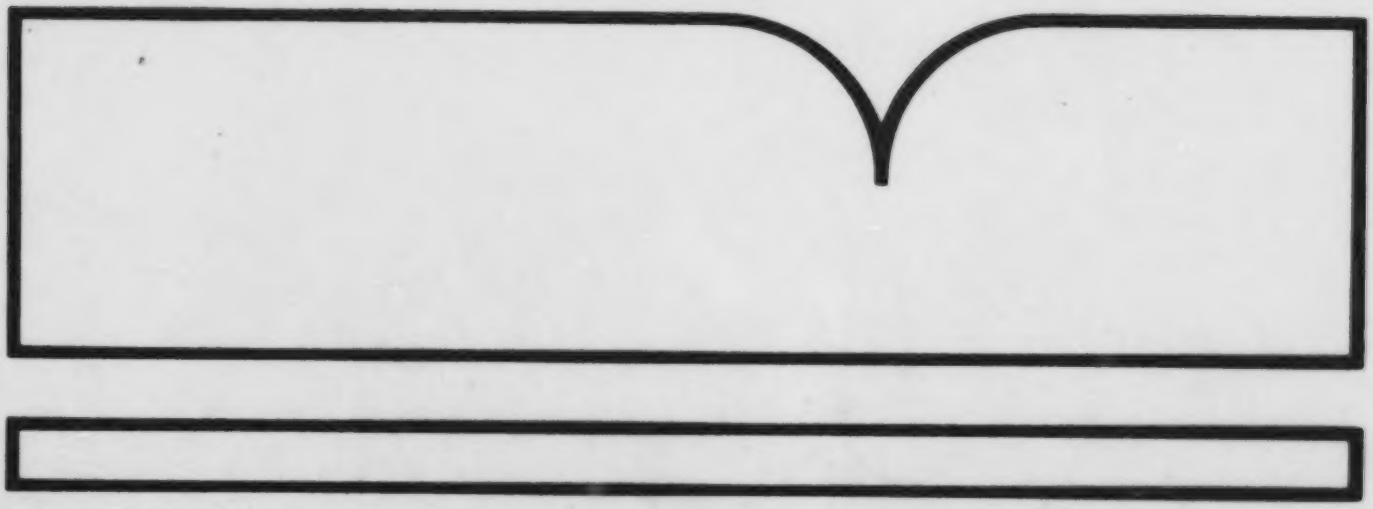

U.S. Department of Commerce
National Technical Information Service
NTIS

PB86-239787

EPA/600/2-86/072
August 1986

CRITICAL REVIEW OF OPEN SOURCE PARTICULATE EMISSION MEASUREMENTS: FIELD COMPARISON

by

Bobby E. Pyle and Joseph D. McCain

Southern Research Institute
2000 Ninth Avenue South
Birmingham, Alabama 35255-5305

EPA Contract 68-02-3696, Task 2

EPA Project Officer: Robert C. McCrillis

Air and Energy Engineering Research Laboratory
Research Triangle Park, North Carolina 27711

AIR AND ENERGY ENGINEERING RESEARCH LABORATORY
OFFICE OF RESEARCH AND DEVELOPMENT
U.S. ENVIRONMENTAL PROTECTION AGENCY
RESEARCH TRIANGLE PARK, NC 27711

REPRODUCED BY
NATIONAL TECHNICAL
INFORMATION SERVICE
U.S. DEPARTMENT OF COMMERCE
SPRINGFIELD, VA. 22161

TECHNICAL REPORT DATA (Please read Instructions on the reverse before completing)		
1. REPORT NO. EPA/600/2-86/072	2.	3. RECIPIENT'S ACCESSION NO. PB86 239787/AS
4. TITLE AND SUBTITLE Critical Review of Open Source Particulate Emission Measurements: Field Comparison		5. REPORT DATE August 1986 6. PERFORMING ORGANIZATION CODE
7. AUTHOR(S) Bobby E. Pyle and Joseph D. McCain		8. PERFORMING ORGANIZATION REPORT NO. SoRI-EAS-85-444R
9. PERFORMING ORGANIZATION NAME AND ADDRESS Southern Research Institute P.O. Box 55305 Birmingham, Alabama 35255-5305		10. PROGRAM ELEMENT NO. 11. CONTRACT/GRANT NO. 68-02-3696, Task 2
12. SPONSORING AGENCY NAME AND ADDRESS EPA, Office of Research and Development Air and Energy Engineering Research Laboratory Research Triangle Park, NC 27711		13. TYPE OF REPORT AND PERIOD COVERED Task Final; 6/83 - 6/85 14. SPONSORING AGENCY CODE EPA/600/13
15. SUPPLEMENTARY NOTES AEERL project officer is Robert C. McCrillis, Mail Drop 65, 919/541-2733.		

16. ABSTRACT The report gives results of a review of sampling and analytical procedures used by various testing firms to quantify particulate emissions from open sources; e.g., roads and storage piles. Seven firms, who account for nearly 100 percent of all open source data in the literature, described their current sampling and analytical procedures. Five of these firms then participated in a simultaneous side-by-side field test on a simulated unpaved road at a major steel plant. Each firm independently measured the particulate emission concentrations produced by roadway traffic. These measurements produced not only the particle-size-dependence of the emissions but also the concentrations as functions of the distance above the road surface. The results for each firm were expressed as emission factors for total particulate and the mass fractions of the particulate with sizes <30, <15, <10, and <2.5 micrometers diameter. Based on an analysis of the results, it was found that all five profiling systems could produce equivalent results in terms of total emissions. This was not the case for emissions by particle size. The only technique of those tested that produced reliable emission factors by particle size was inertial sizing.

17. KEY WORDS AND DOCUMENT ANALYSIS			
a. DESCRIPTORS		b. IDENTIFIERS/OPEN ENDED TERMS	c. COSATI Field/Group
Pollution	Analyzing	Pollution Control	13B
Measurement	Roads	Stationary Sources	14G
Particles		Unpaved Roads	
Dust		Storage Piles	11G
Field Tests		Inertial Sizing	14B
Sampling			
18. DISTRIBUTION STATEMENT Release to Public		19. SECURITY CLASS (This Report) Unclassified	21. NO. OF PAGES 134
		20. SECURITY CLASS (This page) Unclassified	22. PRICE

EPA Form 2220-1 (9-73)

NOTICE

This document has been reviewed in accordance with U.S. Environmental Protection Agency policy and approved for publication. Mention of trade names or commercial products does not constitute endorsement or recommendation for use.

ABSTRACT

Current EPA emission trading (bubble) policies allow excessive emissions from one source to be offset by improved controls on other sources within the same industrial complex. In implementing this bubble policy, many industries have opted to reduce particulate emissions from roads, parking lots, and storage locations in lieu of more stringent controls on other plant operations. The predictions of these open sources emissions based upon the existing data for measured emission factors have been found to be subject to high variability. Part of this uncertainty can be attributed to the variations in source characteristics. However, a significant part of the uncertainties are due to variations in the measuring and analytical techniques used to assess sources upon which the emission factor data base was built. In an effort to quantify these technique dependent parameters, a comparative study of the current measuring and data reduction methods was carried out. This study included a simultaneous, side-by-side field test with five independent testing organizations sampling the dust emissions from a simulated unpaved road at a major steel producing facility. Each of the participants independently measured the particulate emission concentrations produced by roadway traffic. These measurements resulted in not only particle-size dependence of the emissions but also concentrations as functions of the distance above the road surface. The results for each testing organization were expressed as emission factors for total particulate and the mass fractions of the particulate with sizes <30, <15, <10, and <2.5 μm diameter. Based on an analysis of the results, it was found that all five profiling systems were capable of producing equivalent results in terms of total emissions. This was not the case for emissions by particle size. The only technique among those tested that was believed to produce reliable emission factors by particle size was the inertial sizing method.

This work was submitted in partial fulfillment of EPA Contract Number 68-02-3693, work assignment 002 by Southern Research Institute under sponsorship of the U.S. Environmental Protection Agency. This report covers a period from 1 January 1984 to 15 March 1985 and work was completed as of 10 May 1985.

CONTENTS

Section	Page
Figures	vi
Tables	xi
Acknowledgment	xii
1. Introduction	1
2. Conclusions and Recommendations	5
3. Fugitive Measurement Methodologies	8
4. Description of Test	28
5. Particle Size Measurements	34
Methods	34
Cyclone/Impactors	34
Stacked Filters	36
Scanning Electron Microscopy	39
Results	41
Stacked Filter	43
Scanning Electron Microscopy	47
Cyclone/Impactors	52
Particle Sizing Recommendation	55
6. Exposures and Emission Factors	57
Methodologies	57
Sampling Isokineticity	57
Exposure Integration	58
Field Test Results	60
Total Particulate Emission Factors	60
Exposure and Emission Recommendations	84
7. Modeling Fugitive Emissions	85
Predictive Emission Factor Equations	85
Modeling Recommendations	94
References	118
Appendix	120

FIGURES

Number	Title	Page
1	Upwind profiling system used by EEM	10
2	Downwind profiling system used by EEM	11
3	Typical sampling head used by EEM	12
4	Upwind profiling system used by MRI	13
5	Downwind profiling system used by MRI	14
6	Typical hi-vol sampler used by MRI (without particle sizing)	16
7	Upwind profiling system used by PEI	17
8	Downwind profiling system used by PEI	18
9	Typical stacked filter sampling head used by PEI	19
10	Upwind sampling system used by TRC	20
11	Downwind profiling system used by TRC	21
12	Typical sampling head used by TRC	22
13	Upwind sampling system used by USS	23
14	Downwind profiling system used by USS	24
15	Typical sampling head used by USS	25
16	Gary test site after covering road with dirt. View is looking west	29
17	Physical layout of the Gary comparative fugitive emission test site	30
18	Total suspended particulate matter by test and sampling position as measured by standard high-volume sampler	33
19	MRI cyclone/cascade impactor combination	35
20	Lundgren cascade impactor	37
21	Collocated Lundgren cascade impactor (left) and MRI Sierra cyclone and impactor (center)	38
22	PEI stacked filter profiler head	40

Figures (Cont.)

Number	Title	Page
23	Particle size distributions as measured by the various techniques	42
24a	Plot of the ratio of PEI's TSP concentration to hi-vol concentration versus the total particulate mass collected by the hi-vol	46
24b	PEI screen penetration dependence on total mass collected by the profiler sampler	46
25	Particle size distribution as measured by a Lundgren cascade impactor and as determined by the CCSEM technique from a collocated profiler sample	48
26	Total particulate emission factors by test as measured by each organization	64
27	Measured total exposures versus height for Test 1 for all contractors providing total particulate exposure data	72
28	Measured total exposures versus height for Test 2 for all contractors providing total particulate exposure data	73
29	Measured total exposures versus height for Test 3 for all contractors providing total particulate exposure data	74
30	Measured total exposures versus height for Test 4 for all contractors providing total particulate exposure data	75
31	Measured total exposures versus height for Test 5 for all contractors providing total particulate exposure data	76
32	Measured total exposures versus height for Test 6 for all contractors providing total particulate exposure data	77
33	Measured total exposures versus height for Test 7 for all contractors providing total particulate exposure data	78
34	Measured total exposures versus height for Test 8 for all contractors providing total particulate exposure data	79
35	Measured total exposures versus height for Test 9 for all contractors providing total particulate exposure data	80
36	Measured total exposures versus height for Test 10 for all contractors providing total particulate exposure data	81
37	Measured total exposures versus height for Test 11 for all contractors providing total particulate exposure data	82

Figures (Cont.)

Number	Title	Page
38	Scatter diagrams of: the test averaged TP emission factor measurements and that predicted by EEM's equation (filled circles) along with the associated regression line (dotted line); and the values of TP emission factor both measured and predicted by EEM (open circles) along with the associated regression line (broken line)	91
39	Scatter diagrams of: the test averaged TP emission factor measurements and that predicted by MRI's equation (filled circles) along with the associated regression line (dotted line); and the values of TP emission factor both measured and predicted by MRI (open circles) along with the associated regression line (broken line)	96
40	Scatter diagrams of: the test averaged TP emission factor measurements and that predicted by TRC's equation (filled circles) along with the associated regression line (dotted line); and the values of TP emission factor both measured and predicted by TRC (open circles) along with the associated regression line (broken line)	97
41	Scatter diagrams of: the test averaged TP emission factor measurements and that predicted by USS's equation (filled circles) along with the associated regression line (dotted line); and the values of TP emission factor both measured and predicted by USS (open circles) along with the associated regression line (broken line)	98
42	Scatter diagrams of: the test averaged TSP emission factor measurements and that predicted by EEM's equation (filled circles) along with the associated regression line (dotted line); and the values of TSP emission factor both measured and predicted by EEM (open circles) along with the associated regression line (broken line)	99
43	Scatter diagrams of: the test averaged TSP emission factor measurements and that predicted by MRI's equation (filled circles) along with the associated regression line (dotted line); and the values of TSP emission factor both measured and predicted by MRI (open circles) along with the associated regression line (broken line)	100
44	Scatter diagrams of: the test averaged TSP emission factor measurements and that predicted by PEI's equation (filled circles) along with the associated regression line (dotted line); and the values of TSP emission factor both measured and predicted by PEI (open circles) along with the associated regression line (broken line)	101

Figures (Cont.)

Number	Title	Page
45	Scatter diagrams of: the test averaged TSP emission factor measurements and that predicted by TRC's equation (filled circles) along with the associated regression line(dotted line); and the values of TSP emission factor both measured and predicted by TRC(open circles) along with the associated regression line (broken line)	102
46	Scatter diagrams of: the test averaged TSP emission factor measurements and that predicted by USS's equation (filled circles) along with the associated regression line (dotted line); and the values of TSP emission factor both measured and predicted by USS (open circles) along with the associated regression line (broken line)	103
47	Scatter diagrams of: the test averaged PM_{15} emission factor measurements and that predicted by EEM's equation (filled circles) along with the associated regression line (dotted line); and the values of PM_{15} emission factor both measured and predicted by EEM (open circles) along with the associated regression line (broken line)	104
48	Scatter diagrams of: the test averaged PM_{15} emission factor measurements and that predicted by MRI's equation (filled circles) along with the associated regression line (dotted line); and the values of PM_{15} emission factor both measured and predicted by MRI (open circles) along with the associated regression line (broken line)	105
49	Scatter diagrams of: the test averaged PM_{15} emission factor measurements and that predicted by TRC's equation (filled circles) along with the associated regression line (dotted line); and the values of PM_{15} emission factor both measured and predicted by TRC (open circles) along with the associated regression line (broken line)	106
50	Scatter diagrams of: the test averaged PM_{15} emission factor measurements and that predicted by USS's equation (filled circles) along with the associated regression line (dotted line); and the values of PM_{15} emission factor both measured and predicted by USS (open circles) along with the associated regression line (broken line)	107
51	Scatter diagrams of: the test averaged PM_{10} emission factor measurements and that predicted by EEM's equation (filled circles) along with the associated regression line (dotted line); and the values of PM_{10} emission factor both measured and predicted by EEM (open circles) along with the associated regression line (broken line)	108

Figures (Cont.)

Number	Title	Page
52	Scatter diagrams of: the test averaged PM_{10} emission factor measurements and that predicted by MRI's equation (filled circles) along with the associated regression line (dotted line); and the values of PM_{10} emission factor both measured and predicted by MRI (open circles) along with the associated regression line (broken line)	109
53	Scatter diagrams of: the test averaged PM_{10} emission factor measurements and that predicted by PEI's equation (filled circles) along with the associated regression line (dotted line); and the values of PM_{10} emission factor both measured and predicted by PEI (open circles) along with the associated regression line (broken line)	110
54	Scatter diagrams of: the test averaged PM_{10} emission factor measurements and that predicted by TRC's equation (filled circles) along with the associated regression line (dotted line); and the values of PM_{10} emission factor both measured and predicted by TRC (open circles) along with the associated regression line (broken line)	111
55	Scatter diagrams of: the test averaged PM_{10} emission factor measurements and that predicted by USS's equation (filled circles) along with the associated regression line (dotted line); and the values of PM_{10} emission factor both measured and predicted by USS (open circles) along with the associated regression line (broken line)	112
56	Scatter diagrams of: the test averaged FP emission factor measurements and that predicted by EEM's equation (filled circles) along with the associated regression line (dotted line); and the values of FP emission factor both measured and predicted by EEM (open circles) along with the associated regression line (broken line)	113
57	Scatter diagrams of: the test averaged FP emission factor measurements and that predicted by MRI's equation (filled circles) along with the associated regression line (dotted line); and the values of FP emission factor both measured and predicted by MRI (open circles) along with the associated regression line (broken line)	114
58	Scatter diagrams of: the test averaged FP emission factor measurements and that predicted by PEI's equation (filled circles) along with the associated regression line (dotted line); and the values of FP emission factor both measured and predicted by PEI (open circles) along with the associated regression line (broken line)	115

Figures (Cont.)

Number	Title	Page
59	Scatter diagrams of: the test averaged FP emission factor measurements and that predicted by TRC's equation (filled circles) along with the associated regression line (dotted line); and the values of FP emission factor both measured and predicted by TRC (open circles) along with the associated regression line (broken line)	116
60	Scatter diagrams of: the test averaged FP emission factor measurements and that predicted by USS's equation (filled circles) along with the associated regression line (dotted line); and the values of FP emission factor both measured and predicted by USS (open circles) along with the associated regression line (broken line)	117

TABLES

Number	Title	Page
1	Profiling system characteristics	9
2	Average emission factors by size class	44
3	Comparative fugitive emission test results	61
4	Average emission factors obtained by each organization	62
5	Correlation coefficients of TP, TSP, PM_{10}, and FP emission factors reported by test participants	65
6	Exposure and emission values by test number and organization	66
7	Size dependent constants for the predictive emission factor	87
8	Size fractions of particulate as reported by MRI and recalculated by Southern Research Institute	88
9	Average emission factors as calculated by Southern Research Institute	90
10	Correlation and regression line coefficients for the emission factor comparisons	92

ACKNOWLEDGEMENT

Several individuals and organizations contributed to the success of this study. The efforts of those associated with the United States Steel Corporation bear individual mention: Victor Nordlund, Supervisor of Environmental Engineering at the Gary Works, and his staff; William Kubiak in particular for assisting in selection and preparation of the test site; and T.F. Eckle with the USS Technical Center who participated in the comparative test at their own expense.

SECTION 1

INTRODUCTION

During the past decade, research has shown that particulate emissions from open sources such as roads and material storage piles contribute significantly to ambient particulate matter concentrations in many areas.[1] The current EPA emission trading policy allows excessive emissions from one source to be offset by improved control of another source within the same plant. In implementing this bubble policy, many steel plants have agreed to reduce fugitive dust emissions in lieu of tighter controls on process emissions.[2] However, the efforts of several groups to develop equipment and methods for quantifying emissions from nontraditional sources such as roadways have resulted in estimates of emission factors and emission rates with substantial variability. Whereas it is generally agreed that emission factor estimates of process emissions from ducted sources are good to ±50% of a specified measured value, predictions of open source fugitive dust emission factors may vary from measured values by as much as an order of magnitude. These large uncertainties are due to both differences in the measuring techniques used and the site examined. Even for sites with closely similar physical characteristics the measured emissions have been found to differ by as much as an order of magnitude. In an effort to resolve these differences, the U.S. Environmental Protection Agency contracted with Southern Research Institute (SoRI) to conduct a critical review of the various measurement and predictive methods and to conduct a side-by-side field test in which testing organizations whose methods represent the principal techniques which have commonly been applied, would simultaneously sample the emissions from an unpaved road.

The first phase of this review was the compilation of documents that describes in detail each of the testing methods and data reduction techniques used in developing the existing data base. A list of these reports is shown in the Appendix. As a result of the initial phase of this study, documents were received from the seven organizations listed below:

*Catizone & Martin Associates, Inc. (CMA)
63 McKee Street
East Hartford, CT 06108
(203) 289-1331

Energy & Environmental Management, Inc. (EEM)
P.O. Box 71
Murrysville, PA 15668
(412) 247-5124

Energy Impact Associates (EIA)
P.O. Box 1893
Pittsburgh, PA 15230
(412) 351-5800

Midwest Research Institute (MRI)
425 Volker Boulevard
Kansas City, MO 64110
(816) 753-7600

PEI Associates, Inc. (PEI)
(Formerly PEDCo Environmental, Inc.)
11499 Chester Road
Cincinnati, OH 45246
(513) 782-4700

TRC Environmental Consultants, Inc. (TRC)
800 Connecticut Boulevard
East Hartford, CT 06108
(203) 289-8631

United States Steel Corporation (USS)
Research Laboratory
125 Jamison Lane
Monroeville, PA 15146
(412) 372-1212

*CMA is no longer in operation.

Each of these current procedures documents (CPD) specifically addressed the following points:

1. A description of the testing methods and data reduction schemes employed in a specific field test conducted by that organization for the measurement of both the total particulate (TP) and the size distribution of that particulate resulting from open source fugitive emissions and other ancillary measurements such as surface loading of silt on roadway.

2. A discussion of the historical development of the current technique with particular emphasis upon any changes that have been made and the reasons for those changes. If either the sampling or data analysis techniques have undergone change, the respective organization described how data obtained before the modifications were instituted could be correlated with that obtained afterward or detail why such correlations cannot be made when such is the case.

3. One or more detailed test reports from recent field tests which utilized the sampling and data reduction techniques described in (1) above. Included in these reports were sufficient raw data to enable the reader to reproduce the final results quoted.

4. A discussion of how the testing and data reduction procedures described above would be modified for use at various site locations and under varying site conditions.

As a result of review of the CPD's, four organizations were selected to participate in the simultaneous field comparison during Part II of this study. These organizations were selected according to the following criteria:

1. Those organizations which have made a significant contribution to the existing fugitive emission data base using different methodologies.

2. A representative organization for each alternative methodology not included in those selected by criterion number 1.

The four organizations originally selected to participate in the field comparison were CMA, EEM, MRI, and PEI. However, before the field test could be carried out CMA had to withdraw from consideration and were replaced by TRC, the next choice in line. Another organization, USS, participated in the field

comparison at their own expense and thus, a total of five organizations were included in the field comparison, EEM, MRI, PEI, TRC, and USS. The individual field test reports from these five organizations are also listed in the Appendix.

Because much of the use of the emissions trading policy with respect to roadways had been in the iron and steel industry, the desired test site was an unpaved road within an integrated iron and steel facility. Negotiations were undertaken with several companies with regard to possible plant access for the tests; the United States Steel Corporation responded favorably, offering the use of their Gary Works. The nature of the tests to be conducted made it necessary to use a moderately long, straight stretch of roadway that was oriented more or less perpendicular to the prevailing wind and clear of local perturbing influences for a length of a few hundred meters. It was also desirable that the road have a moderately high traffic density for emissions generation. Unfortunately, all suitable roads on the property of the Gary Works were either paved or had been treated with chemical dust suppressant. The most suitable road section in terms of physical layout and traffic density was a paved slag haul road parallel and adjacent to Lake Michigan. Consequently, this road was made to simulate an uncontrolled unpaved road by applying a 5-10 cm thick layer of dirt to one 300 meter section. This portion of the road was located well away from other potentially confounding sources and wind flow obstructions. Five side-by-side test positions, each approximately 15 meters wide, were then laid out on both sides of the road near the center of the simulated unpaved road section. A total of eleven tests were conducted over a five-day period in June 1984. The results of these tests are the subject of the following report.

SECTION 2

CONCLUSIONS AND RECOMMENDATIONS

Each of the profiling systems used in these tests exhibited both pros and cons in terms of their versatility and ease of deployment. Consequently, no conclusions are drawn as to the optimum mechanical design of the profiling towers or associated hardware. However, several conclusions may be drawn regarding the methods of sampling. These conclusions and recommendations are discussed in detail at the ends of Sections 5, 6 and 7 and are summarized in the paragraphs below.

The data from this test series clearly indicate that there is significant exposure at heights up to at least the 9m level. Consequently, the placement of a sampler at the 9m or 10m (preferably 10m) elevation is highly recommended. Also, because the maximum exposure values usually occur at a height of 1.5 to 2.0 meters, any future profiling system should include a sampler at this level. The "ideal" profiling system would have mass samplers at 1.5, 2.5, 4.0, 6.0, 7.5, and 10.0 meters with concurrent particle sizing devices at 1.5, 4.5, and 7.0 meters. This configuration would better characterize both the exposure and size distribution of the particulates in the plume. It was also demonstrated that sampling isokineticity can be maintained for each sampling head on the profiler tower. Therefore, it is recommended that each sampler be equipped with a servo system and individual velocity sensors to provide continuous adjustment of the flow rate based on wind speed at that elevation.

The five profiling systems were found to be capable of producing equivalent results in terms of total emissions. This was not the case for particle size distributions and emissions by particle size. Long recognized problems in reconstituting size distributions of airborne particles from resuspensions of collected bulk material lead to the conclusion that for fugitive emission sampling of the type undertaken here the sizing should take place prior to collection (or concurrent with collection as in cyclones and impactors). The recommended procedure for measuring the particle size distribution is MRI's cyclone/impactor technique with some modifications. With regard to field

operations, first, a further reduction in the sampling flow rate from 20cfm to 15cfm would help minimize errors from particle bounce. Alternatively, adhesive coated substrates could be used at the current 20cfm flow rate. Second, potential errors resulting from the possible transfer of material from the outlet tube of the cyclone to the first stage of the impactor can be avoided by counting only the material collected in the body of the cyclone as its catch. The outlet tube catch would then be combined with that of the first impactor stage. At the current 20cfm flow rate, this would result in a cyclone D50 of 22μm being used rather than the current 14μm value. Lastly, while particle size was measured at the lower elevations (1.5 and 4.5m) an additional cyclone/impactor unit located at a height of about 7m would provide additional information regarding the changes in size distribution as a function of height within the dust plume.

A better data analysis technique than the current MRI procedure would be that commonly used in reducing impactor data from industrial sources. In the latter, a spline fit is made to the cyclone/impactor data in the cumulative percentage form of the distribution. The fit is made in a manner that requires continuity in the slope of the curve and the solution is forced to be asymptotic to 100% at a diameter equal to the maximum diameter present in the sample. The fitted curve is then used to interpolate or extrapolate as needed to obtain the mass fractions in the selected size intervals. This technique avoids the requirement of assuming a functional form for the distribution and makes use of the complete data set rather than just two of the data points.

With regard to the exposure integration procedure, the resultant emission factor appears to be relatively insensitive to the technique used so long as the exposure is adequately characterized with regard to height. The most critical area is that where the peak exposures occur (usually at 1.5 to 2.5m). With samplers at 1.5, 2.5, and 4.0 meters this should not be a major source of error. However, under greatly different site conditions (road type, silt content, etc) the samplers at the lower elevations may need to be positioned at different heights.

The utility of an emission factor predictive equation is that of predict -ing the emissions from a particular site in lieu of actual measurements. In order that the equation be applicable over a wide range of site locations and conditions, it should include as many of the relevant parameters describing the site as possible. This requires that the predictive equation be developed from as large a data base as possible. The equation currently described in the AP-42 manual was developed from a fairly broad data base using multiple linear regression techniques. The data base has some uncertainties particularly with regards to the particle size distributions. These uncertainties most certainly cast some doubt upon the accuracy of the values used for the particle size multiplier, k, in this equation. However, without an extensive evaluation of the existing unpaved road emissions data base, there are no justifications for invalidating the relation. This equation is probably the most reliable predictor of unpaved road emissions currently available. Because of past problems in the particle sizing techniques, the values used for the size multiplier (k) are less reliable than the overall equation. It is recommended that these values be re-evaluated in the future as the data base is expanded with more reliable particle size information.

SECTION 3

FUGITIVE MEASUREMENT METHODOLOGIES

All five of the participating organizations utilized variants of the exposure profiling tower system first developed by MRI[3] to measure emission rates. However, there were potentially significant differences in the actual applications of the method with respect to such items as the number and heights of the profiler samplers, the filter orientation within the samplers, the sampling flow rates, the methods used for establishing and maintaining isokinetic sampling conditions, and the methods used to apportion the total emissions among the various particle size fractions. Fractions of interest were TSP (assumed to be the weight fraction smaller than 30 μm), PM10 (the weight fraction contained in particles smaller than 10 μm), and the fine particle fraction (defined as the weight fraction contained in particles smaller than 2.5 μm). All particle diameters used herein are on an aerodynamic (density = $1 g/cm^3$) basis unless specifically noted otherwise. Brief summaries of the methods used by the participants are given in Table 1.

The profiling methods used by each of the organizations were as follows:

EEM - System composed of an upwind and downwind tower containing three and five sampling heads, respectively, as shown in Figures 1 and 2. Each sampling head consisted of a hi-vol sampler motor, a vertically mounted filter, and an inlet nozzle as shown in Figure 3. The samplers on each tower were raised and lowered vertically by a concatenated pulley arrangement. The samplers were operated at preset fixed flow rates based on a 15-minute average wind speed at a height of 4 m for the period immediately preceding the test. The vertical velocity distribution of wind speed was assumed to be uniform.

MRI - System used for these tests differed somewhat from that used in the past as indicated in Table 1. The system used here was composed of a two head upwind tower and a five head downwind tower as shown in Figures 4 and 5. Each nonsizing sampler head contained a horizontally mounted hi-vol filter and an

TABLE 1. PROFILING SYSTEM CHARACTERISTICS

	Organization				
	EEM	MRI	PEI	TRC	USS
No. of heights					
(upwind)	3	2(1)	4	1	1
(downwind)	5	5(4)	4	5	4
Minimum height (m)					
(upwind)	2	3	1	2	2(3)
(downwind)	2	1.5	1	1	2
Maximum height (m)					
(upwind)	6	6(3)	9(7)	2	2(3)
(downwind)	10	7.5(6)	9(7)	9	9(9.5)
Flow control	manual, fixed	manual, variable	manual, variable	automatic	automatic
Sampler flow set by wind speed at (m):	4	1.5 & 4.5	3	each sampler	each sampler
Particle size method	CCSEM	cyclone/ impactor	stacked filter	CCSEM	CCSEM
No. of heights for particle size					
(upwind)	2(1)	1	4	1	1
(downwind)	3(1)	2	4	3(1)	4
Sampling rate (m^3/hr)	34	34	6.8	34	34
(ft^3/min)	20	20	4	20	20

Note: Values in parentheses ( ) are those used in the past where different from those used in this test.

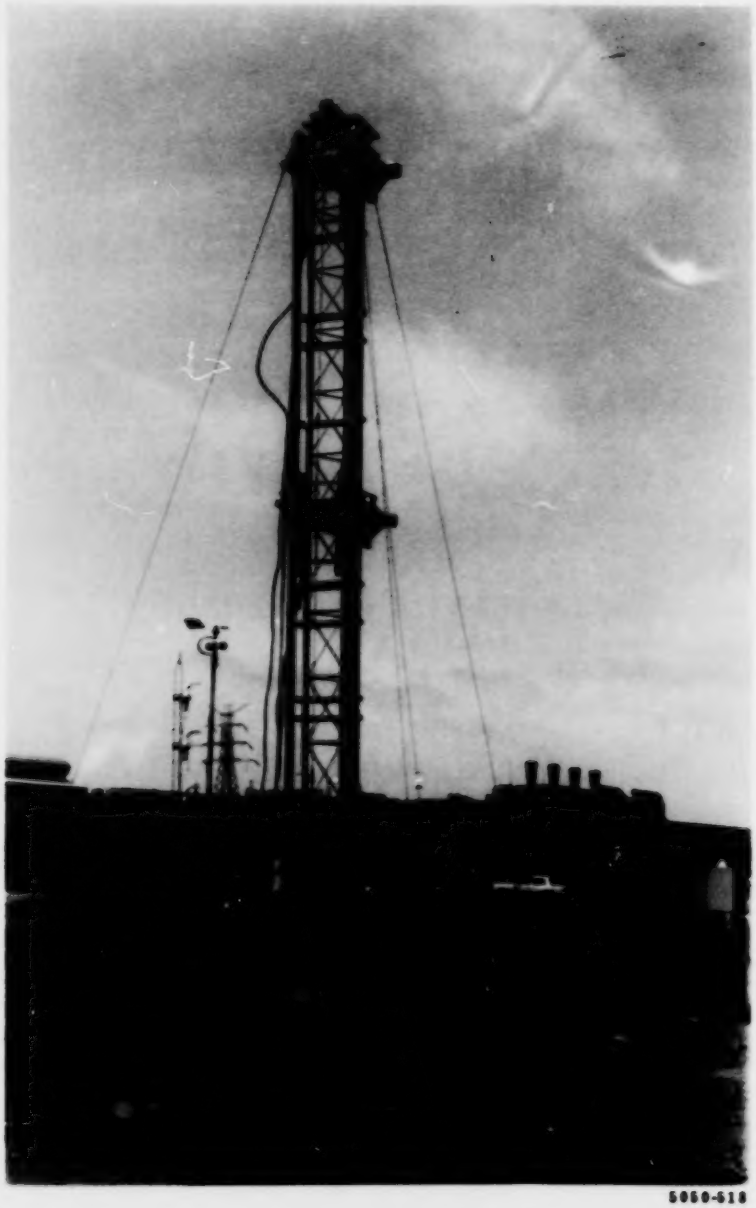

Figure 1. Upwind profiling system used by EEM.

Figure 2. Downwind profiling system used by EEM.

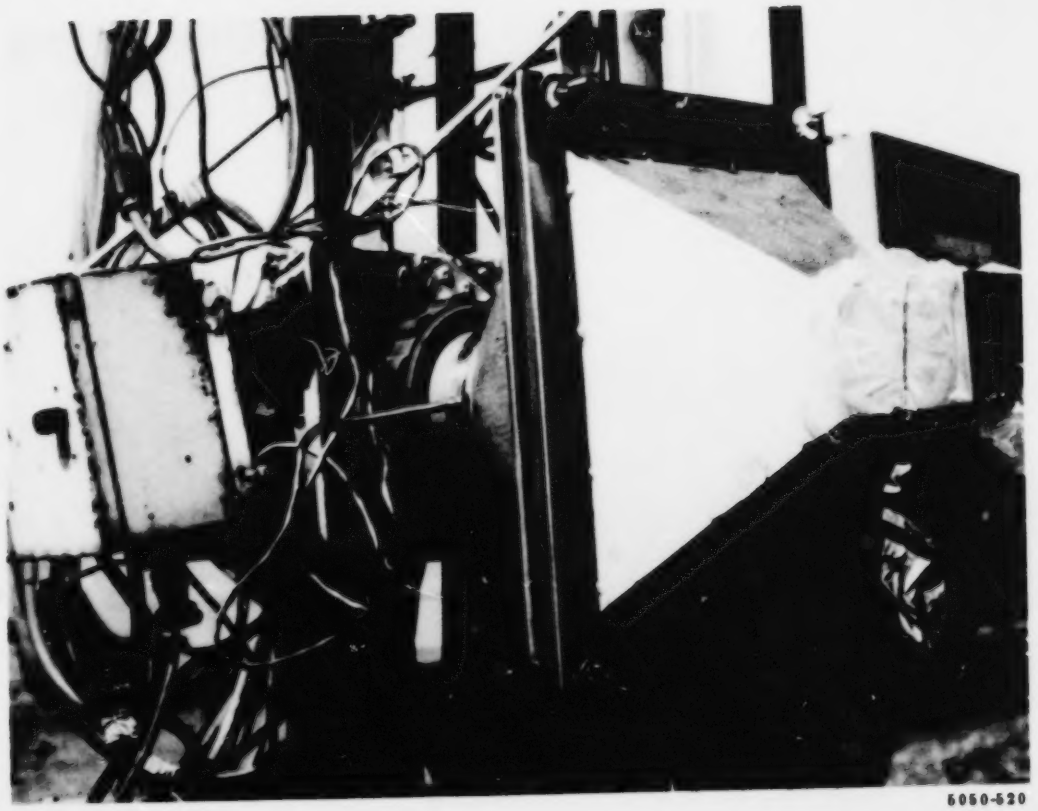

Figure 3. Typical sampling head used by EKM.

Figure 4. Upwind profiling system used by MRI.

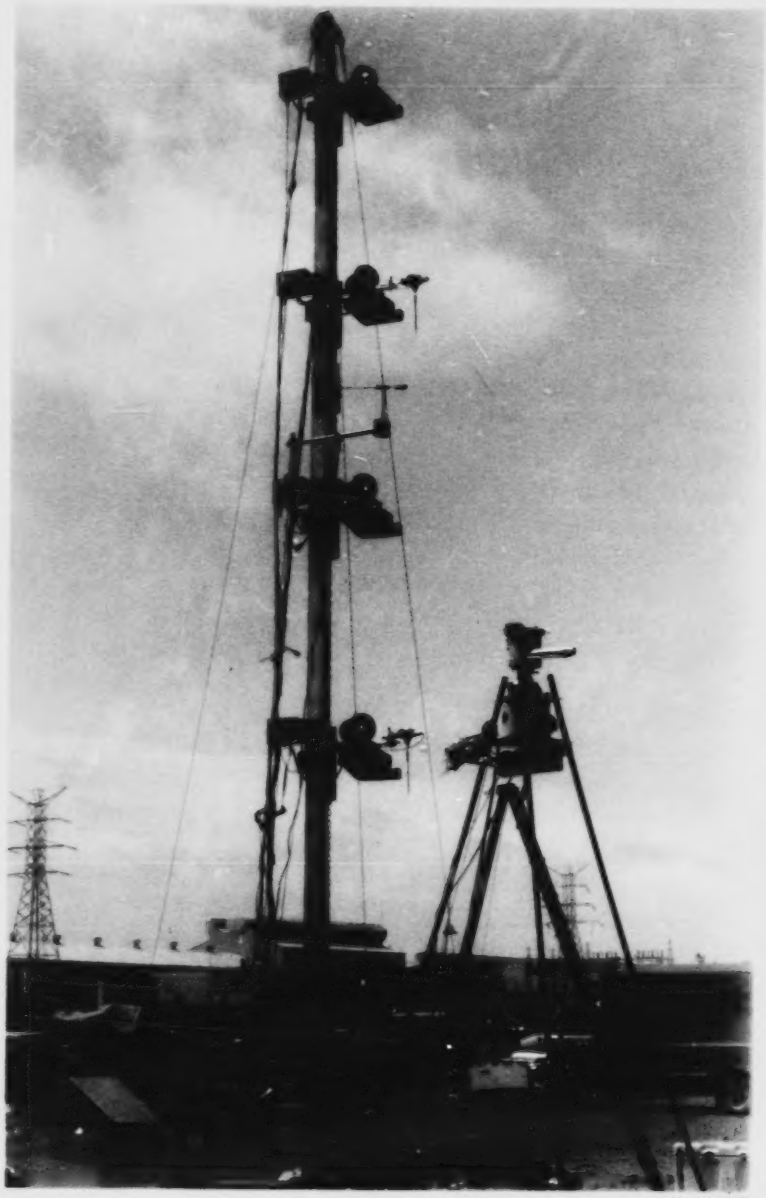

Figure 5. Downwind profiling system used by MRI.

inlet nozzle below the filter as seen in Figure 6. The sampling heads are raised and lowered vertically by a system of pulleys. Periodic manual flow adjustments were based on wind speeds from a logarithm wind shear curve fit to measured wind speeds at heights of 1.5 m and 4.5 m.

PEI - System composed of identical upwind and downwind towers each containing four sampling heads as shown in Figures 7 and 8. Each sampling head consisted of a hi-vol motor and several circular, stacked filters and an inlet nozzle as shown in Figure 9. Sampling heads are raised and lowered vertically while attached to a telescoping tower. In the current tests the maximum height of the profiler was higher than in previous tests (see Table 1). Periodic manual flow adjustments were based on wind speed at a height of 3 m with the vertical velocity profiles adjusted for wind shear by means of an assumed power function.

TRC - System composed of an upwind tower containing one sampler head and a downwind tower with five sampling heads as illustrated in Figures 10 and 11, respectively. Each sampling head contained a hi-vol filter mounted horizontally and an air intake transformer above as shown in Figure 12. The sampling heads were gimbal mounted to the tower and maintained their orientation as the tower was lowered to a horizontal position. Continuous, servo-controlled flow adjustments were based on wind speeds measured by thermal anemometers located adjacent to each sampling inlet.

USS - System consisted of one sampling head upwind tower and a downwind tower containing four samples as shown in Figures 13 and 14, respectively. Each sampling head consisted of a hi-vol filter mounted horizontally and an intake nozzle above as illustrated in Figure 15. The sampling heads were gimbal mounted to the tower and maintained their orientation as the tower was lowered by inclining. Continuous, servo-controlled flow adjustments were based on wind speeds measured by thermal anemometers located adjacent to each sampling inlet.

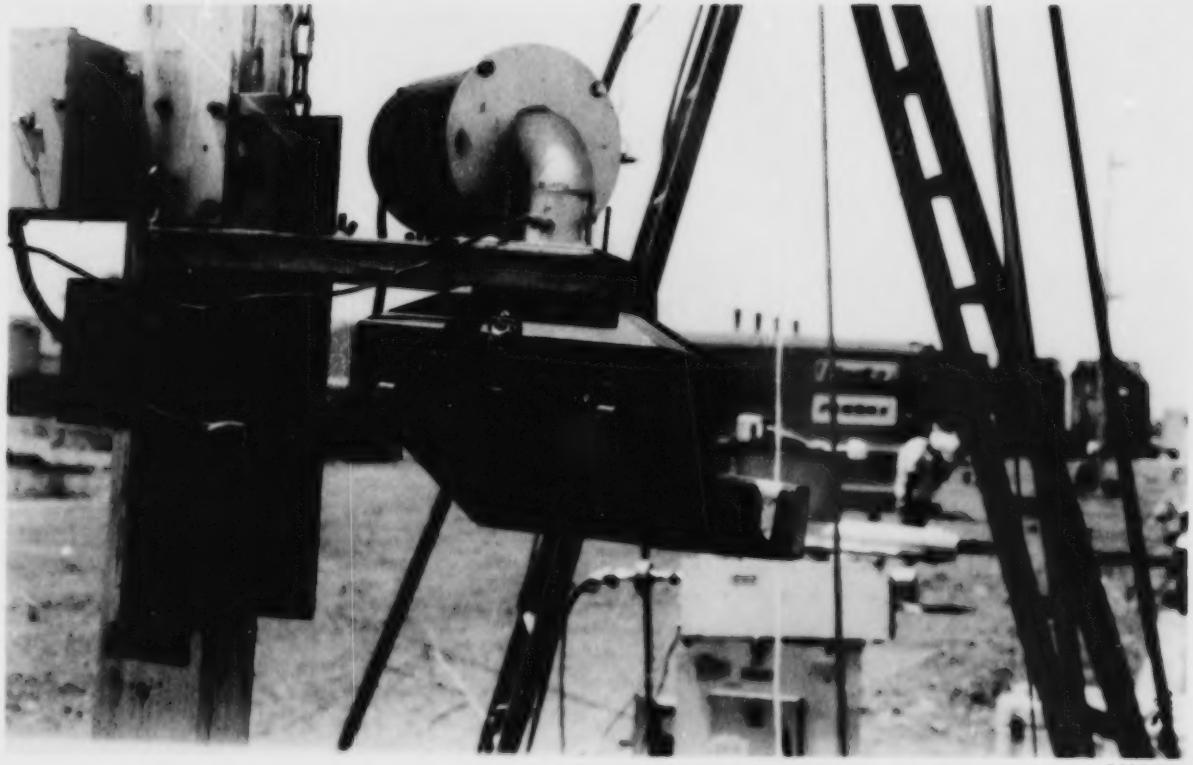

Figure 6. Typical hi-vol sampler used by MRI (without particle sizing).

Figure 7. Upwind profiling system used by PEI.

Figure 8. Downwind profiling system used by PEI.

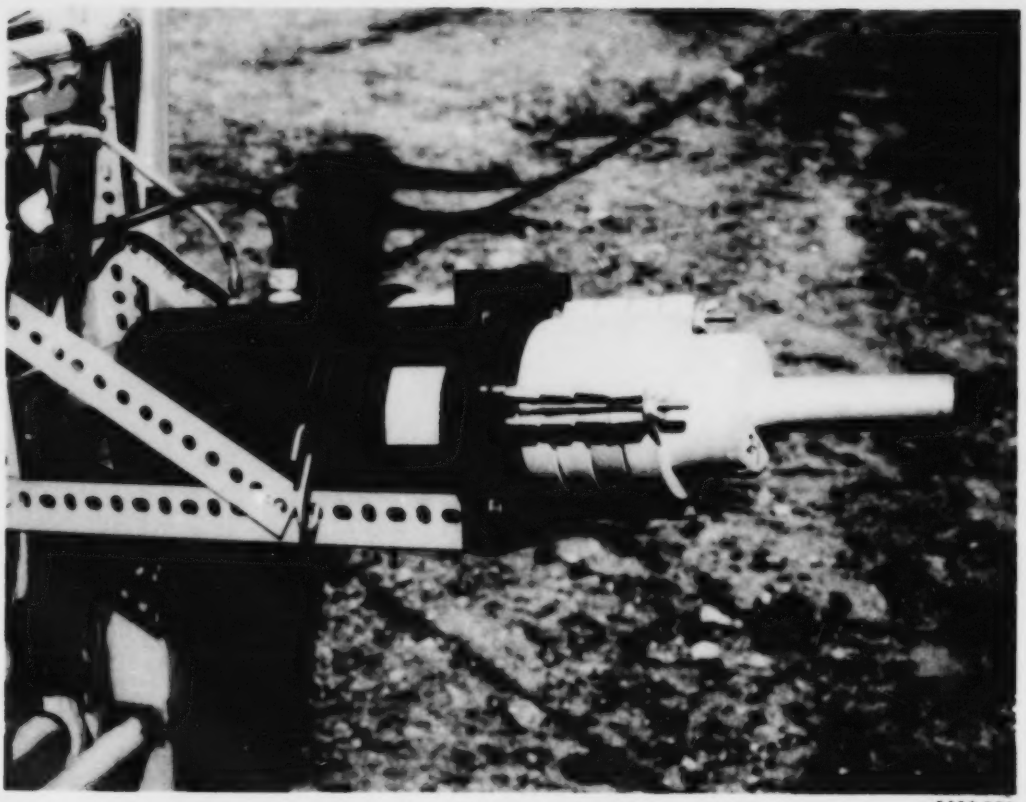

Figure 9. Typical stacked filter sampling head used by PEI.

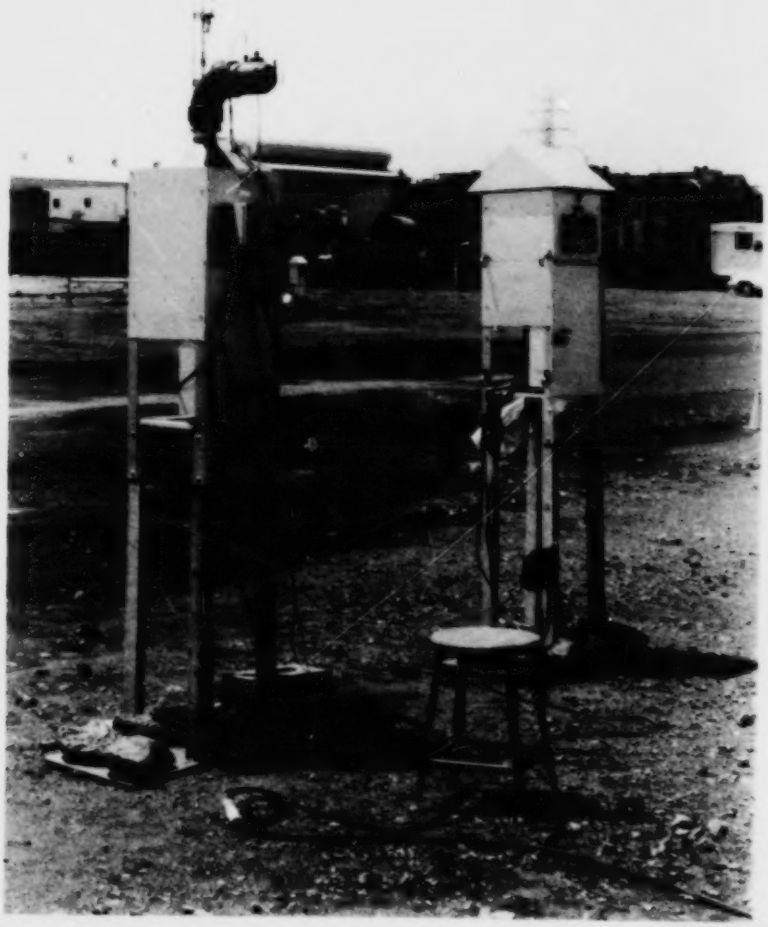

Figure 10. Upwind sampling system used by TRC.

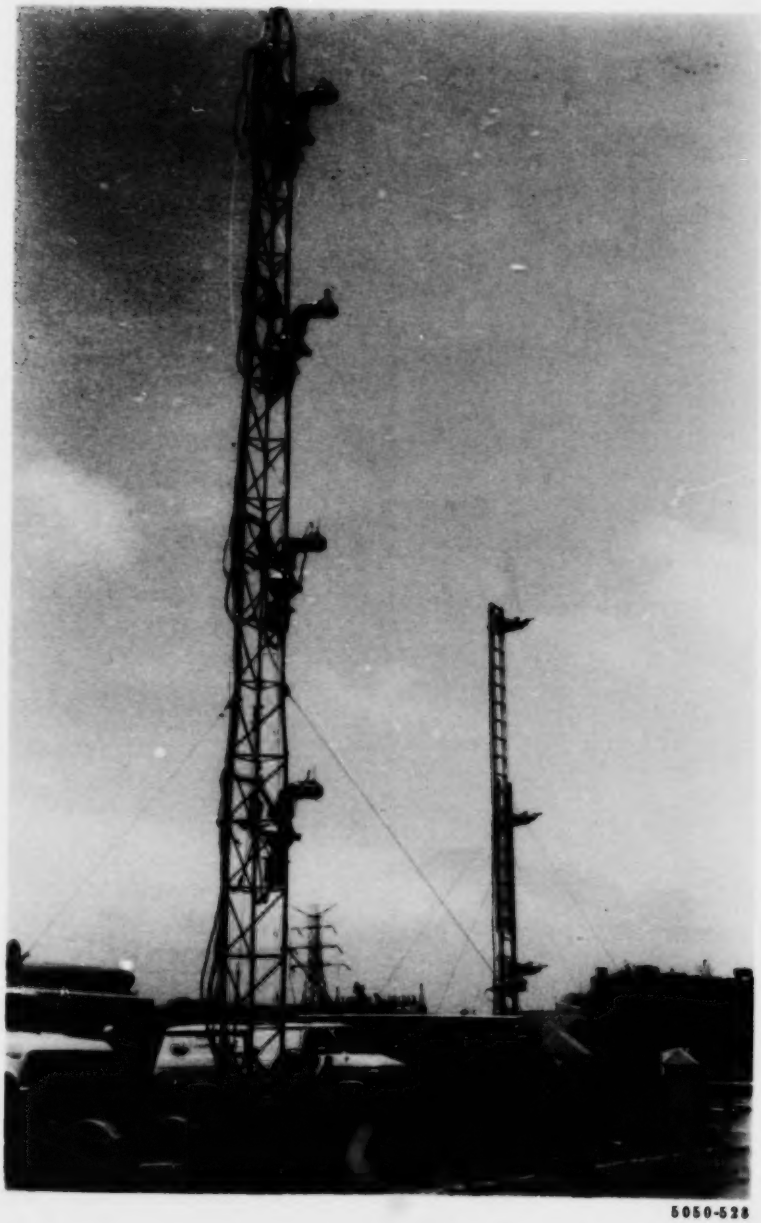

Figure 11. Downwind profiling system used by TRC.

Figure 12. Typical sampling head used by TRC.

Figure 13. Upwind sampling system used by USS.

Figure 14. Downwind profiling system used by USS.

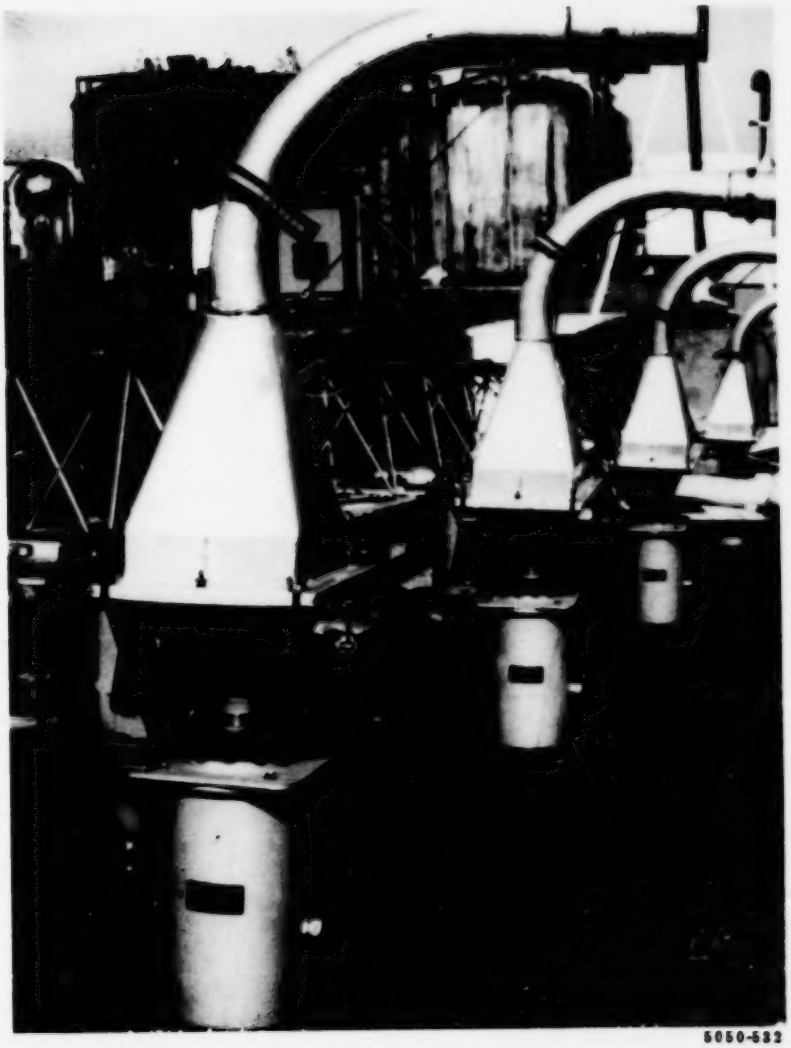

Figure 15. Typical sampling head used by USS.

Three different methods were used for the determination of particle size distributions. Both MRI and PEI used forms of inertial sizing while the remaining three organizations used electron microscopy of the material collected by the profiler samplers.

MRI used a combination of a specially fabricated cyclone for the removal of large particles followed by a Sierra Model 235 Hi-volume cascade impactor.[4] Two such samplers were used, located adjacent to the profiler tower, one at a height of 1.5 m and the other at 4.5 m. These samplers operated at fixed flow rates of 34 cubic meters per hour (20 cfm) with intake nozzles of selected sizes such that the samples would be obtained at near isokinetic conditions.

PEI used the stacked filter concept developed by Cahill, et al.[5] In the PEI implementation of the concept, a stainless steel inlet screen having a 30 μm pore size was used to provide a supposed nominal 30μm fractionation point. The screen was followed by two Nuclepore filters, the first of which had a pore size (8 μm) selected to provide a 2.5μm aerodynamic diameter cutoff while the second, which had a pore size of 0.8μm, served as the final filter.

EEM, TRC, and USS all used computer controlled scanning electron microscopy (CCSEM) for measuring particle size distributions.[6] USS performed their own analyses while Energy Technology Consultants (ETC) performed the analyses for both EEM and TRC. In this method, selected portions of the filters from the profilers were removed, placed between finely perforated stainless steel screens, and backwashed with acetone to remove the collected particles. The particle in acetone suspension was then agitated, and the particles were redeposited by vacuum filtration onto 0.2μm pore size Nuclepore filters. A thin coating of carbon was evaporated onto the redeposited specimen after mounting on SEM sample stubs. The SEM was used in conjunction with an automated image analysis system to detect and determine the dimensions of the projected surface of the particles. Particle volumes were estimated by categorizing the particle's shapes and estimating overall dimensions based on the measurements and assigned category. X-ray fluorescence emissions were used to assign a probable composition class to each particle from which a density

was assigned to it. After measuring approximately 1000 particles and assigning estimated volumes and densities to them, a physical size-weight distribution curve was constructed. Aerodynamic diameters were also estimated for each particle based on the assigned category, the measured dimensions, and aerodynamic shape factors.

In addition to the profilers and sizing systems described above, SoRI performed a limited number of particle size distribution measurements using Lundgren cascade impactors. These samplers were collocated with various samplers of the other participants at different times during the test program. They can be seen hanging under the upper MRI cyclone/impactor and above the lower MRI cyclone/impactor in Figure 5, and below the second lowest PEI sampler in Figure 8. The Lungren impactors sampled at a fixed flow rate of 5 cubic meters per hour (3cfm). The cross-sectional area of the inlet was masked for each test so that the sampling would be done at near isokinetic conditions. These samplers provided a means of obtaining data with an inertial (aerodynamic) classifier collocated with each of the other techniques. A description of the Lundgren cascade impactor is given in Section 5.

SECTION 4

DESCRIPTION OF TEST

The physical layout of the simultaneous field comparison test site is illustrated in Figure 16. The test site was located along a portion of a paved slag haul road adjacent to and approximately 50 meters due south of Lake Michigan. The road was made to simulate an unpaved, uncontrolled, road by covering it with a 5 to 10 cm thick layer of fine aggregate. The material used was a nondescript mixture of clay, iron ore, and boiler ash (composition information is available in TRC's Field Comparison report). The average silt content of the material (fraction passing through a 200 mesh screen) was approximately 10% as measured by all five testing parties.

The average mass concentration (TSP) as measured throughout the testing period by standard high-volume samplers (hi-vols) positioned three meters from the roadway edge was 13.3 mg/m^3. Thus, for all intents and purposes, the test section represented an unpaved and uncontrolled road. In the middle of this 300 meter section of treated roadway, five testing stations were laid off as described in Figure 17. This configuration minimized the distance between sampling systems while allowing sufficient space to each system. Through the use of identical stations on either side of the road the upwind and downwind locations could be swapped across the road when the wind direction reverses as it typically does near the lake.

In an effort to minimize the confounding effects which might be produced by small portable electric generators usually used by the sampling parties, two high capacity diesel generators were positioned on each side of the roadway and approximately 25 meters west of the last sampling location (No. 5 in Figure 17). This also enabled the sampling equipment to be moved from any location to another with a minimum amount of time and effort.

The traffic over the test road was a mixture of service vehicles (pickup trucks) and dump trucks hauling solidified slag from the blast furnaces to the

5050-533

Figure 16. Gary test site after covering road with dirt. View is looking west.

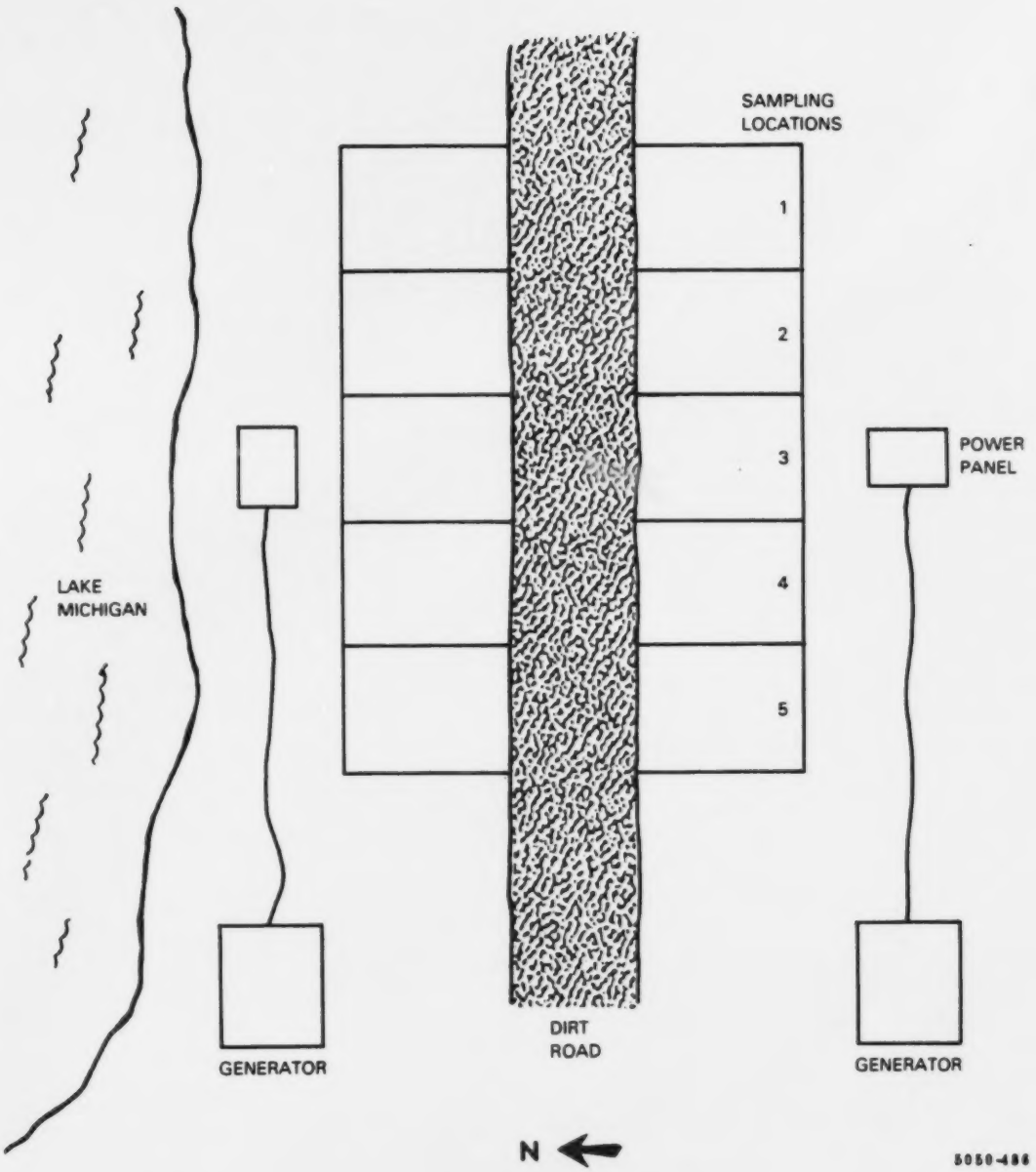

Figure 17. Physical layout of the Gary comparative fugitive emission test site.

slag yards and returning with loads of crushed slag. Average vehicle speed in the test section normally ran as high as 50 to 60 kph. However, after covering the test section with aggregate the average vehicle speed was reduced, because of poor visibility, to approximately 40 kph.

Exposure profiling measurements of the test site were carried out over the period June 11 to June 15, 1984. In this five day period a total of 11 data runs were accomplished. In terms of downwind direction, six tests occurred with the wind coming out of the north (off the lake) and the remaining tests with the wind out of the south. Background concentrations for total particulate (TP) varied with wind direction. When the wind came from the north, off Lake Michigan, the background concentration at 3 meters above the ground was approximately 100 $\mu g/m^3$. During those periods when the wind was from the south the concentration was about 600 $\mu g/m^3$. The difference was due mostly to particulate produced south of the test site where considerable industrial activity was concentrated. This presented no problem for these tests because the TP concentrations produced by the test road were generally several times greater.

The procedure used during each of the eleven tests was as follows: all parties commenced sampling at the same time, during a break in traffic flow; sampling continued until a predetermined number of vehicles had crossed the testing section, and sampling was discontinued simultaneously during a break in traffic flow. Following each test run, sufficient time was allowed for each party to recycle their equipment preparatory to the next test.

One factor of great concern during pretest planning was the possibility of nonuniformity of particle concentrations over the length of the road test section. If the particle concentrations were in fact nonuniform with respect to concentration or size distribution, then comparable results could not have been expected from the various sampling systems, even if they were functionally identical. Any potential effect of nonuniformity of conditions along the test zone was partially obviated by rotating the participant's locations so that each spent one day at each of the five test positions. The lack of a reference

standard for particle size distribution measurement made it difficult to verify uniformity of size distribution; however, uniformity of concentration was checked by means of a conventional high volume sampler at each test location and by comparison of concentrations calculated directly from the various profiler results.

Bar graphs of the concentrations by test and location are shown in Figure 18. The data shown in the figure reveal no systematic bias with respect to sampling position. The overall average concentration for all tests at each test position ranged from 11 mg/m^3 to 15 mg/m^3. The differences were not statistically significant from the grand average of 13.3 mg/m^3 at the 90% confidence level. Average concentrations at each position at a height of 2 m as measured by the profilers ranged from 11.7 mg/m^3 to 17.4 mg/m^3 with a grand average of 13.0 mg/m^3. Again, statistical tests indicated that no significant positional biases existed. In comparing the hi-vol data from each position with the others, the correlation coefficients, with one exception, ranged from 0.52 to 0.97 indicating that the test to test concentration variations were reasonably uniform along the test strip.

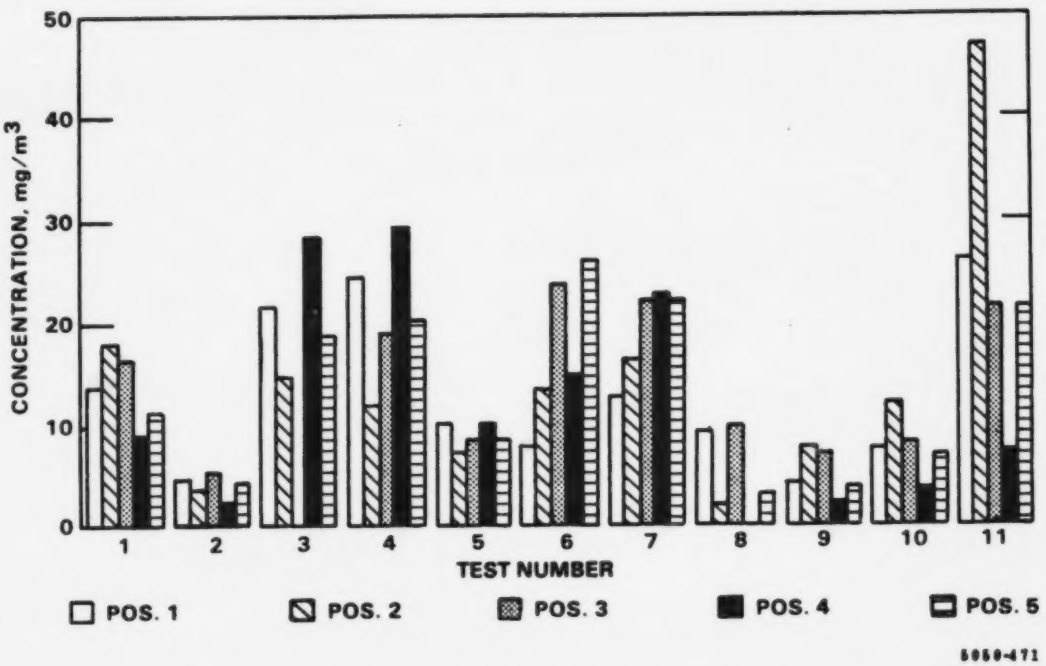

Figure 18. Total suspended particulate matter by test and sampling position as measured by standard high-volume sampler.

SECTION 5

PARTICLE SIZE MEASUREMENT

METHODS

Three fundamentally different particle sizing methods were utilized by the test participants. Three of the organizations - USS, TRC, and EEM - used Computer Controlled Scanning Electron Microscopy (CCSEM); one, MRI, used inertial particle sizing devices; and one, PEI, used a combination of forms of sieving and inertial devices. In addition, SoRI operated collocated inertial sizing samplers at selected locations during some of the tests. Unfortunately, the lack of standard reference methods for particle size distribution measurement under circumstances like those encountered in roadway emissions testing makes it difficult to arrive at unequivocal conclusions regarding the actual distributions during these tests and in the departures from those distributions in the data obtained by the participants.

Cyclone/Impactors

MRI used a combination of a specially fabricated cyclone for the removal of large particles followed by a Sierra Model 235 Hi-volume cascade impactor for size distribution measurement. The setup is illustrated in Figure 19. The size distribution measurements are made separately from the exposure measurement. The analysis of the particulate material collected by their device is by gravimetric methods. Particle collection in the cyclone takes place in two distinct zones: the body of the device, and the outlet tube. If the body catch is taken alone, the cyclone cut diameter is 22μm (aerodynamic diameter); if the body and outlet tube catches are combined, the cut diameter is reduced to 14μm. The treatment of the cyclone data with respect to the handling of the catch(es) and the two possible cut diameters will be deferred to the discussion of the test results. With respect to the impactor portion of the sampling system, MRI used a total of five impaction stages (plus filter) in the impactor producing size cuts at 0.6μm, 1.2μm, 2.0μm, 4.1μm, and 10μm. It should be noted, however, that in past tests only the first three of the five

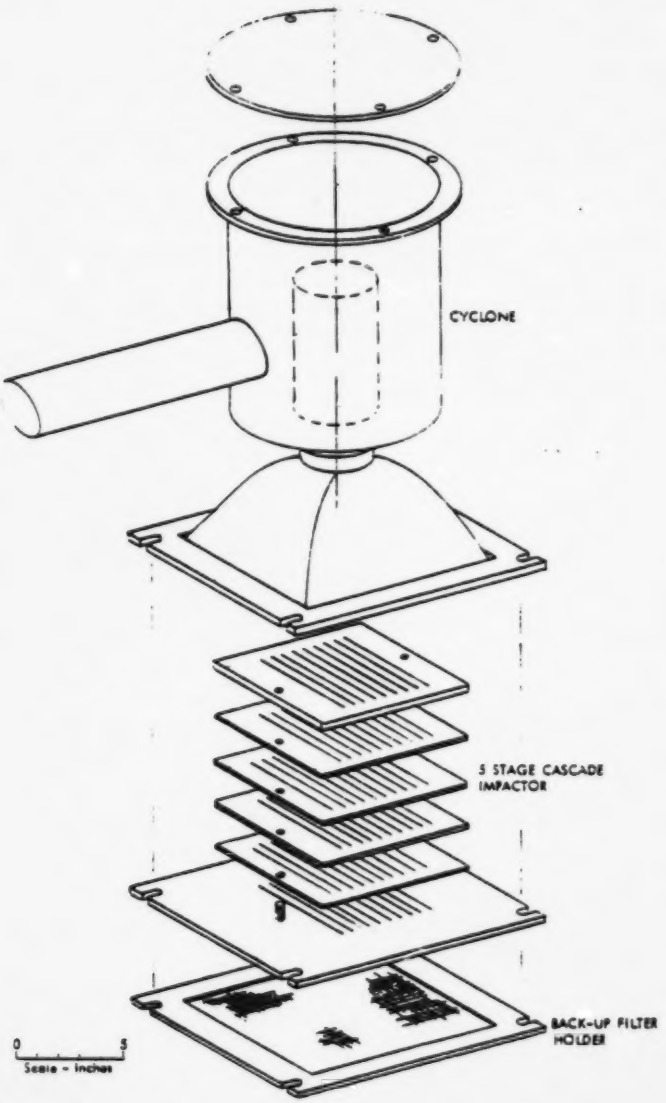

Figure 19. MRI cyclone/cascade impactor combination.

stages were used. The omission or inclusion of the last two stages can have an effect on the interpretation of the data as will be discussed later. Three such cyclone/impactor samplers were used, one upwind to measure both concentration and size distribution, and two more downwind for size distribution measurement only. The latter were located adjacent to the profiler tower, one at a height of 1.5m and the other at 4.5m. These samplers operated at fixed flow rates of 34 cubic meters per hour (20cfm) with intake nozzles of selected sizes such that the samples would be obtained at near isokinetic conditions.

SoRI obtained several samples with Lundgren cascade impactors during the tests as well. These impactors, illustrated in Figure 20, are four stage (plus filter) inertial classifiers[7,8,9], providing size fractionation at diameters of 0.44 μm, 1.4 μm, 4.2 μm, and 14 μm as operated in these tests. The samples were taken quasi-isokinetically with inlet nozzle cross-sections adjusted in accordance with the mean wind speed at the start of the test, but the flow rate was held constant at about 5 cubic meters per hour (3 cfm). Particle collection in this impactor takes place on a moving plastic film coated with an adhesive. The adhesive is used to insure retention of the impacted particles. The particle size distribution is measured gravimetrically. However, by collecting the particles on the moving film, overlapping of particles in the collected sample is largely avoided, permitting individual particles collected on each stage to be easily examined by microscope. Three of these samplers were set up collocated at various times with samplers of EEM, MRI, and PEI as illustrated for one case in Figure 21. Although the Lundgren impactor results are used as a basis for some comparisons through the remaining discussions of particle size distribution, they should not be construed as reference standards.

Stacked filters

PEI used the stacked filter concept developed by Cahill.[5] In the PEI implementation of the concept, a stainless steel inlet screen having a 30 μm pore size is used to provide a supposed nominal 30 μm fractionation point. The screen is followed by two Nuclepore filters, the first of which has a pore size (8 μm) selected to provide a 2.5 μm aerodynamic diameter cutoff while the second, which has a pore size of 0.8 μm, serves as the final filter. These

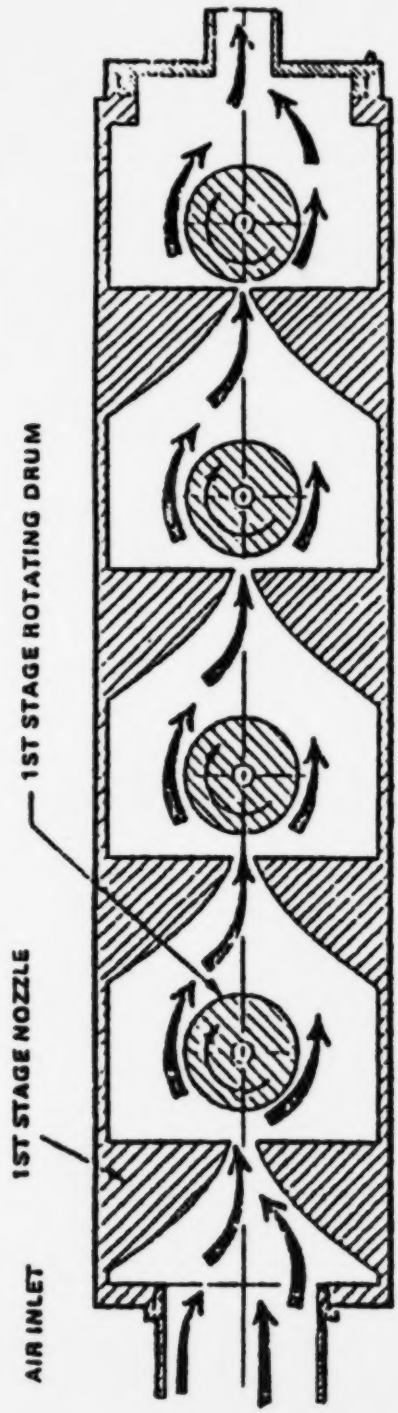

Figure 20. Lundgren cascade impactor.

5050-534

Figure 21. Collocated Lundgren cascade impactor (left) and MRI Sierra cyclone and impactor (center).

stacked filter units constituted the exposure samplers on the identical upwind and downwind profiler towers. A schematic diagram of the sampler is shown in Figure 22.

Scanning Electron Microscopy

EEM, TRC, and USS all used computer controlled scanning electron microscopy (CCSEM) for measuring particle size distributions.[6] USS performed their own analyses while Energy Technology Consultants (ETC) performed the analyses for both EEM and TRC. In this method, selected portions of the filters from the profilers are removed, placed between finely perforated stainless steel screens, and backwashed with acetone (ETC) or backblown with compressed air (USS) to remove the collected particles. In ETC's procedure the acetone particle suspension is then agitated and the particles are redeposited by vacuum filtration onto 0.2μm pore size Nuclepore filters. USS recollects the air suspended particles on similar Nuclepore filters for analysis. A thin coating of carbon is evaporated onto the redeposited specimen after mounting on SEM sample stubs.

A SEM is used in conjunction with an automated image analysis system to detect and determine the dimensions of the projected surface of the particles. The same hardware and software is used by both ETC and USS for their respective analyses. Particle volumes are estimated by categorizing the particle shapes and estimating overall dimensions based on the measurements and assigned shape category. X-ray fluorescence emissions are used to assign a probable composition class to each particle from which a density is assigned to it. After measuring approximately 700 to 1200 particles and assigning estimated volumes and densities to them, a physical diameter - weight distribution curve is constructed. Aerodynamic diameters are also estimated for each particle based on the assigned category, the measured dimensions, and aerodynamic shape factors. The method by which the particles to be measured are selected and the way in which the decision is reached that a sufficient number of particles have been measured are considered proprietary information by both the USS and ETC; therefore this information was not available for use in critiqueing the CCSEM methodology used in this application. Because the distributions are heavily skewed to the small particle end of the size spectrum in terms of number

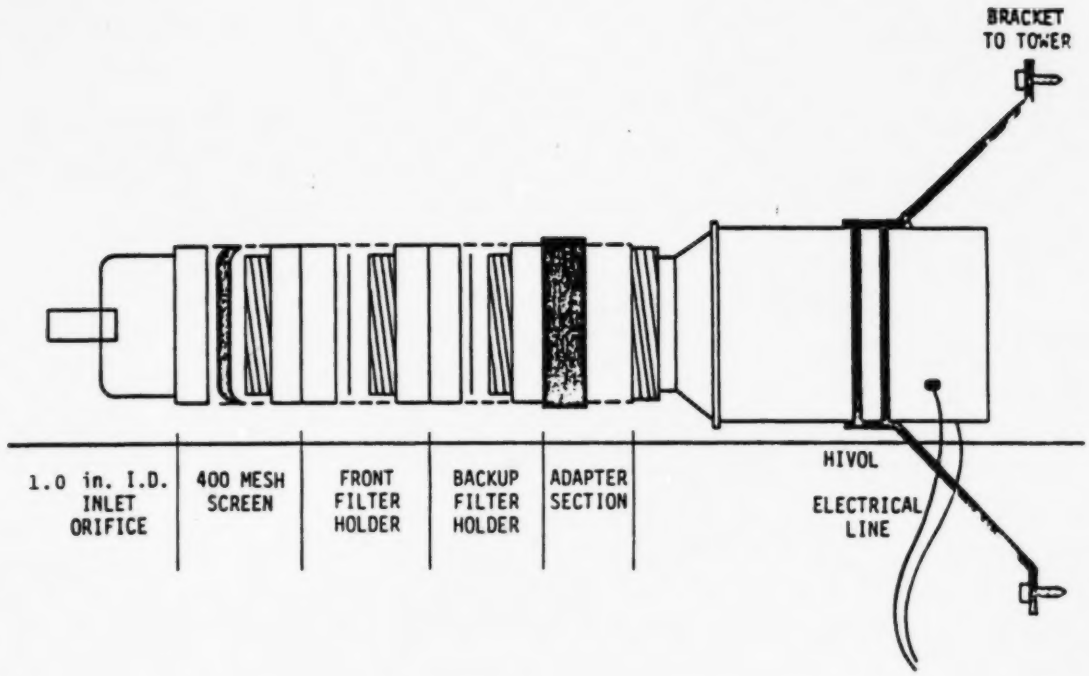

Figure 22. PEI stacked filter profiler head.

population, the counting statistics for the large particles, which contain the preponderance of the mass, would be poor unless a technique like stratified counting were used. A technique like the latter may indeed have been used, however this could not be verified.

RESULTS

The PEI profiling system provided data in two size fractions at each profiler level for each test. MRI's system provided data for each test in seven size fractions at each of two heights for a location adjacent to their profiler. The remaining three participants used CCSEM analysis of varying numbers of the filters from their profilers. USS performed size analyses on all of the filters from their profiler. TRC had CCSEM analyses performed on two or three filters from selected heights from one test each day. EEM had analyses performed on complete profiler filter sets from two tests which were selected as representative of typical conditions through the week.

The results from disparate methods were not found to be mutually consistent. Comparative particle size distribution results from Test 4 (PEI data from Test 9) are shown in Figure 23, in which marked differences can be seen to exist among the results from the various methods. The particle size distributions measured by a given contractor were generally similar for all tests. Test to test variations for each contractor were smaller than the differences resulting from using different techniques. These differences and their probable causes will be discussed in detail in the following paragraphs. This test was selected for illustration because it is one for which inertial sizing devices (Lundgren impactors) were collocated with samplers for which CCSEM size analyses were performed (EEM). The results from this test for all participants were generally comparable to those from the other tests for which size data were available. No results are shown for TRC because they, like EEM, had size analyses done for only a subset of the complete test series and samples from this date were not included in that subset. The distributions for all three users of CCSEM size analysis were quite similar to that illustrated in Figure 23 throughout the entire test series. The PEI data in the illustration were from a different day (Test 9), since complete measurements, which

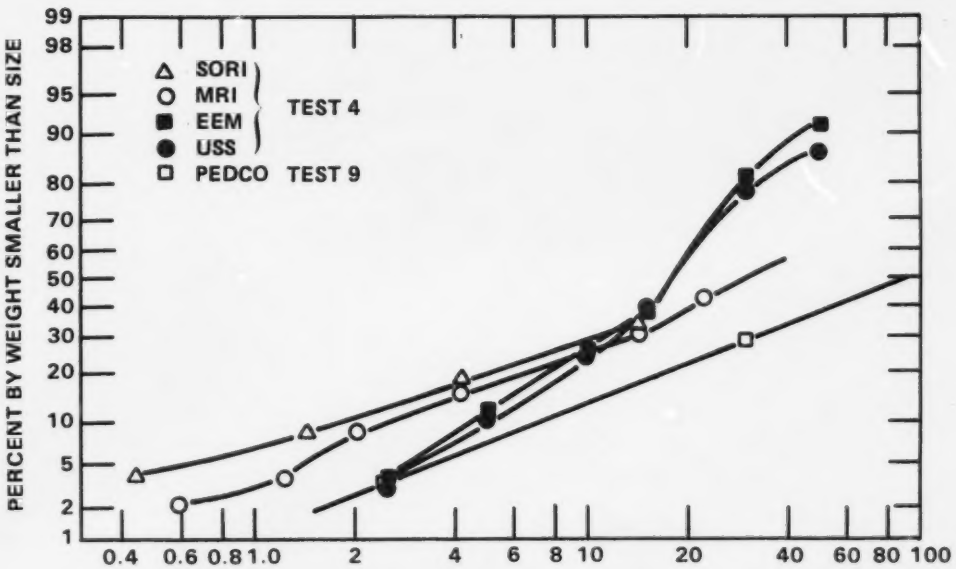

Figure 23. Particle size distributions as measured by the various techniques. 5050-473

included all particle sizes were obtained on only one day by PEI. Again, since day-to-day variations in the distributions measured by the other participants were small, conclusions based on comparison of the PEI distribution with the others shown in the figure should be valid.

Averages and standard deviations of emission factors for total particulates, TSP (<30μm), PM_{10} (<10μm), and FP (<2.5μm) for each participating organization are given in Table 2. In general, at the 95% confidence level, no significant differences are found in the total emission factors other than the slightly low value from TRC. In the case of the TSP emission factors, the results from the three contractors using CCSEM analysis show no differences which are significant at the 95% confidence level. However, the MRI results are significantly lower than of the CCSEM users at the 95% confidence level, and the PEI results are lower than those of MRI at that same confidence level.

Stacked Filter

Looking first at PEI's results, we find that they were systematically low for all particle sizes considered. PEI's method provides data only at nominal sizes of 2.5μm and 30μm from which 10 μm values are inferred by interpolation, thus if both the 2.5μm and 30μm data are low compared to the other inertial techniques, then it is highly likely that the 10μm value will be as well. The 30μm cutoff was presumed based on the pore size of the screen and was not verified by calibration. In the runs with collocated Lundgren impactors, in two of three cases the concentrations of fine particles and of particles smaller than 30μm as measured by PEI were respectively one-third and two-thirds as large as those measured by the impactors in two of the three cases. In a third run the concentrations were approximately equal.

The physical mechanism used to provide the 30μm size cut in the PEI system is a wire mesh screen with 30μm openings. The assumption is then made that this inlet screen will provide a particle size cutoff of 30μm. However, it is probable that significant collection of particles smaller than 30μm will take place by impaction and interception, even with clean screens, thereby reducing

TABLE 2. AVERAGE EMISSION FACTORS BY SIZE CLASS

	Emission factor, kg/VKT							
	TP (total)		TSP (<30 μm)		PM_{10} (<10μm)		FP (<2.5 μm)	
	Average	σ	Average	σ	Average	σ	Average	σ
EEM	8.3	2.5	6.6	2.0	1.9	0.63	0.21	0.10
TRC	5.7	1.4	5.3	1.3	1.8	0.45	0.16	0.04
USS	8.4	3.4	7.1	3.2	2.6	1.10	0.32	0.21
MRI	8.3	3.8	3.6	1.7	1.9	0.88	0.61	0.28
PEI	5.8*	1.8	2.4	0.99	1.2	0.53	0.30	0.21

* Tests 8, 9, and 10 only. Average TP Emission Factor measured by other contractors for these three tests was 6.22 kg/VKT (see Table 4).

the effective cutoff diameter to a value substantially smaller than 30μm in much the same way the the 8μm pores of the Nuclepore filter produce an inertial separation near 2.5μm. Further, as particles are collected by the screen, the openings are reduced in size, thus making the screen become a progressively more efficient filter. This filtration effect will then result in depressed values for particle concentrations and emission factors for all particle sizes that are assumed to be passed by the screen. It is worth noting that the openings in the weaves of fabric filters used for particulate control devices are comparable to or larger than the 30μm openings used here.[10] In Figure 24a the PEI data obtained in this test series is used to illustrate that the screens undoubtedly do become more efficient filters as a test proceeds.

Data from other participants, which will be discussed shortly, indicated that the particle size distribution remained fairly constant at heights between 1.5m and 4.5m throughout the test series, leading us to expect that the ratio of TSP concentration to total concentration would be constant as well. The particulate concentrations obtained from the hi-vols were previously shown to be consistent with those measured by the profilers at a height of two meters. Since the profiler and the hi-vol sampling periods were identical, the hi-vol filter weights can be used as surrogates proportional to the missing total weights for the PEI profiler samples at the two meter level, and the hi-vol concentrations as surrogates for the total concentrations that would have been obtained by the profiler. The points plotted in Figure 24a are the ratios of the TSP (<30μm) concentrations at the two meter height from PEI's profiler to those of the collocated hi-vols plotted versus the corresponding hi-vol catch weight. As can be seen, the ratio declines as the filter weight, and hence the expected total catch weight of the profiler, increases. Washes of the sampler screens and inlets were obtained in each of tests 8, 9, and 10; consequently, complete data on the system catches were available for those sets. The ratios of apparent TSP to total concentrations from the lower samplers of PEI's profiler, where the distribution might be expected to be fairly constant, are shown in a similar way for tests 8, 9, and 10 in Figure 24b. Again, the ratios tended to decline as the catch weights increased. This is indicative of decreasing screen penetration as the profiler samplers loaded up during a sampling run. This filtration effect, together with the misassignment of the initial particle size cutoff of the clean screen, is the probable explanation

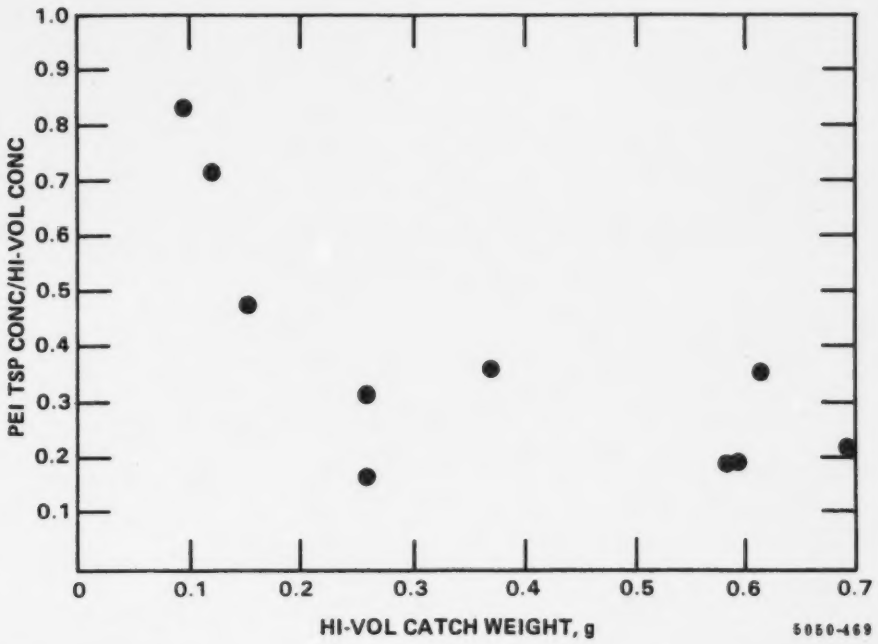

Figure 24a. Plot of the ratio of PEI's TSP concentration to hi-vol concentration versus the total particulate mass collected by the hi-vol.

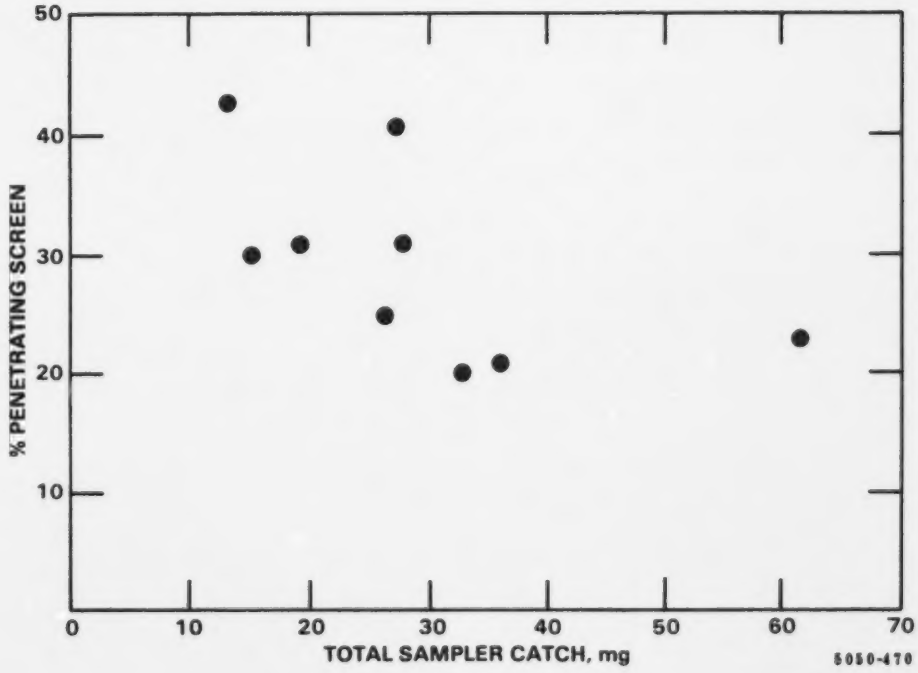

Figure 24b. PEI screen penetration dependence on total mass collected by the profiler sampler.

of why PEI's particle size distribution curve, shown in Figure 23, fell below those of the other participants.

The catch weights of the PEI samplers were very near the detection limits in many cases so operation with shorter sampling times in order to avoid loading the screens is not feasible. Even in the absence of these problems, the PEI system can provide, at best, questionable data with respect to PM_{10} emissions. The system is purported to provide size distribution information at only two particle sizes - 2.5μm and 30μm, - both of which are relatively far removed from 10μm. Thus, the 10μm fraction must be estimated by means of some assumptions regarding the shape of the distribution at each height. Even the most commonly used distribution form, the log-normal approximation, cannot be used in PEI's normal practice as the total concentrations are not usually determined but only the concentrations of particles nominally smaller than 30μm and 2.5μm.

Scanning Electron Microscopy

Turning now to the CCSEM method, Figure 25 shows a particle size distribution obtained by EEM/ETC using CCSEM methodology and the distribution measured by SoRI using a collocated Lundgren cascade impactor. Six such collocated sampling runs were carried out and each resulted in particle size distributions like that illustrated in Figure 25. The points shown for the impactor results for sizes smaller than 15 μm are from gravimetric determinations. The results which are shown for the impactor for sizes larger than 15um were obtained in two ways. Both of these involved microscopic measurement of the size distribution of the material collected on the first stage of the impactor and then apportioning the mass collected by the stage accordingly. In the first case SoRI personnel performed manual counts of random regions of the first stage substrate of the Lundgren sample using optical microscopy. These counts were made in eight size classes based on Feret's diameter. Similar measurements were made of all of the Lundgren first stage catches with total of approximately 500 particles being measured on each. Secondly, one half of each of the Lundgren substrates were then sent to ETC for analysis of the catches by CCSEM. Time and cost constraints led to only one of these actually being analyzed.

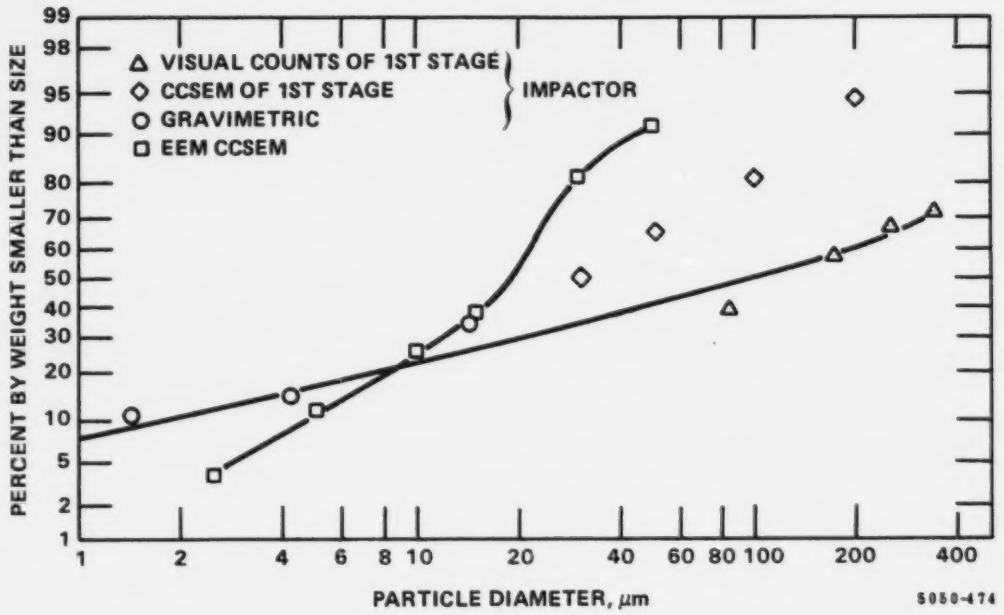

Figure 25. Particle size distribution as measured by a Lundgren cascade impactor and as determined by the CCSEM technique from a collocated profiler sample.

The one selected was the particular sample used in the illustration and the results of that analysis are also incorporated in the figure. Discussion of the comparative results of the optical and CCSEM analyses of this sample will be deferred for the moment.

A total of nine valid downwind Lundgren impactor runs were made over the course of the tests, cursory examination of which revealed that all had collected particles with sizes up to 300μm. Six had particles larger than 400 μm and two contained particles larger than 500μm. Similarly, MRI reported particles as large as 300μm in their cyclone catches and examination of randomly selected filters from the collocated hi-vol samplers revealed the presence of particles having sizes of a few hundred micrometers. The average combined results from the nine valid downwind Lundgren impactor runs showed 50% (range of 34% to 78%) of the mass to be contained in particles larger than 14 μm, the first stage cutoff. Inlet losses, which were not accounted for in the Lundgren results, would probably increase the latter figure to about 60%, if included. In aggregate, the SoRI microscopically determined mass median diameter of the material on the first stages of the Lundgren samples was 200μm, meaning that typically some 25% to 30% of the total mass in the roadway emissions was contained in particles larger than 200μm. On the other hand, no particles physically larger than 80μm were reported in the data from any of the three groups using CCSEM for size distribution measurement and in the case of the TRC results, none larger than 50μm were reported.

USS states that the particle sizing range capacity of their CCSEM system, is 0.2μm to 80μm, and it appears from the results reported by ETC (EEM and TRC) that the same upper limit applies in practice to their method as well, although ETC quotes the method as covering sizes to 300μm.[6] The filter retention screens used in transferring the sample from the profiler filters to the Nuclepore material for analysis will themselves act as filters and bias the sample taken from the original profiler filters by suppressing the transfer of large particles. Indeed, in ETC's description of their technique, the screen is said to prevent the transfer of (large) filter shards which would otherwise contaminate the sample. The screen used by ETC was a metal shim with an array of 210μm diameter round holes resulting in a total open area of 41%. Thus no particle larger than 210μm physical diameter could be transferred from the

filter. More importantly, the probability of transfer would be low (less than 50%) for any particle larger than 50μm with the probability dropping to zero at 210μm. The omission of the particles in the size classes larger than 50 to 80 micrometers obviously introduces a bias into the final reported distribution, the severity of which depends on the relative fraction of the mass actually contained in that fraction. In the present instance as much as 25 to 50 percent of the total mass was probably contained in particles physically larger than 50 to 80μm. This mass would be reassigned to smaller particles in the CCSEM results. Thus the reported CCSEM distributions would be expected to rise much more steeply than the true distributions in the size region above about 50μm.

Returning now to the results depicted in Figure 25, we find that although the optical and CCSEM analyses are not in complete agreement, both sets of results show non-negligible fractions of the total catch to consist of particles larger than 50μm, 60% and 35% respectively, with 50% and 75% respectively being larger than 30μm. These analyses were carried out directly on the original specimens with no particle removal and transfer from the original substrate taking place in either case. (The actual results of the CCSEM measurements of the substrate showed less than one percent of the mass consisted of particles smaller than 10μm, 22% in the 10 to 30μm range, 25% in the 30 to 50μm range, 24% in the 50 to 100μm range, 20% in the 100 to 200μm range, and 9% in the 200 to 500μm range.) In contrast, only 5% of the mass on the collocated profiler sample was assigned to particles larger than 50μm and only 20% was assigned to particles larger than 30μm by the CCSEM analysis. Even though the size range of the particles on the substrate was limited as compared to that of the profiler filter, measurements of a total of about 4500 particles were needed in order to obtain reasonable statistical validity in the data. In contrast, only about 1000 particles were measured from the profiler filter even though the size range was presumably much larger. This raises a question as to whether the number of particles examined in the routine CCSEM analyses is in fact sufficient for obtaining reliable data.

The lack of large particles in the CCSEM results for all of the profiler samples may arise from three factors. First, the analysis may not include sufficient particles to provide valid results for the statistically rare large

particles. Second, the screens used in the sample transfer and preparation procedures for the CCSEM analyses result in a bias against the inclusion of large particles. And third, the large particles may simply be lost from the surfaces of the filters in handling and transport after the sampling takes place. Large particles are not strongly attached to the filters and are commonly observed to become detached from filter surfaces. In the cases of hi-vol filters which are folded and placed in envelopes for transport, the large particles are frequently found to migrate to the vicinity of the fold or off the filter into the envelope while in transit. Thus the lack of large particles in the CCSEM results may simply be a result of a failure in maintaining sample integrity and representativeness throughout delivery to the analytical laboratory. ETC reported that visual scans of the surfaces of the EEM and TRC profiler filters from these tests revealed no particles larger than about 100μm present on any of the samples. (In the case of the Lundgren samples, the adhesive used on the substrates insures that none are lost.) Thus the validity of the application of the CCSEM technique to filter samples containing the large particles encountered in roadway emissions testing is highly questionable.

At the other end of the size spectrum, it is unlikely that the techniques used to remove the particles from the filters would be effective for removing individual small particles. Thus the bulk of the small particles removed would be in the form of agglomerates which would be counted as a lesser number of larger particles. This would have the effect of transferring mass from the fine particle end of the distribution to the midrange thereby depressing the fine particle end of the distribution and again steepening the apparent distribution. Manifestation of these potential problems can be illustrated using data taken during these tests. Six Lundgren runs were made with the impactors collocated with EEM profiler samplers. For these runs, the total particulate concentrations measured by the profilers and by the impactors were within 6% of each other on the average (range of 75% to 118%). At the same time, however, the average of the ratio of the fine particle concentration as measured by EEM/ETC to that measured by the impactors was only 18% (range 6% to 31%). At 10μm the average ratio of the EEM concentrations to those from the impactors was 72% (range of 32% to 109%).

Thus aside from the difficulties in estimating particle volumes and assigning aerodynamic diameters to irregular, inhomogenous particles of the types encountered here, there appear to be fundamental difficulties at both the large and small ends of the size spectrum in the CCSEM analyses of roadway emission samples. These problems render the CCSEM methodology, as used by the participants of this test, unsuitable for applications of this type.

Cyclone/Impactors

One of the primary advantages attributed to PEI's system and to the CCSEM particles sizing methodology is that the methods permit the particle size determinations to be made directly on the profiler samples. Thus the size distributions can be obtained at each height from a sample which was acquired isokinetically. The MRI methodology on the other hand provides data obtained directly on an aerodynamic basis using the well characterized and widely accepted techniques of inertial separation by cyclones and cascade impactors. The particle size cuts span the range over which data are needed with adequate resolution. However, MRI's data are obtained at only two heights (1.5m and 4.5m) from samples that are taken under only quasi-isokinetic conditions. The lack of true isokinetic sampling should constitute no real problem except for tests conducted under conditions of widely varying wind velocity. However, it would be desirable to have particle size data for at least one more height, say about 7m.

Although MRI measures the particle size distribution by a means for which the results are inherently on an aerodynamic basis, there are potential problems related to the operation of the actual hardware used. First, particle collection in the cyclone takes place in two distinct zones, the main body of the cyclone and the outlet tube. Particles caught in the main body are fully contained by the body cavity and cannot be transferred to succeeding parts of the sampler by jostling or vibration during and after sampling. However, a large part of what is considered by MRI to be the cyclone catch in reality collects on the wall of the exit tube and transform to the impactor. There is no way to insure that this material will remain in place during sampling or transport and cleanup after sampling. The cutoff diameter for the cyclone body catch is about 22μm at the nominal operating flow rate while the cutoff diame-

ter for the combination of the body and outlet tube is about 14μm. (These cut diameters are based on the results of recent recalibrations[11] that were performed on MRI's behalf and differ significantly from previously reported values.[12] The new calibrations would alter the results of PM_{15} and PM_{10} emissions which were reported in some of MRI's previous work.) If the combined body and outlet catches are used, as is MRI's practice, the possibility exists that some part of the catch will be dislodged and transferred from the plus 14 μm part of the size distribution defined by the cyclone to the 10μm to 14μm fraction collected by the first stage of the impactor. Uncertainties from this can be avoided by separate recovery of the material from the cyclone body and the outlet tube and treating the outlet tube catch as part of the catch of the first impaction stage.

A second area of potential concern in MRI's sizing methodology is related to their treatment of the impactor backup filter data. Particle bounce has long been a problem plaguing cascade impactor usage and the Sierra Model 235 is no exception in this regard. In developing their roadway emissions protocol, MRI tried a number of approaches, including greases on the collection substrates, the use of the inlet cyclone to reduce overloading and bounce problems at the first stage, and operation at reduced flow rate - approaches which had all proven useful in other cascade impactor operations in the past. Originally the Sierra impactor was quoted by the manufacturer as being usable at the standard hi-vol flow rate of 68 cubic meters per hour (40 cfm); however, it soon because apparent to MRI that particle bounce and blowoff were very real problems under those conditions.

At the time these problems were being resolved the complete five-stage impactor was being used. Because the principal error resulting from particle bounce is to transfer material which should be collected by the upper stages of the impactor to the backup filter, MRI began compensating for the effect of bounce by using the lesser of two weights for the backup filter catch. These weights being either the actual filter catch or the average of the catches of the two previous stages. The magnitude of the bounce errors were greatly reduced by adding the cyclone and dropping the sampling rate to 34 cubic meters per hour (20 cfm). But in spite of the reduction in the potential errors

arising from bounce with the revised procedures, the filter catch correction protocol continued to be used. This probably resulted in overcorrection and subsequently the introduction of a negative bias in the fine particle end of the size spectrum for tests carried out using the revised sampling procedures. A further change in operating protocol then greatly magnified the potential bias - MRI began to operate the impactor without the last two stages. Now the material which had been collected by the last two stages was also being passed to the filter, which reduced the relative magnitude of the bounce error still more, but the same correction procedure was being used. In this test series, MRI reverted to their old procedure of using all five impactor stages, although this was not the method described in their Current Procedures document.

Two valid Lundgren impactor runs were obtained collocated with the MRI impactors; for those the ratios of fine particle concentrations as calculated directly from the uncorrected MRI catch weights to those from the Lundgren were 1.01 and 1.14, respectively. Had MRI not used the last two impactor stages, as had become their normal practice, and then followed their data treatment protocol, the MRI fine particle concentrations would have been about half that of the Lundgren results. The same ratios for the results after correction, as reported by MRI, were somewhat higher than 0.5, (0.66 and 0.71), since the last two impactor stages were actually used in this test.

Finally, the method used by MRI for obtaining the fine particle, PM10, and TSP fractions is not the best available. MRI makes the assumption that the distribution is both unimodal and lognormal although extraneous sources and the nature of the road dust itself might result in the distributions being multimodal. They then use the percentage assigned to the backup filter and the percentage passed by the cyclone to fit a lognormal distribution to the data, ignoring any deviations from lognormality that might be indicated by the data from the remaining impactor stages. Thus as the data are currently handled, this fit is based entirely on the two most suspect values from the entire data set - the possibly erroneous or ficticious filter weight and the cyclone catch weight which currently includes the suspect outlet tube catch. The desired fractions for the size ranges of interest are then found from this two point lognormal fit.

PARTICLE SIZING RECOMMENDATIONS

The recommended procedure for measuring the particle size distribution is MRI's cyclone/impactor technique with some modifications. With regard to field operations.

With regard to field operations, first, a further reduction in the sampling flow rate from 20cfm to 15cfm would help minimize errors from particle bounce. Experience has shown that the product of jet velocities, V, and D50's of impactor stages must be limited to values below maximums which depend on the type of substrate used. If the jet velocities are expressed in meters per second and the D50's are expressed in micrometers, the limits for the product are 15μm•m/s for glass fiber substrates and 25μm m/s if adhesive coated substrates are used. Operation of the impactor at a flow rate of 20cfm results in V•/D50 products in excess of the limit for the glass substrates which are used. Operation at 15cfm reduces the products to acceptable values. Alternatively, adhesive coated substrates could be used at the current 20cfm flow rate. Second, potential errors resulting from the possible transfer of material from the outlet tube of the cyclone to the first stage of the impactor can be avoided by counting only the material collected in the body of the cyclone as its catch. The outlet tube catch would then be combined with that of the first impactor stage. At the current 20cfm flow rate, this would result in a cyclone D50 of 22μm being used rather than the current 14μm value. Lastly, while particle size was measured at the lower elevations (1.5m and 4.5m) an additional cyclone/impactor unit located at a height of about 7m would provide additional information regarding the changes in size distribution as a function of height within the dust plume.

With respect to data analysis, a better technique than the current MRI procedure would be that commonly used in reducing impactor data from industrial sources.[13,14] In the latter, a spline fit is made to the cyclone/impactor data in the cumulative percentage from of the distribution. The fit is made in a manner that requires continuity in the slope of the curve and the solution is

forced to be asymptotic to 100% at a diameter equal to the maximum diameter present in the sample. The fitted curve is then used to interpolate or extrapolate as needed to obtain the mass fractions in the selected size intervals. This technique avoids the requirement of assuming a functional form for the distribution and makes use of the complete data set rather than just two of the data points.

SECTION 6

EXPOSURES AND EMISSION FACTORS

Exposure is defined as the total incident particulate mass, in the selected size range, per unit area in a vertical plane parallel to the roadway. The integral of exposure versus height is thus equal to the particulate emissions per unit length of roadway during the test. The emission factor is obtained by dividing by the number of vehicles passing the sampler during the test. Accurate measurement of emission rates from the resuspension of road dust by vehicular traffic thus hinges on the exposure measurements and subsequent integrations.

METHODOLOGIES

All participants in the program, both during the methods review (Phase I) and the field test (Phase II), use variants of the profiling technique first developed by MRI[1]. However, there are several differences among the various organizations in the detailed manner with which the method is employed. Specific differences include the number of samplers employed, the heights at which exposures are measured, the approach used to obtain representative (isokinetic) samples, the method used to measure the background aerosol, the method used to integrate the exposure curves to obtain emission factors, and the method used to partition the emissions into the various particle size classes of interest. The following paragraphs discuss all of these differences except for those related to particle size. Discussions of particle sizing are contained in Section 5 of this report.

Sampling Isokineticity

All organizations involved in both phases of the study attempt, to varying extents, to perform the exposure sampling in an isokinetic fashion. USS and TRC use servo systems with individual velocity sensors at each sampling inlet to provide continuous adjustment of the flow rate for each sampler. EIA, EEM, and PEI sample at fixed flow rates which are set based on the wind velocity measured during a short time period immediately prior to the start of

sampling. EIA and PEI do alter sampling flows in the event of sustained gross changes in windspeed. The latter three organizations (EIA, EEM, and PEI) use a measured windspeed at a single height coupled with an assumed functional form for wind shear to obtain the velocities for setting the flow rates of the individual exposure samplers. Finally, MRI periodically adjusts the sampling flows based on an assumed logarithmic vertical windspeed distribution fit to measured speeds at two heights. Those organizations not using continuous individual servo controls to maintain isokinetic sampling flow rates correct their resulting exposure values by factors based on the mean inlet velocity for each sampler, the mean calculated windspeed at each sampling height, and the particle size distribution. Tests for which the ratio of mean sample inlet velocity to mean windspeed falls outside the range 0.8 to 1.3 are voided by all participants. The velocity ratio approximates the limit of the ratio of true exposure to measured exposure so the condition imposed insures that the errors caused by deviations from isokinetic sampling will be relatively small.

All organizations maintain the pointing angle of the sampler inlets no greater than 30 degrees from the mean wind direction (20 degree limits for EIA and EEM, and a 15 degree limit for PEI). No correction is made for the mean angle of the wind with respect to the road by any of the organizations. This causes a positive bias in the results proportional to the secant of the wind angle with respect to the road. At a 15 degree angle the error is 3 percent and at 45 degrees it increases to 40 percent. All of the testing organizations void tests in which the mean angle of the wind with respect to the road is greater than 45 degrees, so 40 percent is the greatest error which can be introduced by ignoring the angle factor.

Exposure Integration

Integration of the measured exposures for calculating emission rates are performed using the trapezoidal rule by EEM, PEI, and USS. EIA has also used this method in the past, but their Phase I current procedures documents suggested that in the future they would use a least squares fit of a half-gaussian distribution to the measured exposure profile. This procedure was proposed to eliminate difficulties in extrapolation of exposures near the ground and above

the height of the uppermost sampler on the profiler and to provide a completely objective method for defining and integrating the exposure profile. However, tests carried out by SoRI of this method using field data obtained during this program resulted in values of integrated exposures which were three to five times greater than those calculated using current procedures. TRC utilizes planimeter integration of a smooth spline fit to the data points (exposures) and MRI uses Simpson's rule with linear interpolation to provide any extra values needed.

In treating cases in which the measured exposures, after background correction, do not go to zero within the height spanned by the profiler, all but TRC used linear extrapolation from the two uppermost measurements to approximate the unmeasured top of the plume. TRC uses a "freehand" extension of the spline curve for extrapolation. No satisfactory method has been developed to cover the case in which the measured exposures at the upper end of the profiler increase with height. Extrapolations to the ground are made in a linear fashion based on the exposures measured at the two lowest heights by EEM and USS while TRC again uses a "freehand" extension of their spline curve. If the concentration gradient near the ground has a positive slope, USS uses a constant value of exposure equal to the exposure measured at the lowest height for the extrapolation. Both PEI and MRI use a constant value equal to the exposure at the lowest height for extrapolation to the ground in all cases. Integrated exposures calculated in the latter fashion will be lower than those from the former by amounts which depend on the steepness of the concentration gradient between the two lowest samplers. The differences in the field results obtained in this program using each integration method on all sets of exposure data ranged from about 2% to 12% with an average difference of about 4%. Therefore it was concluded that the method of integration will usually have little effect on the results. However, significant differences could occur if the exposure gradient was very steep (or exhibited a maximum) between the two lowest heights of the profiler. This appears to have been the case in this test series for at least one testing party (TRC).

FIELD TEST RESULTS

The results obtained by the five sampling organizations during the five-day field comparison are summarized in Table 3. As shown in this table eleven separate tests were carried out to characterize the emissions from the simulated unpaved road. Rotation of the testing parties through the sample locations was carried out on a daily basis as seen in columns 2 and 3. Data in columns 6 through 18 were extracted from the Field Comparison Final Reports produced by each of the five testing companies. As seen in these entries, some test parameters were either not measured or not explicitly reported by the various organizations. Some of the data variations between contractors for a given test are explained by the fact that occasionally some of the testing parties were late in starting and stopping their profiler systems and consequently sampled over either a different number and/or type of vehicle passes. Also there were some variations reported in the vehicle weight estimates, but these differences were not significant.

In column 24 of Table 3, the values of particulate concentrations obtained with standard high volume samplers are tabulated. In obtaining these data, standard hi-vol samplers were placed at each sample location. These samplers were not rotated with the sampling parties and served as monitors of the changes that took place throughout the test for each sampling location.

Total Particulate Emission Factors

Of the five field test participants, four purportedly measure total particulate emission factors while the fifth, PEI, normally measures only the fraction nominally smaller than 30 μm. The average total emission factors for the complete test series are summarized in Table 4. For the four contractors whose methods normally provide total emission factors, the average values were 8.34, 8.25, 8.41, and 5.73 kg/VKT. The last value (5.73 kg/VKT) is significantly different from the other three at the 90% confidence level. TRC, whose data produced that result, stated in their report that their values were generated from profiler filter catches only and did not include nozzle and inlet washes. Although the omission of the latter material could explain the

Table 3. COMPARATIVE FUGITIVE EMISSION TEST RESULTS.

TEST NUMBER	TEST DATE	SITE LOCAT.	TEST ORGAN-IZATION	On Win side (1=N) (2=S)	WIND SPEED (4ft) (M/S)	WIND DIRECTION (degN)	WIND STD. DEV. (M/S)	AMB. TEMP (degF)	AMB. HUMID. (%)	ROAD SILT FRACTION <45um (%)	ROAD SILT FRACTION 45-75um (%)	ROAD SILT FRACTION <75um (%)	SOIL MOISTURE (%)	AVE. NO. WHEELS	AVE. SPEED (KPH)	AVE. WEIGHT (MG)	NUMBER OF VEHICLE PASSES	EMISSION FACTORS TP <100um (KG/VKT)	EMISSION FACTORS TSP (KG/VKT)	EMISSION FACTORS PM10	EMISSION FACTORS PM15	EMISSION FACTORS FP PM2.5	HI-VOL TSP (ug/m3)
1	6/11/4	1	PEI	2	2.42			67	70			4.3	2.9	12.1	34.4	22.8	40		2.03			1.2	0.49	13601.3
1	"	2	USS	2	3.34	22		84				14.5		12.8	35.9	16.4	41	8.56	6.93	3.74	2.50	0.24	17569.3
1	"	3	MRI	2	2.8			64				11.1		12.0	30	20.0	40	9.33	3.69	2.65	2.02	0.618	16202.7
1	"	4	EEN	2	2.90	348	4.96	72	49	5.2	12.2	17.4	1.0	12.1	34.4	19.2	40	10.24	8.09	4.09	2.46	0.31	8548.5
1	"	5	TRC	2	2.97			64.2				8.17		12.1	34.41	20.7	40	7.11	6.53	3.63	2.17	0.20	11118.0
2	"	1	PEI	2	2.91			67	70			4.3	2.9	5.1	37.5	7.0	30		0.86			0.5	0.16	4256.4
2	"	2	USS	2	4.01	41		84				14.5		6.1	33.3	9.3	30	5.29	3.60	1.76	1.06	0.11	3308.5
2	"	3	MRI	2	2.8			64				11.1		5.2	32	7.0	31	4.26	1.82	1.12	0.860	0.274	4938.8
2	"	4	EEN	2	3.62	340	2.46	73	49	5.2	12.2	17.4	1.0	5.1	37.5	11.1	30	6.32	5.15	2.61	1.56	0.20	2121.7
2	"	5	TRC	2	3.71			66.4				8.17		5.13	37.54	11.7	30	4.29	3.97	2.23	1.34	0.12	4468.2
3	6/12/4	1	TRC	1	4.11			87.5				12.26		13.46	32.57	26.0	41	6.67	6.18	3.51	2.12	0.19	21184.8
3	"	2	PEI	1	3.58			87	58			3.9	5.4	13.75	32.2	25.1	40		3.45		1.8	0.45	14266.4
3	"	3	USS	1	4.56	190		90				16.0		13.0	28.8	18.2	41	9.20	8.28	4.53	2.95	0.26	0.0
3	"	4	MRI	1	3.4			80				10.6		14.0	31	26.0	41	12.2	4.57	2.96	2.23	0.713	28160.2
3	"	5	EEN	1	3.68	188	5.59	92	60	9.0	12.0	21.0	1.5	13.7	32.8	23.5	40	11.30	8.93	4.52	2.71	0.34	18790.7
4	"	1	TRC	1	5.28			92.1				12.26		13.1	37.54	20.2	42	8.80	8.10	4.58	2.77	0.25	24104.2
4	"	2	PEI	1	4.43			87	58			3.9	5.4	13.0	34.2	23.8	42		2.18		1.0	0.18	11605.7
4	"	3	USS	1	5.26	177		90				16.0		12.8	33.8	20.1	40	15.92	14.14	6.96	4.39	0.79	18713.4
4	"	4	MRI	1	4.1			80				10.6		13.0	32	24.0	41	15.9	7.13	4.82	3.75	1.23	29105.6
4	"	5	EEN	1	4.74	194	3.04	94	53	9.0	12.0	21.0	1.5	13.1	37.5	23.0	42	11.24	8.88	4.50	2.70	0.34	20080.4
5	"	1	TRC	1	4.72			98.1				12.26		4.71	43.11	6.67	42	5.90	5.38	3.04	1.84	0.17	9979.5
5	"	2	PEI	1	5.14			87	58			3.9	5.4	4.7	43.1	6.4	42		2.50		0.8	0.02	6834.7
5	"	3	USS	1	4.01	239		94				16.0		4.6	34.1	5.9	41	4.84	4.15	2.39	1.60	0.17	8358.8
5	"	4	MRI	1	4.0			80				10.6		4.7	32	6.4	42	2.54	1.75	1.39	1.14	0.431	9487.3
5	"	5	EEN	1	5.54	225	6.79	95	50	9.0	12.0	21.0	1.5	4.7	43.1	5.7	42	5.00	3.95	2.00	1.20	0.15	8761.8
6	6/13/4	1	EEN	1	2.41	221	6.26	87	62	10.8	5.0	15.8	1.5	14.0	35.7	24.0	46	5.49	4.34	2.20	1.32	0.16	7516.3
6	"	2	TRC	1	2.39			95.8				13.69		14.04	35.52	26.1	46	4.40	4.09	2.43	1.51	0.14	13084.6
6	"	3	PEI	1	2.59			90	56			10.8	3.2	14.0	35.5	25.8	43		3.24		1.8	0.58	23599.5
6	"	4	USS	1	2.90	220		90				16.0		14.0	30.6	19.0	46	7.79	6.94	4.37	2.94	0.34	14542.1
6	"	5	MRI	1	2.4			73				11.0		14.0	28	26.0	42	11.5	5.05	3.38	2.64	0.877	26176.1
7	"	1	EEN	1	2.46	256	3.31	88	78	10.8	5.0	15.8	1.5	15.9	35.7	29.4	41	11.58	9.14	4.63	2.78	0.35	12351.1
7	"	2	TRC	1	2.26			94.4				13.69		15.8	35.73	31.7	41	5.85	5.27	2.87	1.71	0.15	16184.0
7	"	3	PEI	1	2.95			90	56			10.8	3.2	15.8	35.7	30.8	41		4.11		2.1	0.60	21810.0
7	"	4	USS	1	2.80	227		94				16.0		15.5	31.0	22.0	40	12.28	10.01	6.19	3.49	0.45	22451.7
7	"	5	MRI	1	2.1			73				11.0		16.0	29	30.0	40	7.16	4.06	2.90	2.29	0.750	22080.8
8	6/14/4	1	MRI	2	4.9			59				6.9		15.0	40	28.0	67	6.26	1.99	1.33	1.03	0.352	8886.1
8	"	2	EEN	2	4.38	346	3.31	64	67	2.8	7.9	10.7	0.4	14.6	38.5	27.6	61	7.46	5.82	3.28	1.57	0.11	1647.0
8	"	3	TRC	2	4.93			59.1				6.92		14.62	38.38	29.4	61	4.54	4.16	2.31	1.38	0.12	9616.6
8	"	4	PEI	2	4.12			59	78			4.5	7.0	14.6	38.4	28.9	61	7.818	1.64		0.9	0.27	0.0
8	"	5	USS	2	5.05	344		70				11.7		14.1	32.6	21.5	62	6.59	5.79	3.06	1.86	0.17	2993.1
9	"	1	MRI	2	5.4			59				6.9		5.6	32	8.2	50	6.06	2.26	1.19	0.922	0.327	4205.6
9	"	2	EEN	2	4.78	340	2.50	57	62	2.8	7.9	10.7	0.4	5.6	42.3	6.2	51	5.71	4.45	2.51	1.20	0.09	7542.0
9	"	3	TRC	2	4.93			60.9				6.92		5.65	42.28	9.6	51	4.06	3.70	2.04	1.21	0.11	6835.3
9	"	4	PEI	2	4.12			59	78			4.5	7.0	5.6	42.1	8.4	51	4.168	1.29		0.5	0.04	2087.1
9	"	5	USS	2	5.65	346		75				11.7		5.7	36.0	5.8	49	4.19	3.18	1.68	0.96	0.05	4000.1
10	"	1	MRI	2	6.5			59				6.9		6.3	32	9.8	50	6.88	2.88	2.02	1.58	0.524	7255.4
10	"	2	EEN	2	5.63	341	2.32	57	62	2.8	7.9	10.7	0.4	6.3	45.1	7.2	50	9.06	7.07	3.99	1.90	0.16	11660.2
10	"	3	TRC	2	5.16			60.9				6.92		6.28	45.06	11.4	50	5.65	5.15	2.83	1.69	0.15	7972.6
10	"	4	PEI	2	4.12			59	78			4.5	7.0	6.3	45.0	10.2	50	5.568	2.02		1.0	0.18	3542.1
10	"	5	USS	2	6.82	333		70				11.7		6.1	39.2	7.6	50	8.22	6.46	3.95	2.71	0.40	7046.1
11	6/15/4	1	USS	2	3.13	23		74				11.0		14.3	29.1	19.3	39	9.61	8.26	5.77	3.76	0.49	26701.5
11	"	2	MRI	2	2.7			60				10.3		15.0	26	29.0	39	8.68	4.17	2.88	2.20	0.623	46984.5
11	"	3	EEN	2	1.61	353	2.14	63	75	1.7	4.7	6.4	0.2	14.7	34.0	26.8	40	8.16	6.36	3.39	1.71	0.12	21283.8
11	"	4	TRC	2	2.59			62.9				6.39		14.7	34.00	29.1	40	5.74	5.28	2.92	1.74	0.16	6855.8
11	"	5	PEI	2	1.60			65	85			6.0	15.2	14.7	34.0	28.9	40		2.52		1.2	0.29	21675.5

a This value calculated b SoRI

TABLE 4. AVERAGE EMISSION FACTORS OBTAINED BY EACH ORGANIZATION

	Organization					
	EEM	MRI	TRC	USS	PEI	All
TP All Tests						
Mean (kg/VKT)	8.34	8.25	5.73	8.41	--	7.68
Std. deviation	2.49	3.83	1.43	3.43	--	1.30
TP Tests 8,9,10 only						
Mean (kg/VKT)	7.4	6.4	4.8	6.3	5.8	6.15*
Std. deviation	1.7	0.4	0.8	2.0	1.8	1.55
TSP All Tests						
Mean (kg/VKT)	6.56	3.58	5.26	7.07	2.37	4.97
Std. deviation	1.98	1.66	1.31	3.15	0.99	1.98
PM_{10} All Tests						
Mean (kg/VKT)	1.92	1.88	1.77	2.57	1.16	1.86
Std. deviation	0.63	0.88	0.45	1.10	0.53	0.50
FP All Tests						
Mean (kg/VKT)	0.21	0.61	0.16	0.32	0.30	0.32
Std. deviation	0.10	0.28	0.04	0.21	0.21	0.17

* Average includes PEI's value.

low values, USS, using a virtually identical profiling system, also did not include nozzle and inlet losses and their results produced the highest of the four averages, making the omission of the washes by TRC less likely as the explanation of their low values.

Since PEI did not ordinarily measure TP they are excluded from the first row of averages shown in Table 4. However, at the request of SoRI, the inlet nozzles and screens of PEI's profiler were washed in three of the tests (8, 9, 10) to provide a limited basis of comparison of their results with those of the remaining contractors. For those tests, PEI's total emission factors averaged 5.8 kg/VKT while those of the others averaged 7.4, 6.4, 4.8, and 6.3 kg/VKT, shown in Table 4. Thus we have no reason to believe that PEI's system would produce values which differed from those of the other contractors if total emission factors were desired.

A histogram of the total emission factor results is shown in Figure 26. In general, the values reported for the total particulate emission factor are well correlated with correlation coefficients among the four sets of data ranging from 0.584 to 0.802. The correlation matrix for the reported emission factors is tabulated in Table 5.

Individual test results in terms of exposures versus height are tabulated for each contractor in Table 6. Plots of exposure versus height are given for the combined data in Figures 27 through 37. Again it can be seen that the results of the various participants are in reasonable agreement in terms of the total exposure data. It is worth noting that the maximum value of the exposure was almost always measured at a height of 1.5 to 2.0 meters. Three of the four test participants who normally measure the total emission factor had a sampler in that range of heights, TRC being the exception. If a profiling system does not have a sampler located at or near the height at which the exposure is greatest, the resulting integrated exposure will be systematically low. This may have been a contributing factor in TRC's low values for the emission factors.

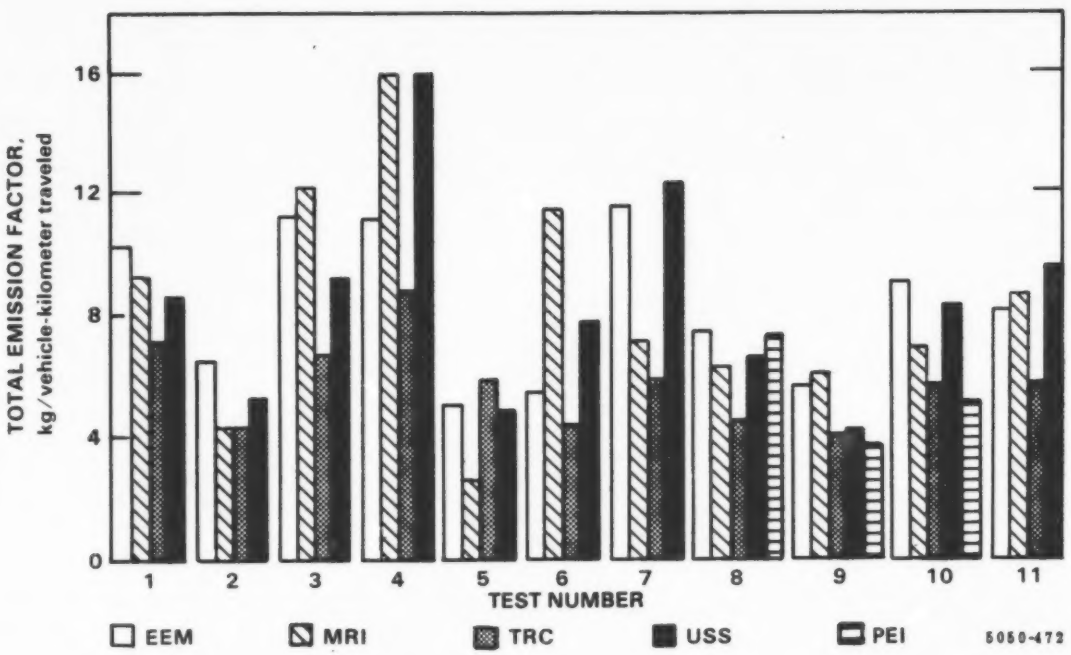

Figure 26. Total particulate emission factors by test as measured by each organization.

TABLE 5. CORRELATION COEFFICIENTS OF TP, TSP, PM_{10}, AND FP EMISSION FACTORS REPORTED BY TEST PARTICIPANTS

	TP					TSP (<30 μm)				
	USS	MRI	EEM	TRC	PEI	USS	MRI	EEM	TRC	PEI
USS	-	.770	.802	.787	-	-	.904	.772	.795	.504
MRI	.770	-	.584	.645	-	.904	-	.594	.705	.490
EEM	.802	.584	-	.728	-	.772	.594	-	.728	.486
TRC	.787	.645	.728	-	-	.795	.705	.728	-	.286
PEI	-	-	-	-	-	.504	.490	.464	.286	-

	PM_{10} (<10 μm)					F.P. (<2.5 μm)				
USS	-	.915	.669	.703	.625	-	.865	.472	.703	.224
MRI	.915	-	.636	.780	.566	.865	-	.612	.764	.434
EEM	.669	.636	-	.718	.564	.472	.612	-	.700	.520
TRC	.703	.780	.718	-	.251	.703	.764	.700	-	.124
PEI	.625	.566	.564	.251	-	.224	.434	.520	.124	-

TABLE 6. EXPOSURE AND EMISSION VALUES BY TEST NUMBER AND ORGANIZATION

EXPOSURE, mg/cm^2

	1					2				
ORGANIZATION	PEI	USS	MRI	EEM	TRC	PEI	USS	MRI	EEM	TRC
POSITION	1	2	3	4	5	1	2	3	4	5
HEIGHT, m										
10									0.05	
9		0.29		0.35	-0.10		0.11			-0.05
8				0.16					0.46	
7.5			0.30					0.06		
7					0.64					0.33
6.5		1.11					0.43			
6			1.45	1.98				0.39	1.10	
5					3.31					0.95
4.5		4.95	4.25				1.70	1.14		
4				5.15					2.89	
3			6.19		5.10			2.26		2.06
2.5										
2		6.35		7.61			3.15		3.37	
1.5			8.12					3.22		
1					5.21					2.99
Reported Emission Factor, kg/VKT		8.56	9.33	10.24	7.11		5.29	4.26	6.52	4.29
SoRI Emission Factor, kg/VKT		8.16	8.82	9.31	7.26		4.85	4.05	6.21	4.30

NOTE: SoRI Emission Factor is from integration by the trapezoidal rule with linear extrapolation to zero at the top of the profiler and constant exposure from the lowest height to the ground.

TABLE 6. (continued)

EXPOSURE, mg/cm^2

TEST	3					4				
ORGANIZATION	TRC	PEI	USS	MRI	EEM	TRC	PEI	USS	MRI	EEM
POSITION	1	2	3	4	5	1	2	3	4	5
HEIGHT, m										
10					0.21					0.58
9	-0.06		0.41			0.21		0.59		
8					0.93					1.58
7.5				1.01					1.50	
7	0.43					1.28				
6.5			1.24					2.45		
6				(3.1)	2.35				3.57	2.77
5	2.53					3.93				
4.5			5.01	5.23				7.93	6.52	
4					4.42					6.57
3	4.53			9.88		4.50			11.50	
2.5										
2			6.88		8.48			11.74		7.75
1.5				9.89					13.50	
1	6.02					8.18				
Reported mission Factor, kg/VKT	6.67		9.20	12.20	11.30	8.80		15.92	15.90	11.20
SoRI Emission Factor, kg/VKT	6.61		8.98	12.57	9.94	8.41		15.50	15.81	18.94

NOTE: SoRI Emission Factor is from integration by the trapezoidal rule with linear extrapolation to zero at the top of the profiler and constant exposure from the lowest height to the ground.

TABLE 6. (continued)

EXPOSURE, mg/cm^2

TEST	5					6				
ORGANIZATION	TRC	PEI	USS	MRI	EEM	EEM	TRC	PEI	USS	MRI
POSITION	1	2	3	4	5	1	2	3	4	5
HEIGHT, m										
10					0.43	0.45				
9	0.34		0.42				-0.32		1.10	
8					0.71	1.06				
7.5				1.14						3.46
7	1.02						0.57			
6.5			1.09						2.04	
6				0.78	1.44	2.15				4.04
5	2.56						2.19			
4.5			2.08	1.21					4.32	6.00
4					2.20	3.15				
3	3.92			2.15			3.11			6.49
2.5										
2			3.51		3.35	3.72			5.67	
1.5				0.60						5.08
1	4.49						4.22			
Reported mission Factor, kg/VKT	5.90		4.84	2.54	5.00	5.49	4.40		7.79	11.50
SoRI Emission Factor, kg/VKT	5.65		4.56	3.73	4.40	5.13	4.46		7.28	10.24

NOTE: SoRI Emission Factor is from integration by the trapezoidal rule with linear extrapolation to zero at the top of the profiler and constant exposure from the lowest height to the ground.

TABLE 6. (continued)

EXPOSURE, mg/cm^2

TEST	7					8				
ORGANIZATION	EEM	TRC	PEI	USS	MRI	MRI	EEM	TRC	PEI	USS
POSITION	1	2	3	4	5	1	2	3	4	5
HEIGHT, m										
10	0.88						0.03			
9		0.62		1.89				0.15	2.41	0.74
8	1.46						0.47			
7.5					2.33	0.55				
7		1.40						0.98		
6.5				2.97						2.03
6	2.78				2.91	1.73	2.54			
5		2.20						2.74	4.46	
4.5				5.03	3.56	4.44				5.21
4	5.71						5.89			
3		3.29			5.77	7.73		4.40		
2.5									3.36	
2	7.76			7.49			8.39			6.99
1.5					2.35	8.89				
1		4.18						5.50	10.40	
Reported Emission Factor, kg/VKT	11.58	5.85		12.28	7.16	6.26	7.46	4.54	7.81	6.59
SoRI Emission Factor, kg/VKT	10.80	5.64		11.44	7.30	6.89	7.05	4.49	7.47	6.60

NOTE: SoRI Emission Factor is from integration by the trapezoidal rule with linear extrapolation to zero at the top of the profiler and constant exposure from the lowest height to the ground.

TABLE 6. (continued)

EXPOSURE, mg/cm^2

TEST	9					10				
ORGANIZATION	MRI	EEM	TRC	PEI	USS	MRI	EEM	TRC	PEI	USS
POSITION	1	2	3	4	5	1	2	3	4	5
HEIGHT, M										
10		0.14					0.08			
9			0.10	0.81	0.22			0.42	1.01	0.72
8		0.25					0.67			
7.5	0.40					0.40				
7			0.79					1.06		
6.5					1.07					2.65
6	2.50	1.35				2.50	2.95			
5			2.49	2.78				2.82	2.53	
4.5	3.58				2.74	3.78				5.34
4		3.05					6.39			
3	5.88		3.42			5.88		4.16		
2.5				3.61					5.19	
2		5.63			3.53		7.88			6.69
1.5	6.99					6.99				
1			3.57	5.23				5.45	5.23	
Reported Emission Factor, KG/VKT	6.06	5.71	4.06	4.16	4.19	6.88	9.06	5.65	5.56	8.22
SoRI Emission Factor, KG/VKT	6.81	5.18	4.00	5.44	4.11	6.87	8.79	5.47	5.90	7.55

NOTE: SoRI Emission Factor is from integration by the trapezoidal rule with linear extrapolation to zero at the top of the profiler and constant exposure from the lowest height to the ground.

TABLE 6. (continued)

EXPOSURE, mg/cm^2

TEST	11				
ORGANIZATION	USS	MRI	EEM	TRC	PEI
POSITION	1	2	3	4	5
HEIGHT,m					
10			0.08		
9	0.39			0.11	
8			0.64		
7.5		0.74			
7				0.83	
6.5	1.24				
6		2.40	2.06		
5				1.95	
4.5	4.35	5.19			
4			3.69		
3		6.52		3.72	
2.5					
2	7.14		5.86		
1.5		5.32			
1				4.78	
Reported Emission Factor, kg/VKT	9.61	8.68	8.16	5.74	
SoRI Emission Factor, kg/VKT	8.87	8.36	7.29	5.40	

NOTE: SoRI Emission Factor is from integration by the trapezoidal rule with linear extrapolation to zero at the top of the profiler and constant exposure from the lowest height to the ground.

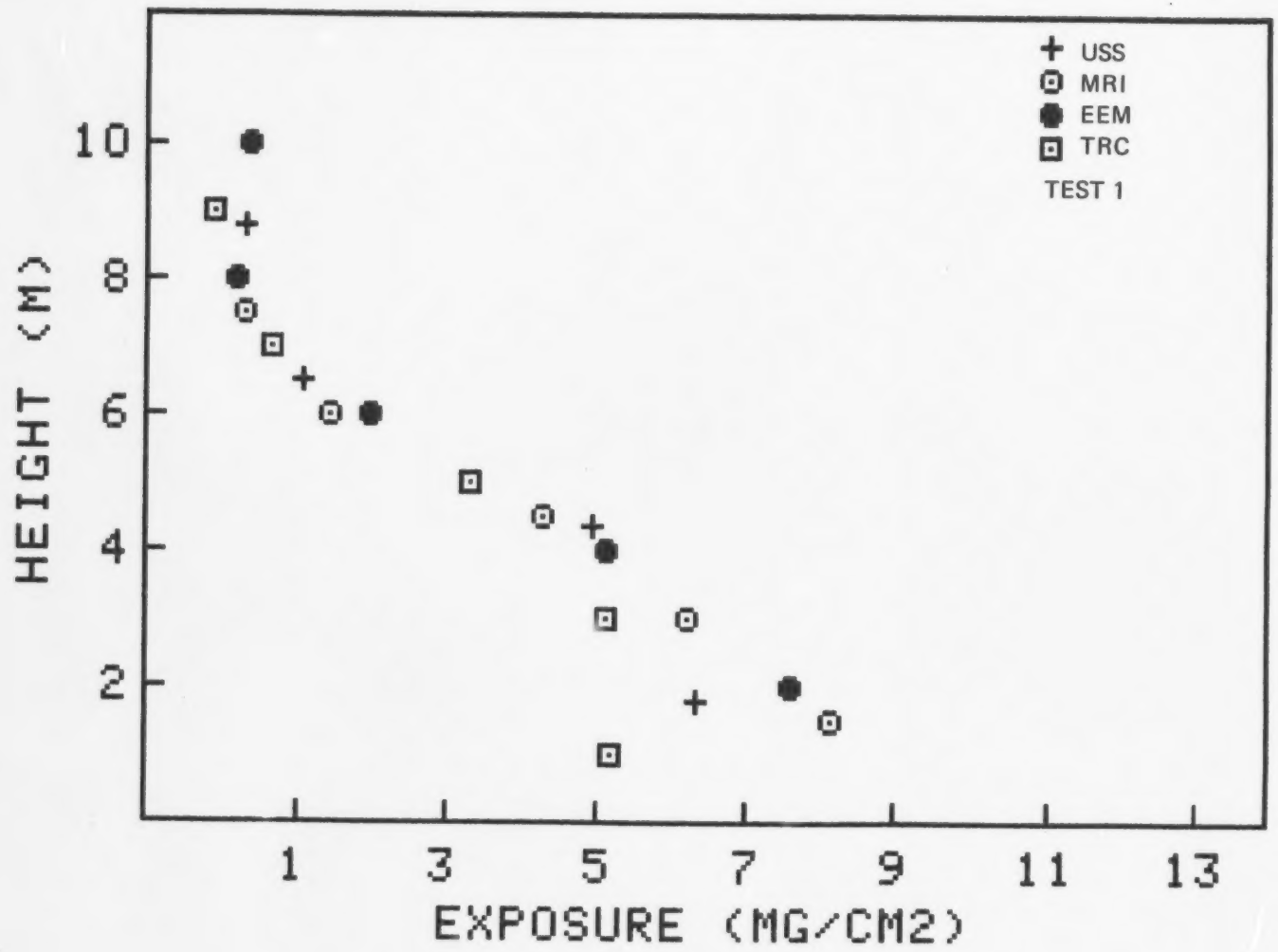

Figure 27. Measured total exposures versus height for Test 1 for all contractors providing total particulate exposure data.

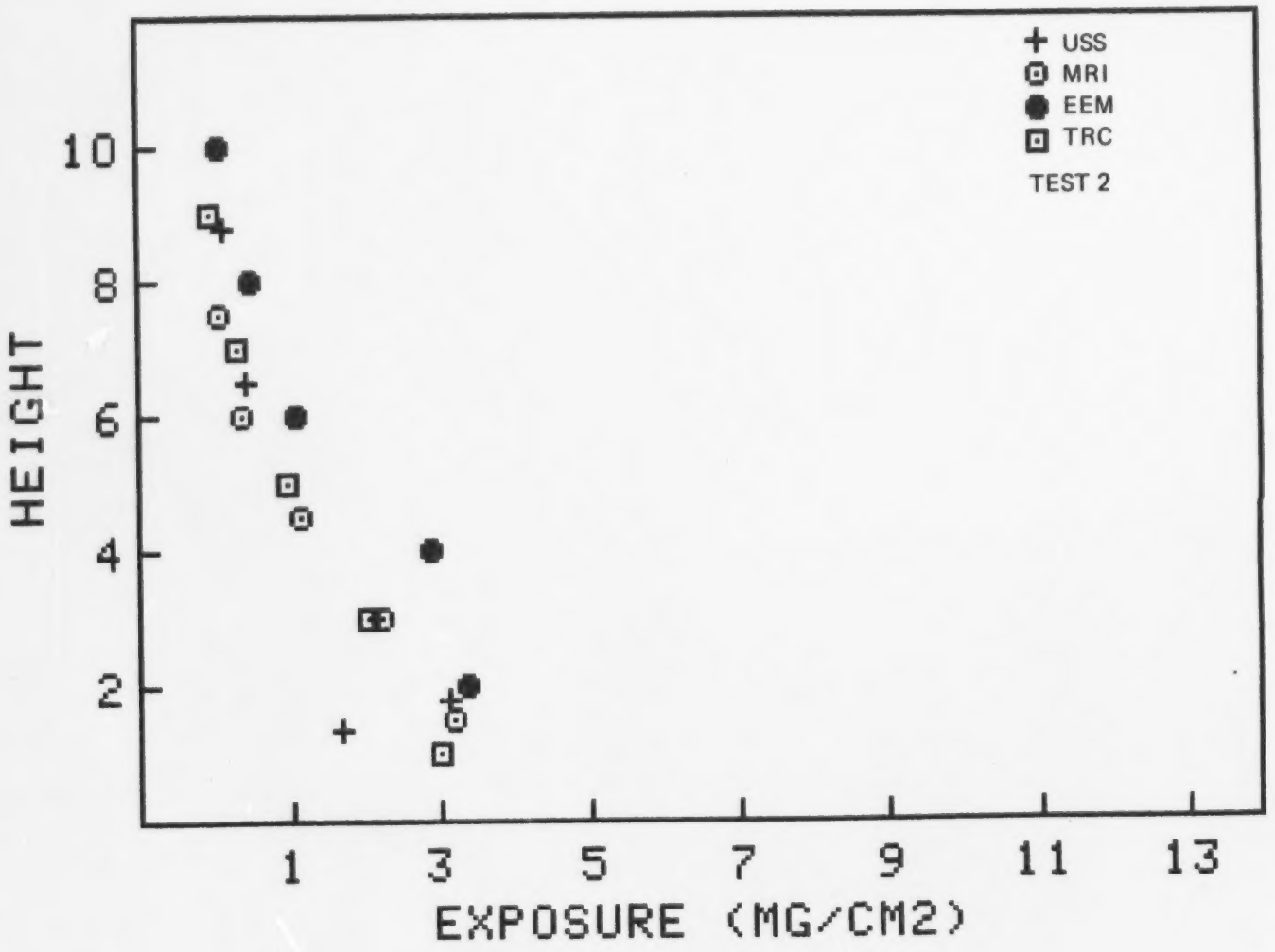

Figure 28. Measured total exposures versus height for Test 2 for all contractors providing total particulate exposure data.

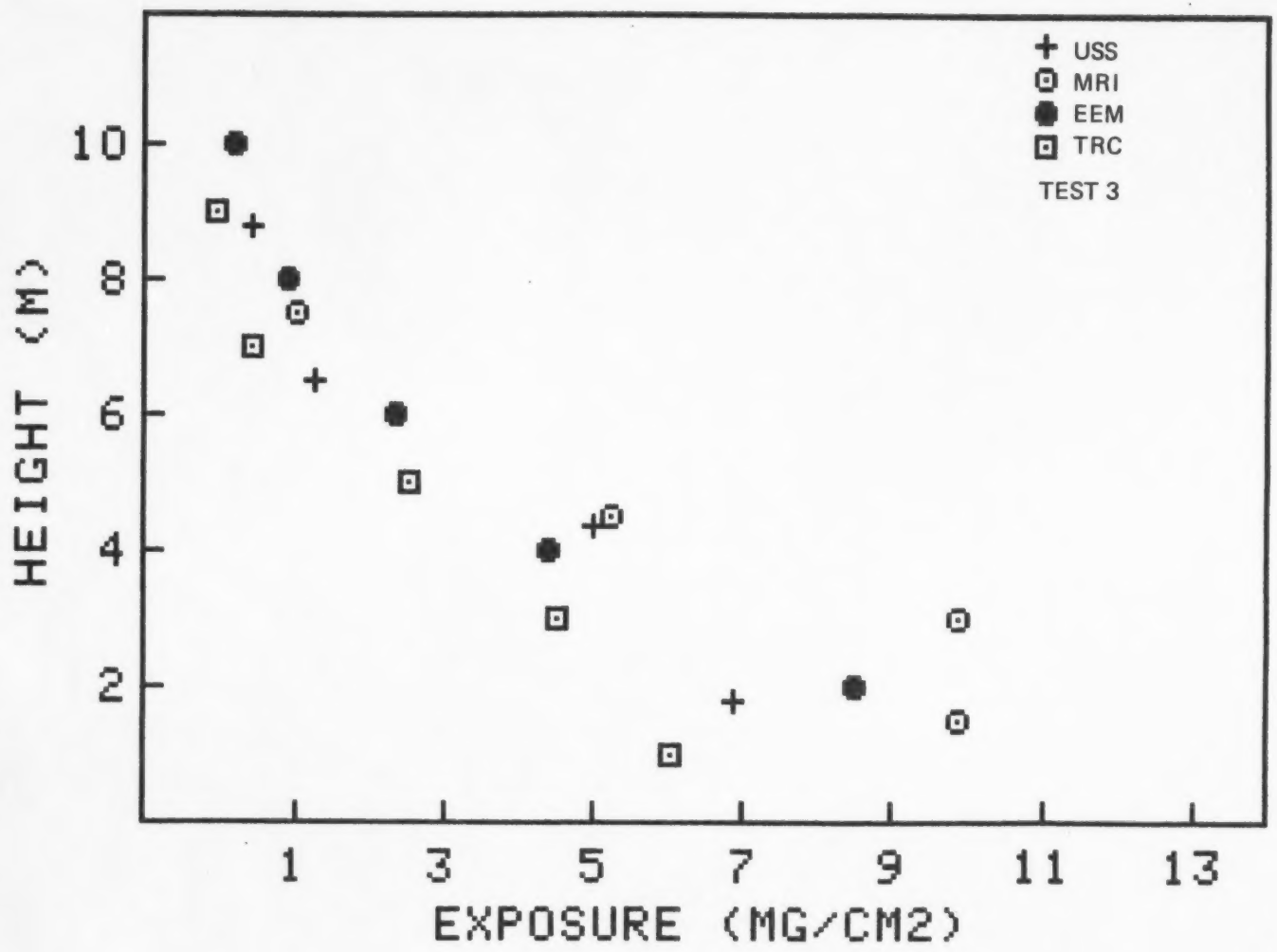

Figure 29. Measured total exposures versus height for Test 3 for all contractors providing total particulate exposure data.

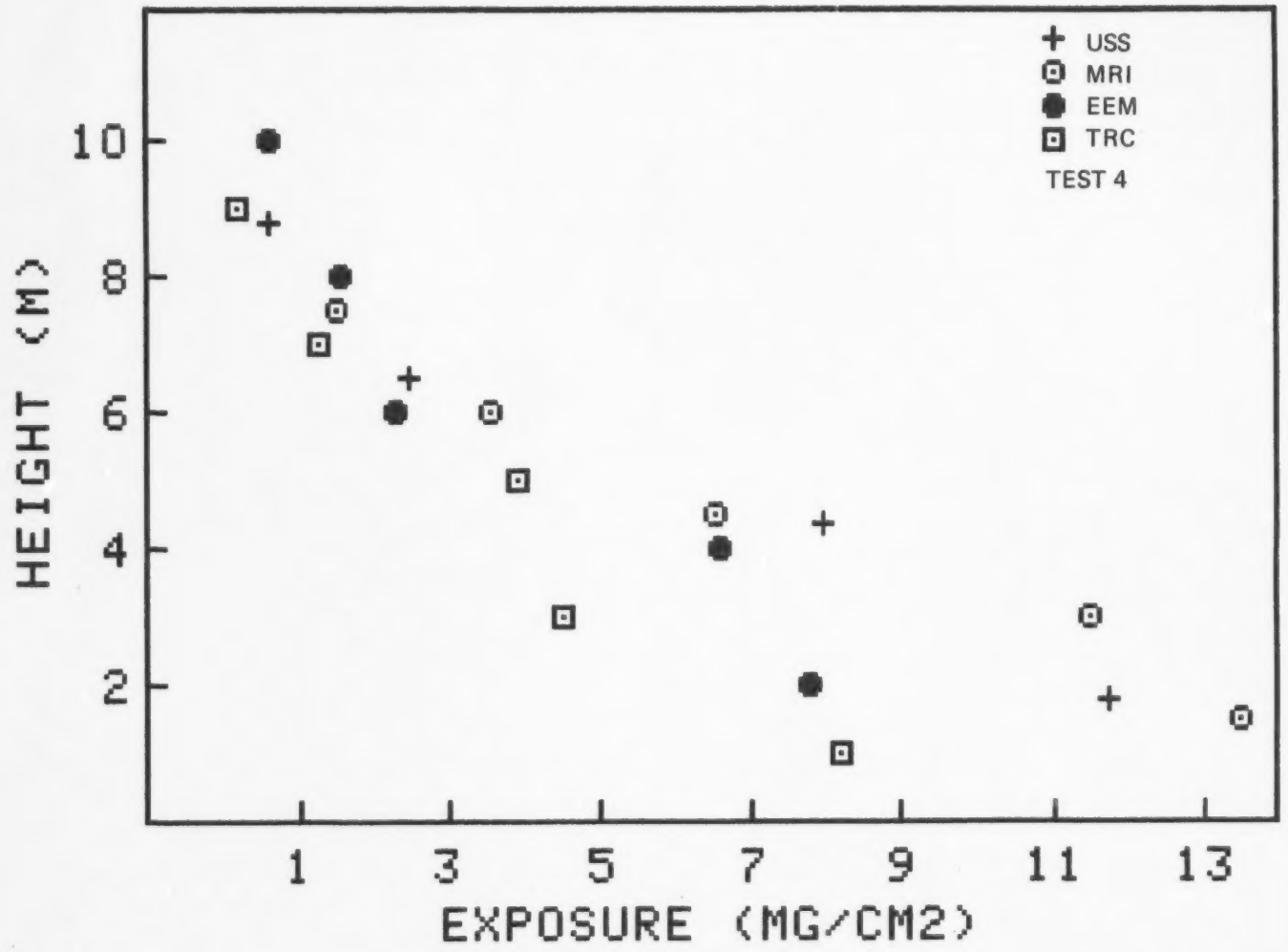

Figure 30. Measured total exposures versus height for Test 4 for all contractors providing total particulate exposure data.

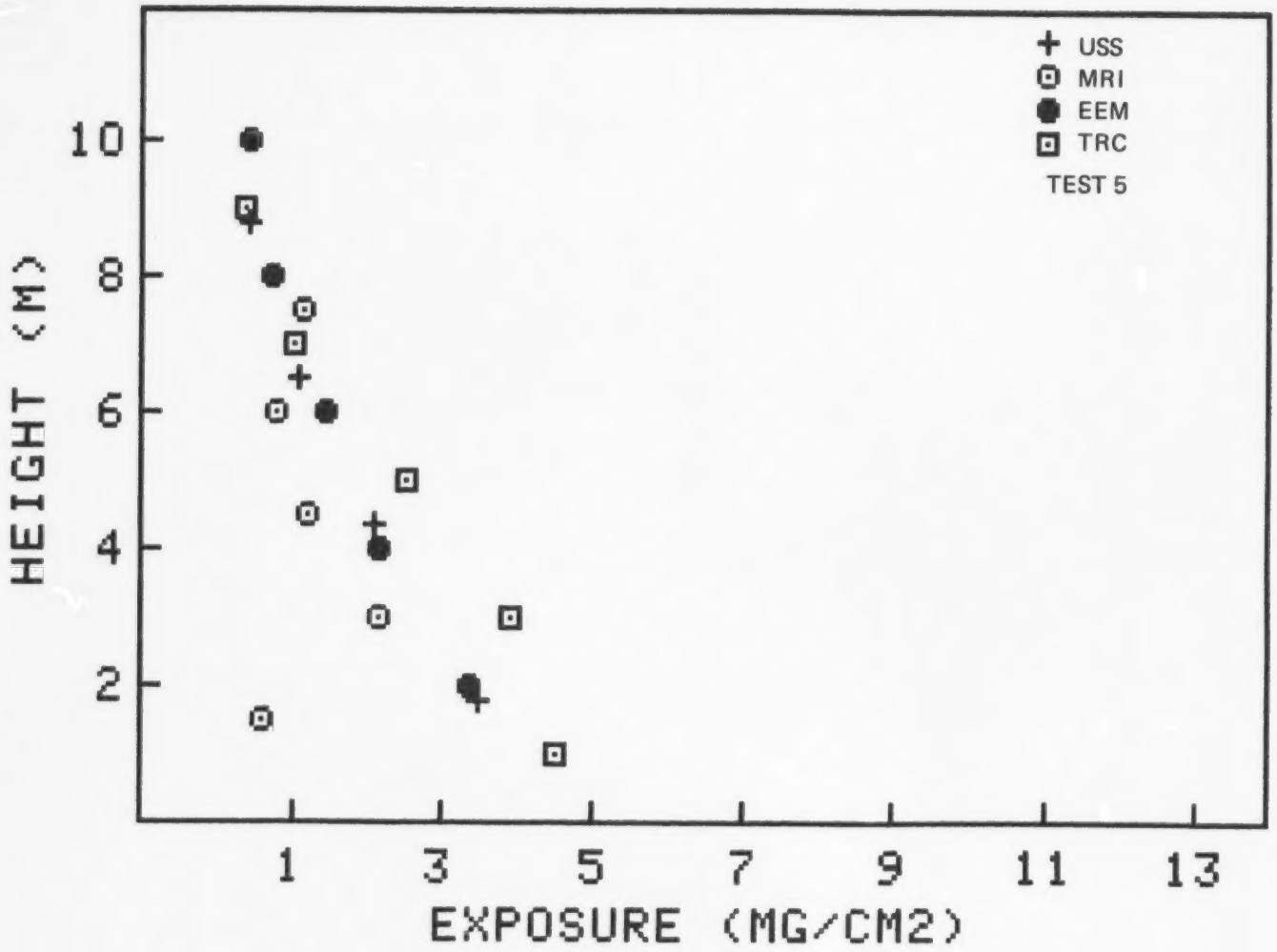

Figure 31. Measured total exposures versus height for Test 5 for all contractors providing total particulate exposure data.

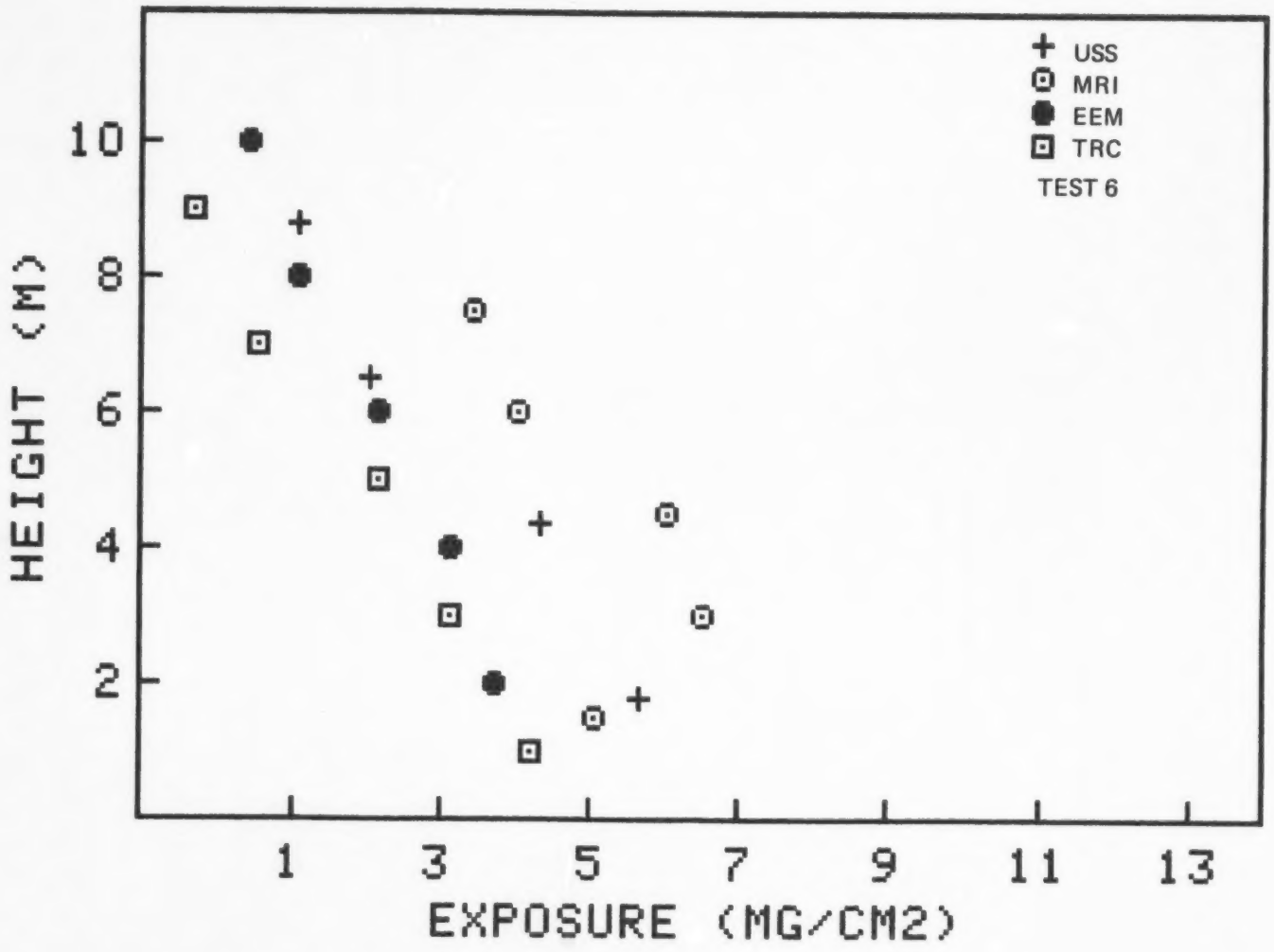

Figure 32. Measured total exposures versus height for Test 6 for all contractors providing total particulate exposure data.

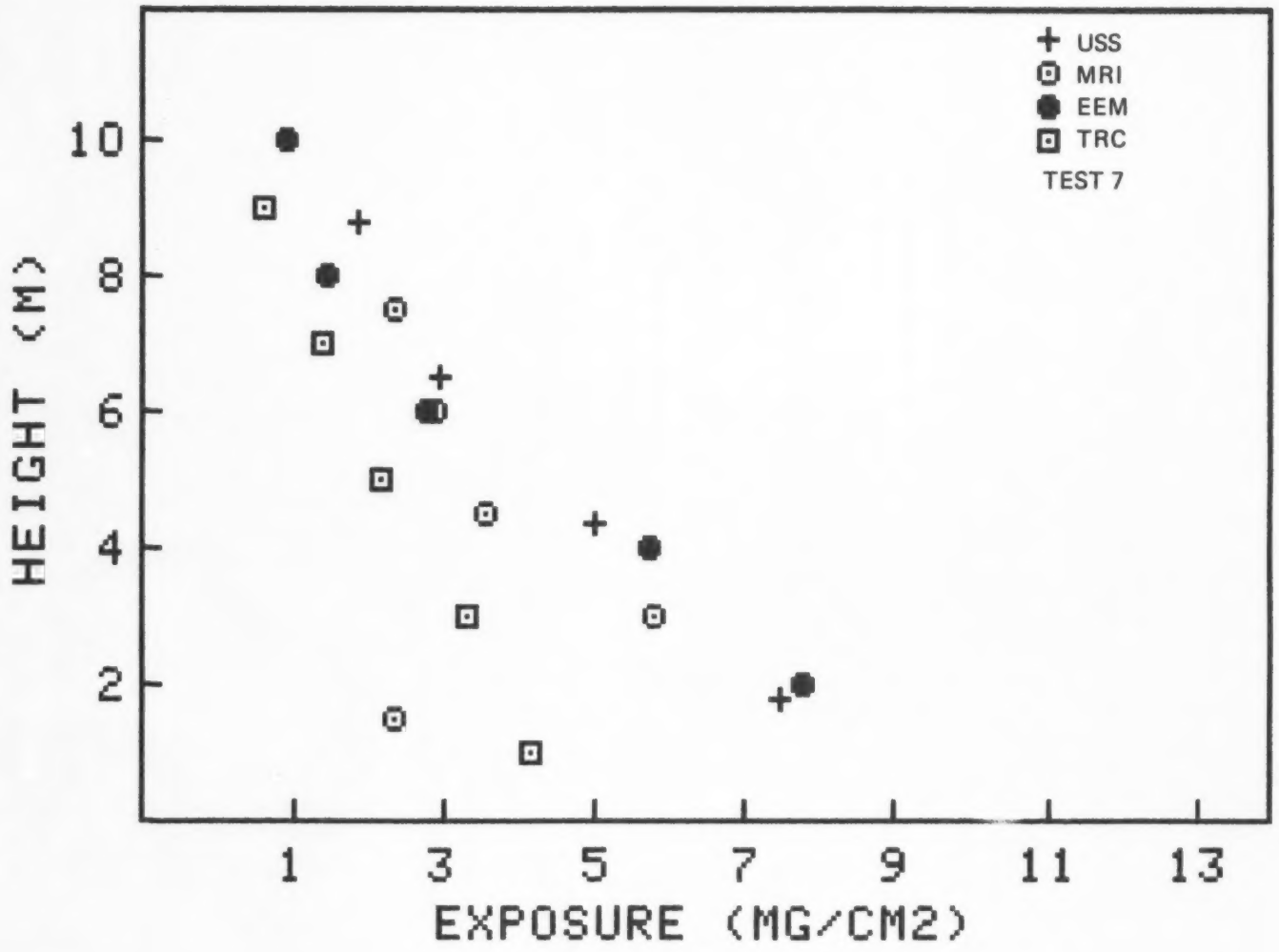

Figure 33. Measured total exposures versus height for Test 7 for all contractors providing total particulate exposure data.

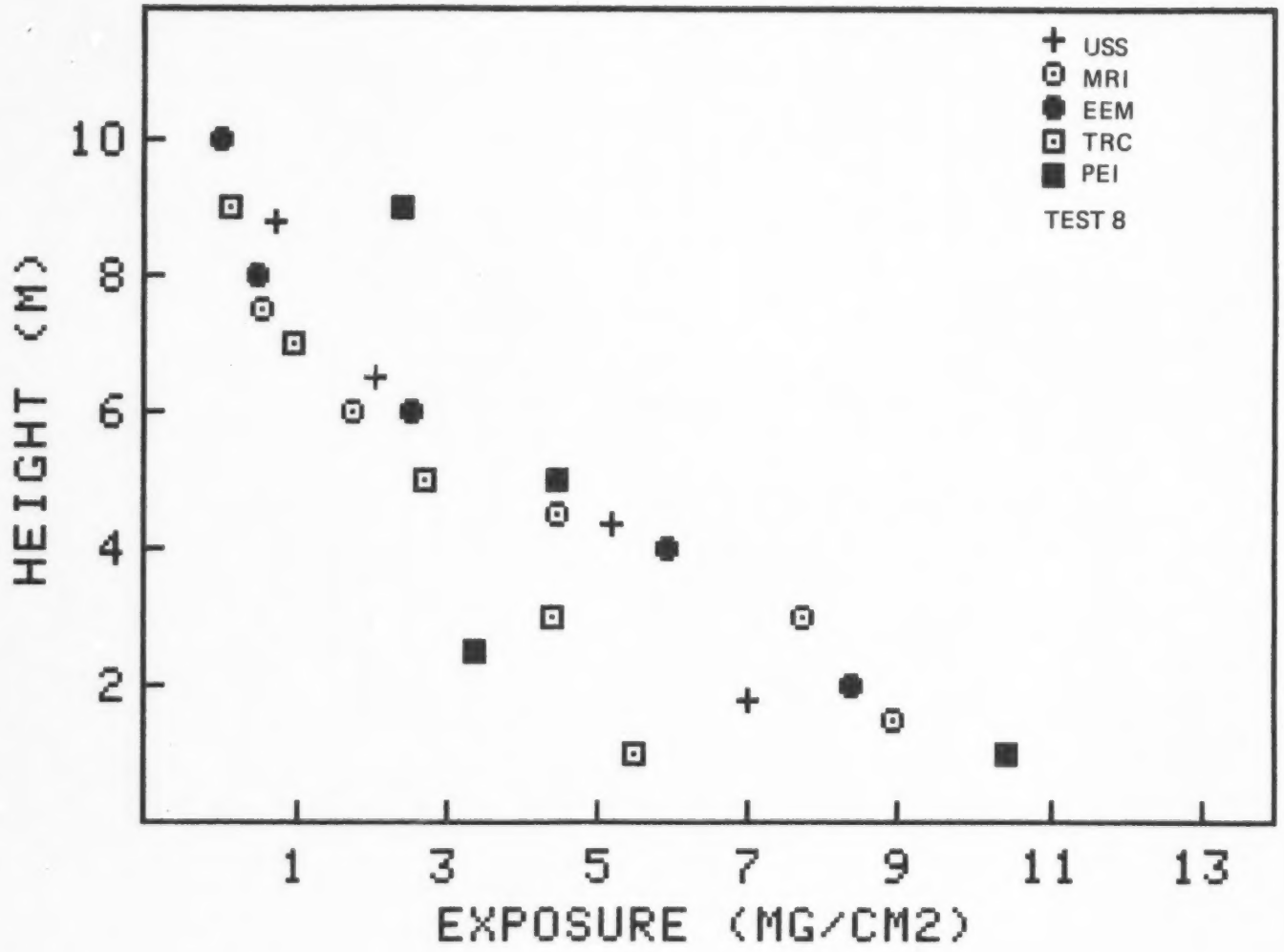

Figure 34. Measured total exposures versus height for Test 8 for all contractors providing total particulate exposure data.

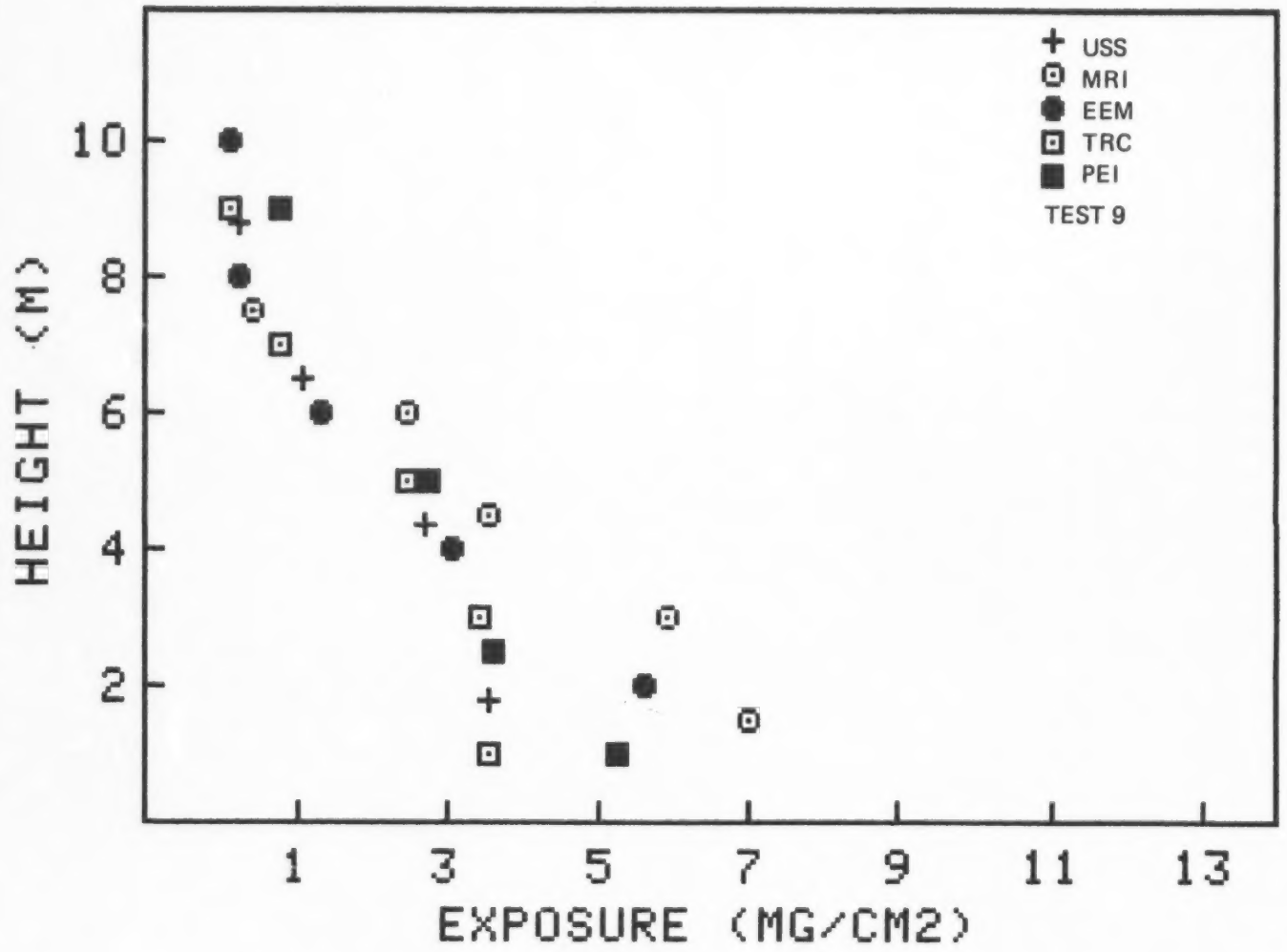

Figure 35. Measured total exposures versus height for Test 9 for all contractors providing total particulate exposure data.

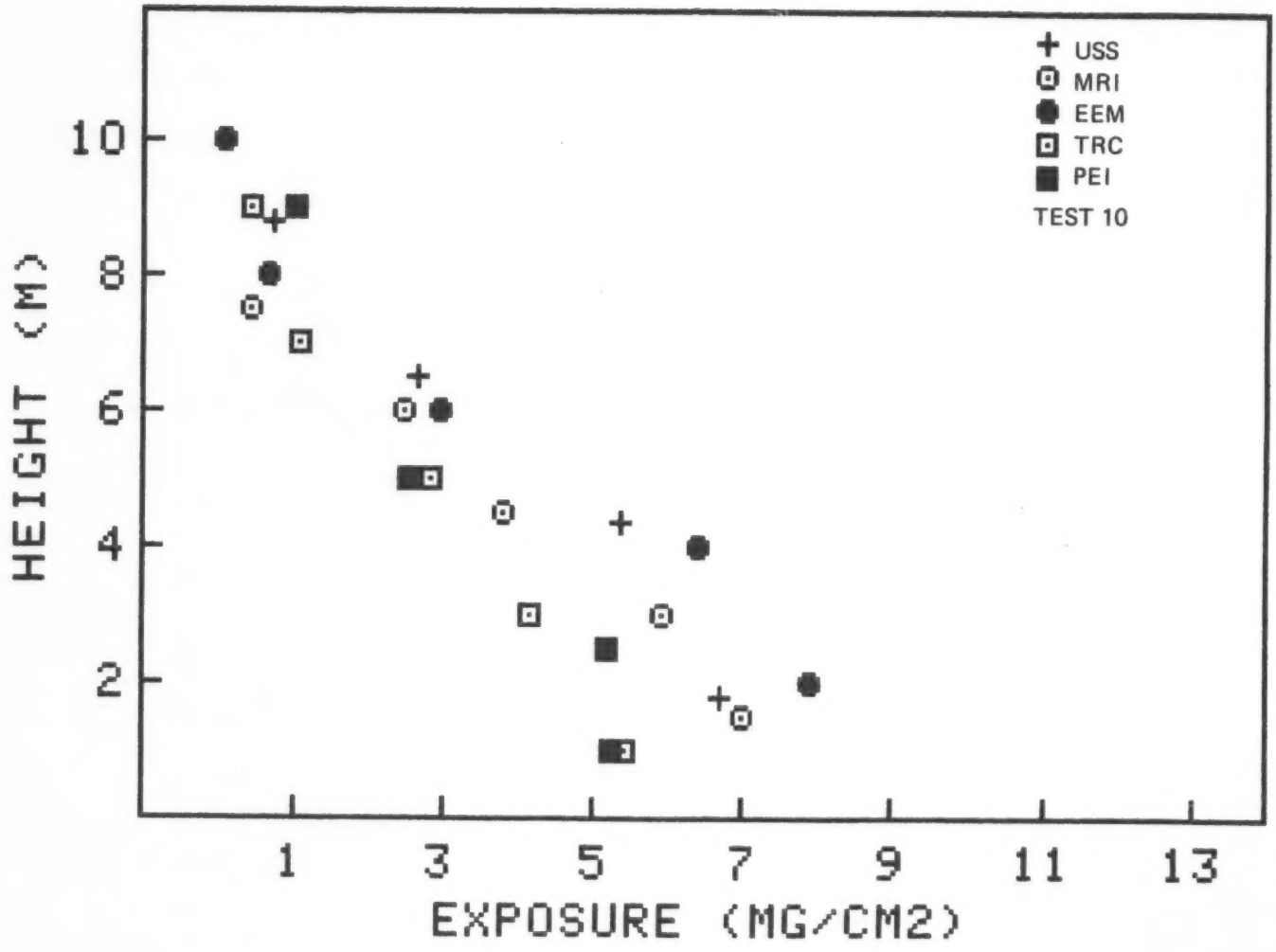

Figure 36. Measured total exposures versus height for Test 10 for all contractors providing total particulate exposure data.

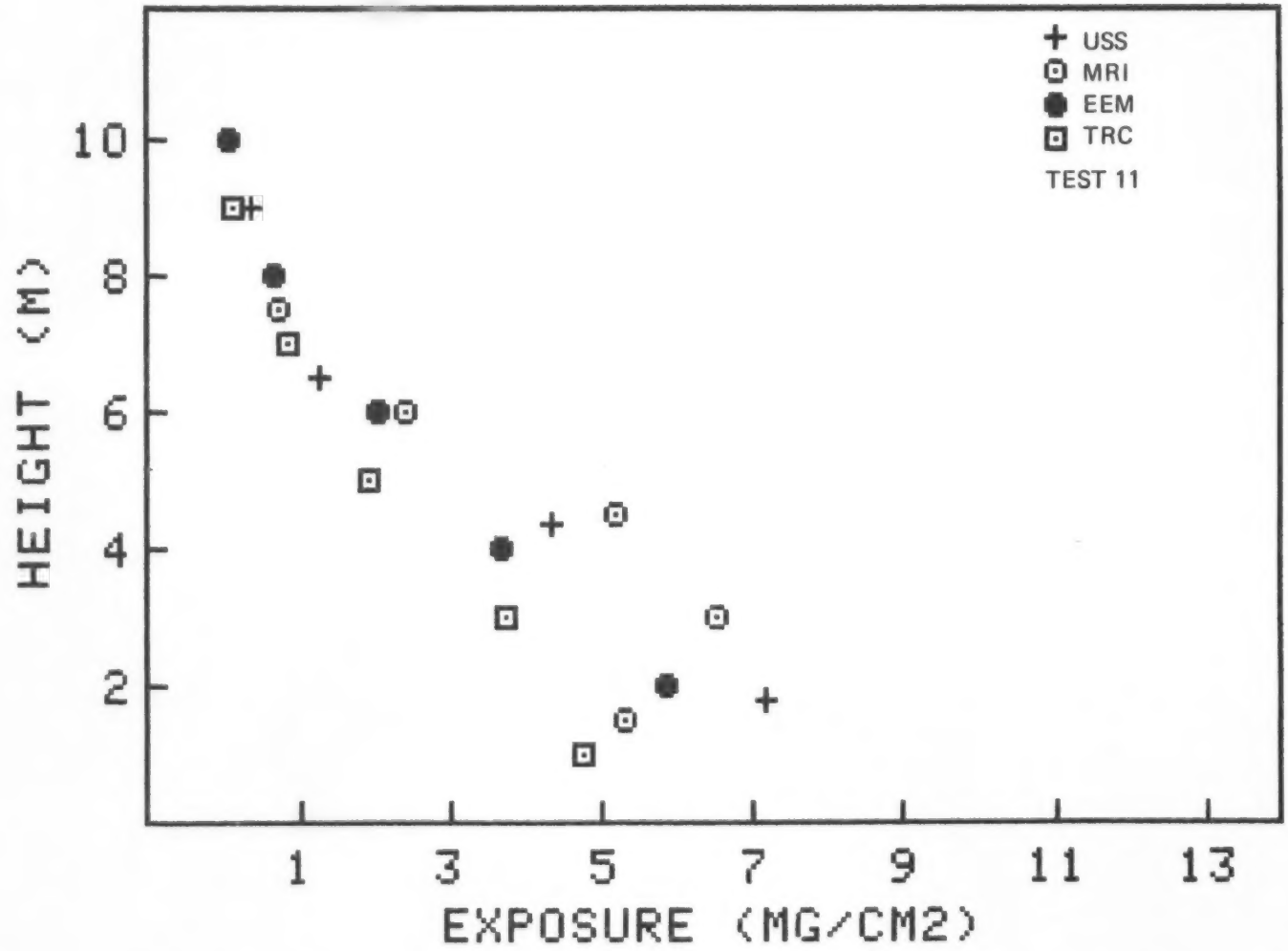

Figure 37. Measured total exposures versus height for Test 11 for all contractors providing total particulate exposure data.

For some size fractions and test numbers the differences between the two entries are small, but for others they are quite significant.

The SoRI recalculated values of particulate size fraction shown in Table 8 were used to define size specific average measured emission factors for each of the 11 tests. This was accomplished in the following manner. For each of the 11 tests, the measured TP emission factor values shown in column 19 of Table 3 were averaged to obtain the values shown in column 2 of Table 9. The entries in the other columns of Table 9 (TSP, PM_{15}, PM_{10}, and FP) were obtained by multiplying the average TP value (column 1, Table 9) by the appropriate SoRI size fraction entry in Table 8. For example, for Test Number 1, the average emission factor for TP is, from column 19 of Table 3: (8.56 + 9.33 + 10.24 + 7.11)/4 = 8.81 kg/VKT as shown in Table 9, column 2. The average emission factor for TSP is calculated using the SoRI Test Number 1 entry in Table 9, column 4 and the average TP above: (0.453) x (8.81) = 3.99 kg/VKT as shown in Table 9, column 3. The remaining entries in this table were calculated in a similar manner. Thus, the values shown in Table 9 were used as a best estimate against which the results of the five predictive equations were compared.

As mentioned in Section 6, there were differences in the reported input values as shown in Table 3. Some of the data variations between contractors for a given test are explained by the fact that occasionally some of the testing parties were late in starting and stopping their profiler systems and consequently sampled over either a different number and/or type of vehicle passes. Also there were some variations reported in the vehicle weight estimates. In an effort to remove the effects of these differences on the predicted values of the emission factor, each of the predictive equations were evaluated using the entire set of test parameters (columns 10 and 13-18 of Table 3) for each of the 11 tests. These predicted emission factor values for TP, TSP, PM_{15}, PM_{10}, and FP were then averaged for each test number and equation used. For example, the average predicted TP emission factor for Test 1 using EEM's equation was determined by using each of the five sets of

EXPOSURE AND EMISSION RECOMMENDATIONS

Each of the profiling systems used in these tests exhibited both pros and cons in terms of their versatility and ease of deployment. With regard to the height of the uppermost sampler, the data from this test series clearly indicate that there is significant exposure at heights up to at least the 9m level. Consequently, the placement of a sampler at the 9m or 10m (preferably 10m) elevation is highly recommended. Also, because the maximum exposure values usually occur at a height of 1.5 to 2.0 meters, any future profiling system should include a sampler at this level. In summary the "ideal" profiling system would have mass samplers at 1.5, 2.5, 4.0, 6.0, 7.5, and 10.0 meters with concurrent particle sizing devices at 1.5, 4.5, and 7.0 meters. This configuration would better characterize both the exposure and size distribution of the particulates in the plume.

As demonstrated by USS and TRC, sampling isokineticity can be maintained for each sampling head on the profiler tower. Therefore, it is recommended that each sampler be equipped with a servo system and individual velocity sensors to provide continuous adjustment of the flow rate based on wind speed at that elevation.

With regard to the exposure integration procedure, the resultant emission factor appears to be relatively insensitive to the technique used so long or the exposure is adequately characterized with regard to height. The most critical area is that where the peak exposures occur (usually at 1.5 to 2.0m). With samplers at 1.5, 2.5, and 4.0 meters this should not be a major source of error. However, under greatly different site conditions (road type, silt content, etc) the samplers at the lower elevations may need to be positioned at different heights.

SECTION 7

MODELING FUGITIVE EMISSIONS

One objective of this study was to correlate the various predictive equations for unpaved roads and to identify or develop, if feasible, an equation or set of equations that best account for observed differences. As a final step in their analysis of the field test data, each participant was to develop a predictive equation for the test road. The results of these efforts along with an analysis of each is presented in the following paragraphs.

PREDICTIVE EMISSION FACTOR EQUATIONS

Three of the five participants (MRI, TRC, and USS) used the existing predictive equation described in Supplement No. 14 of the AP-42 document.[16] This equation is

$$E = k(1.7)\left(\frac{s}{12}\right)\left(\frac{S}{48}\right)\left(\frac{W}{2.7}\right)^{0.7}\left(\frac{w}{4}\right)^{0.5}\left(\frac{365-p}{365}\right) \quad (1)$$

where E = emission factor, kg/VKT

k = particle size multiplier, dimensionless

s = silt content of road surface material, % passing a 200 mesh screen

S = mean vehicle speed, km/hr

W = mean vehicle weight, Mg (metric tons)

w = mean number of wheels, dimensionless

p = number of days with at least 0.254 mm of precipitation per year, dimensionless.

For the current series of tests the factor involving p was omitted. The values for the particle size multiplier k as listed in the AP-42 document are: 0.80 (<30 μm), 0.57 (<15 μm), 0.45 (<10 μm), 0.28 (<5 μm), and 0.16 (<2.5 μm). No value is listed for total particulate TP. Each of those organizations using Equation (1) derived different values for the size multiplier k.

The other two participants (EEM and PEI) developed their own predictive equation based on the parameters measured during this test series. PEI used a multiple linear regression analysis to develop the predictive equation

$$E = k(W)^a(m)^b \qquad (2)$$

where m = road surface moisture content, %, and the constants k, a, and b are dependent upon the size fraction of the particulate being considered. EEM also used a multiple regression technique to develop the following predictive equation

$$E = k(s)^{0.139}(R)^{-0.203}(w)^{0.267}(W)^{0.395} \qquad (3)$$

where R = ambient relative humidity, percent; and the other parameters are as defined previously. The values of the constants in Equations (1), (2), and (3) for all organizations are summarized in Table 7. It is important to notice that PEI's equation is applicable only for predicting TSP, PM_{10}, and FP emissions. Also the term containing soil moisture in Equation (2) is applicable only for the FP fraction.

In evaluating these predictive equations, the question arises as to which of the measured emission factors should be used for comparison. In view of the limitations of the particle sizing techniques as discussed earlier, probably none are truly representative of the actual road conditions with MRI's results being the most nearly representative.

For physical reasons, the particle sizing techniques used by MRI have a higher probability of correctly describing the actual but unknown dust size distributions. However, because of uncertainties in MRI's data reduction process, the "as reported" size distributions are somewhat questionable. As a result, the raw data reported by MRI (filter weighings, cyclone washes, etc.) were independently reduced using the cascade impactor data reduction techniques[13] described at the end of Section 5. The results of these recalculations are tabulated in Table 8 along with the values reported by MRI.

TABLE 7. SIZE DEPENDENT CONSTANTS FOR THE PREDICTIVE EMISSION FACTOR EQUATIONS

Size Fraction		Equation 1			Equation 2			Equation 3
		MRI	TRC	USS	PEI			EEM
		k	k	k	k	a	b	k
TP	(total)	1.80	1.00	1.16	-	-	0.0	2.319
TSP	(<30 μm)	0.80	0.92	1.00	0.62	0.44	0.0	1.832
PM_{15}	(<15 μm)	0.57	0.51	0.57	-	-	0.0	0.928
PM_{10}	(<10 μm)	0.45	0.31	0.36	0.20	0.59	0.0	0.557
FP	(<2.5 μm)	0.16	0.03	0.04	0.0092	1.50	-0.72	0.070

TABLE 8. SIZE FRACTIONS OF PARTICULATE AS REPORTED BY MRI AND RECALCULATED BY SOUTHERN RESEARCH INSTITUTE

Test No.	Organization	TP (total)	Size Fraction as Percent Less Than TSP (<30 μm)	PM_{15} (<15 μm)	PM_{10} (<10 μm)	FP (<2.5 μm)
1	SoRI	1.00	0.453	0.313	0.240	0.094
	MRI	1.00	0.395	0.284	0.216	0.066
2	SoRI	1.00	0.412	0.306	0.234	0.098
	MRI	1.00	0.427	0.263	0.202	0.064
3	SoRI	1.00	0.487	0.350	0.280	0.113
	MRI	1.00	0.374	0.243	0.183	0.058
4	SoRI	1.00	0.527	0.326	0.250	0.107
	MRI	1.00	0.448	0.303	0.236	0.077
5	SoRI	1.00	0.427	0.274	0.212	0.090
	MRI	1.00	0.689	0.547	0.449	0.170
6	SoRI	1.00	0.507	0.352	0.279	0.120
	MRI	1.00	0.439	0.294	0.230	0.078
7	SoRI	1.00	0.506	0.357	0.283	0.117
	MRI	1.00	0.567	0.405	0.320	0.105
8	SoRI	1.00	0.349	0.233	0.177	0.077
	MRI	1.00	0.318	0.212	0.164	0.056
9	SoRI	1.00	0.304	0.216	0.174	0.070
	MRI	1.00	0.373	0.196	0.152	0.054
10	SoRI	1.00	0.333	0.216	0.166	0.074
	MRI	1.00	0.419	0.294	0.230	0.076
11	SoRI	1.00	0.457	0.333	0.240	0.089
	MRI	1.00	0.480	0.332	0.253	0.072

test parameters (columns 10 and 13-18 of Table 3) as inputs to Equation (3). The five resulting values were averaged to represent a best theoretical approximation to the TP emission factor for Test Number 1 using EEM's predictor equation. A similar process was carried out for each predictive equation and all size fractions.

In order to compare these theoretically predicted emission factors to the best estimates of those measured in the field, as shown in Table 9, a correlation/regression analysis was carried out. The results of applying this analysis to EEM's equation are summarized in Figure 38. In this scatter diagram the predicted values of TP emission factor are plotted versus the measured values for each of the 11 tests. In this figure there are shown two sets of data. The filled circles correspond to the paired values of the average predicted emission factors using Equation (3) and the average measured values shown in column 2 of Table 9. The open circles correspond to the paired values of the predicted emission factor based on only one input data set per test, and the values measured by that specific organization. In brief, the filled circles depict how well EEM's equation can predict emission factors based on the average measured values for total particulate from all contractors. The open circles demonstrate the degree in which EEM's equation can predict the actual data measured by EEM. For either set of points, if the predicted and measured values of the emission factor were in a one-to-one correspondence, the points would all lie along the solid diagonal line. The other lines in the figures represent the least squares linear regression lines for the data. The dotted line is the regression line for the filled symbols and the simple broken line that for the open symbols. The values of the least squares correlation coefficients (r), and the coefficients of the regression line in Figure 38 are shown in Table 10.

Thus in Figure 38, EEM's emission factor predictive equation for TP is moderately well correlated with the average of the values measured ($r = 0.68$) and also with their own measured value ($r = 0.61$). Also, the slopes of the regression line for the averaged data and their own data (as shown in Table 10) are within 54% and 80%, respectively, when compared to the one-to-one

TABLE 9. AVERAGE EMISSION FACTORS AS CALCULATED BY SOUTHERN RESEARCH INSTITUTE

Test Number	TP (kg/VKT)	TSP (kg/VKT)	PM_{15} (kg/VKT)	PM_{10} (kg/VKT)	FP (kg/VKT)
1	8.81	3.99	2.76	2.11	0.83
2	5.09	2.10	1.56	1.19	0.50
3	9.84	4.79	3.44	2.76	1.11
4	12.96	6.83	4.23	3.24	1.39
5	4.57	1.95	1.25	0.97	0.41
6	7.30	3.70	2.57	2.04	0.88
7	9.22	4.67	3.29	2.61	1.08
8	6.21	2.17	1.45	1.10	0.48
9	5.00	1.52	1.08	0.87	0.35
10	7.45	2.48	1.61	1.24	0.55
11	8.05	3.68	2.68	1.93	0.72

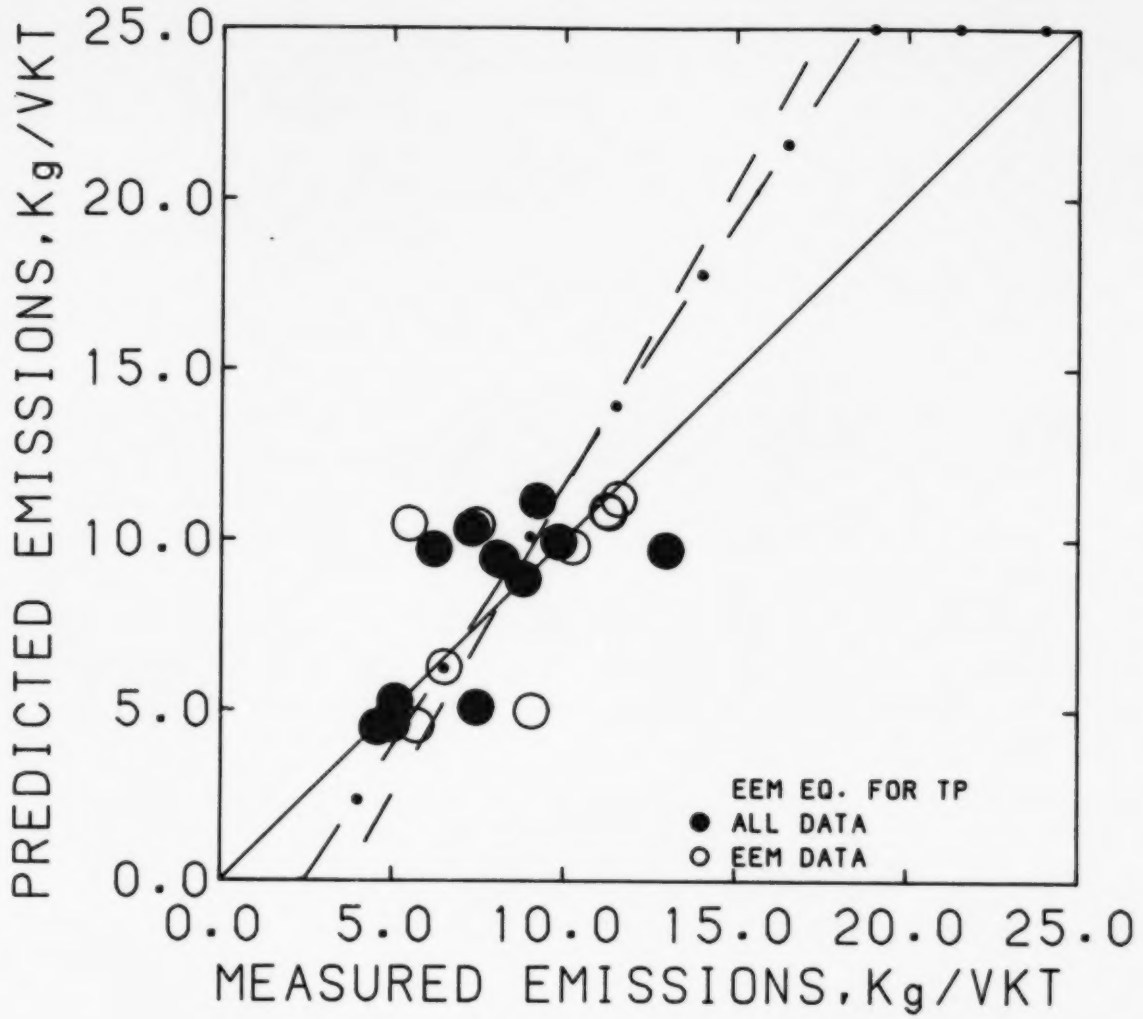

Figure 38. Scatter diagrams of: the test averaged TP emission factor measurements and that predicted by EEM's equation (filled circles) along with the associated regression line (dotted line); and the values of TP emission factor both measured and predicted by EEM (open circles) along with the associated regression line (broken line).

TABLE 10. CORRELATION AND REGRESSION LINE COEFFICIENTS FOR THE EMISSION FACTOR COMPARISONS

Size Fraction	Organization	Averaged Data			Own Data			Figure No.
		Intercept	Slope	r	Intercept	Slope	r	
TP (total)	MRI	19.18	4.18	0.69	-8.92	2.40	0.65	39
	TRC	10.66	2.33	0.69	-66.01	12.82	0.25	40
	USS	12.35	2.70	0.69	-5.07	1.64	0.76	41
	PEI	-	-	-	-	-	-	-
	EEM	-3.79	1.54	0.68	-6.48	1.80	0.61	38
TS (<30μm)	MRI	-3.35	2.65	0.75	-3.71	2.39	0.67	43
	TRC	-3.84	3.04	0.75	-61.38	12.99	0.25	45
	USS	-4.19	3.31	0.75	-3.11	1.51	0.77	46
	PEI	0.46	0.50	0.65	-0.05	0.96	0.59	44
	EEM	0.16	1.80	0.72	-4.95	1.79	0.62	42
PM_{15} (<15μm)	MRI	-2.38	2.77	0.79	-2.37	2.40	0.69	48
	TRC	-2.13	2.48	0.79	-31.24	11.90	0.27	49
	USS	-2.38	2.77	0.79	-2.19	1.60	0.75	50
	PEI	-	-	-	-	-	-	-
	EEM	0.10	1.33	0.76	-3.32	1.95	0.57	47
PM_{10} (<10μm)	MRI	-1.78	2.76	0.80	-1.94	2.49	0.68	52
	TRC	-1.23	1.90	0.80	-17.81	11.36	0.28	54
	USS	-1.43	2.21	0.80	-1.57	1.67	0.72	55
	PEI	-0.02	0.61	0.68	0.02	0.95	0.72	53
	EEM	0.08	1.01	0.76	-1.09	1.63	0.64	51
FP (<2.5μm)	MRI	-0.62	2.35	0.81	-0.83	2.93	0.64	57
	TRC	-0.12	0.44	0.81	-1.86	12.99	0.26	59
	USS	-0.16	0.59	0.81	-0.08	1.21	0.58	60
	PEI	-1.76	2.96	0.33	-0.05	1.14	0.92	58
	EEM	0.01	0.31	0.75	-0.04	1.38	0.58	56

r = Correlation Coefficient

correspondence line. Because of the offset in the intercept values (-3.79 and -6.48) EEM's predictive equation would under predict at low values of the TP emissions and over-predict at higher values.

A similar analysis was applied to each of the five predictive equations and the results shown in Table 10 and Figures 39 through 60. By examining the values in Table 10 it can be seen that for the case of the TP emission factors, the errors in the slopes of the regression lines range from 54% to 318% for the averaged data and from 80% to 1182% for the individual data. Thus, even though the correlation coefficients for the averaged data are very nearly the same, the various predictive equations will in general over-predict the measured values by varying amounts.

Although the data base used for these statistical analyses was limited, some general comments regarding the various predictor models can be made.

- MRI's equation consistently over-predicts the results measured here for all size fractions considered.

- TRC's equation predicts results similar to that of MRI as might be expected. The over prediction at TP is less than MRI's, and the TSP is greater than MRI's results reflecting the different values of k used (see Table 7). This is especially true for FP fraction. Here TRC's equation severely under-predicts the average measured results while predicting their own data quite well as seen in Figure 59. This is due primarily to the fact that those using CCSEM techniques simply do not see the entire fine particulate fraction of the dust.

- USS's equation predicts results very much the same as TRC and is explicable for the same reasons.

- EEM's equation appears to do a better job of predicting the average test results. This is primarily due to the fact that the equation was derived based on the current data base (11 tests). How well this predictive equation can be applied to previous data has not been determined.

The severe under-prediction of the FP fraction as seen in Figure 56 is again due to the inability of the CCSEM techniques to correctly describe the particulate size distribution.

- PEI's equation consistently under-predicts the averaged data from these tests while giving moderately good agreement to their own data. This reflects the conclusions drawn earlier regarding the stacked filter system.

In general the results of this analysis would suggest that either the predictive equation of EEM or that used by MRI, TRC, and USS would adequately represent the results of this test series if appropriate values were chosen for the constants in Table 7. The PEI relation is seen to be inadequate primarily because the underlying TSP data base was systematically low.

MODELING RECOMMENDATIONS

The utility of an emission factor predictive equation is not necessarily that of predicting the emissions from a particular site in lieu of actual measurements. In order that the equation be applicable over a wide range of site locations and conditions, it should include as many of the relevant parameters describing the site as possible. This requires that the predictive equation be developed from as large a data base as possible.

Equation (1) above is just such a relation. It was developed from a fairly broad data base using multiple linear regression techniques. The data base has some uncertainties particularly with regards to the particle size distributions. These uncertainties most certainly cast some doubt upon the precision of the values used for the particle size multiplier, k, in Equation (1). However, without an extensive evaluation of the existing unpaved road emissions data base, there are no justifications for invalidating the relation used by MRI, TRC, and USS.

This predictive equation (Equation (2)) developed by PEI is considered inadequate because it was derived using an invalid TSP data base. Although the relation (Equation (3)) developed by EEM did quite well predicing the results of this test series, the data base from which it was derived is too small to give it much creditability for other sites without extensive validation.

In summary, the predictive emission factor equation used by MRI, TRC, and USS and as described in the AP-42 manual[15] is probably the most reliable predictor of unpaved road emissions currently available. Because of past problems in the particle sizing techniques, the values used for the size multiplier (k) are less reliable than the overall equation. It is recommended that these values be re-evaluated in the future as the data base is expanded with more reliable particle size information.

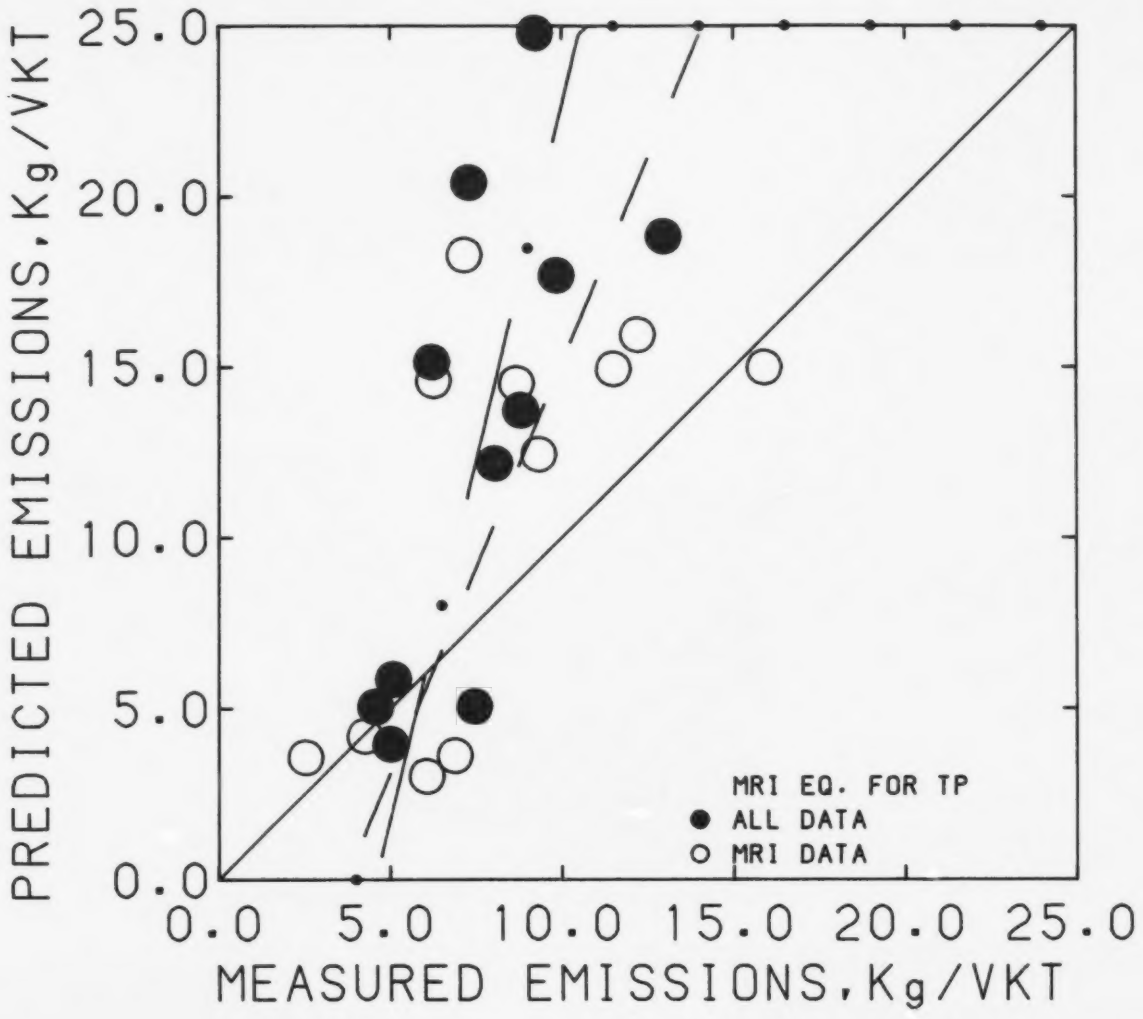

Figure 39. Scatter diagrams of: the test averaged TP emission factor measurements and that predicted by MRI's equation (filled circles) along with the associated regression line (dotted line); and the values of TP emission factor both measured and predicted by MRI (open circles) along with the associated regression line (broken line).

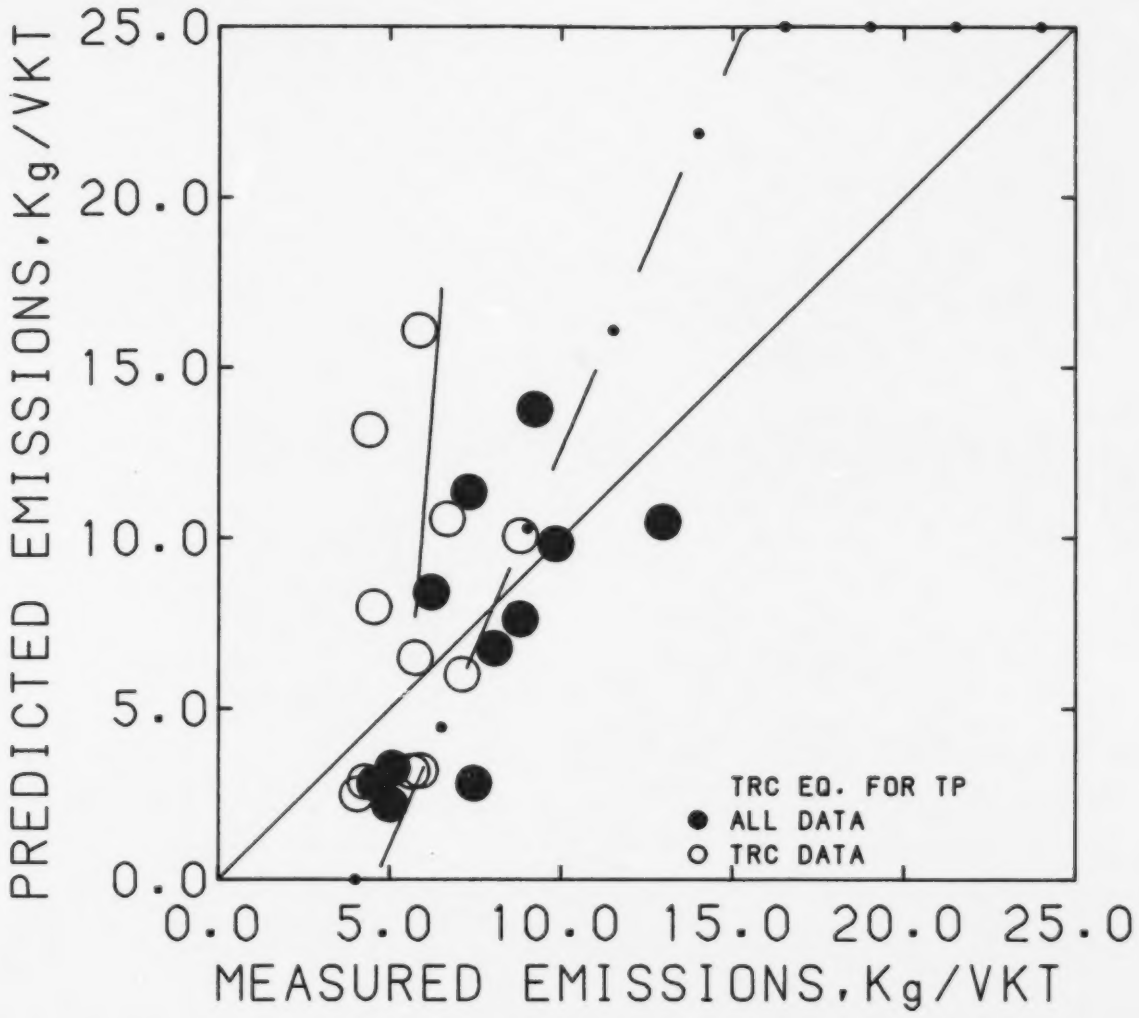

Figure 40. Scatter diagrams of: the test averaged TP emission factor measurements and that predicted by TRC's equation (filled circles) along with the associated regression line (dotted line); and the values of TP emission factor both measured and predicted by TRC (open circles) along with the associated regression line (broken line).

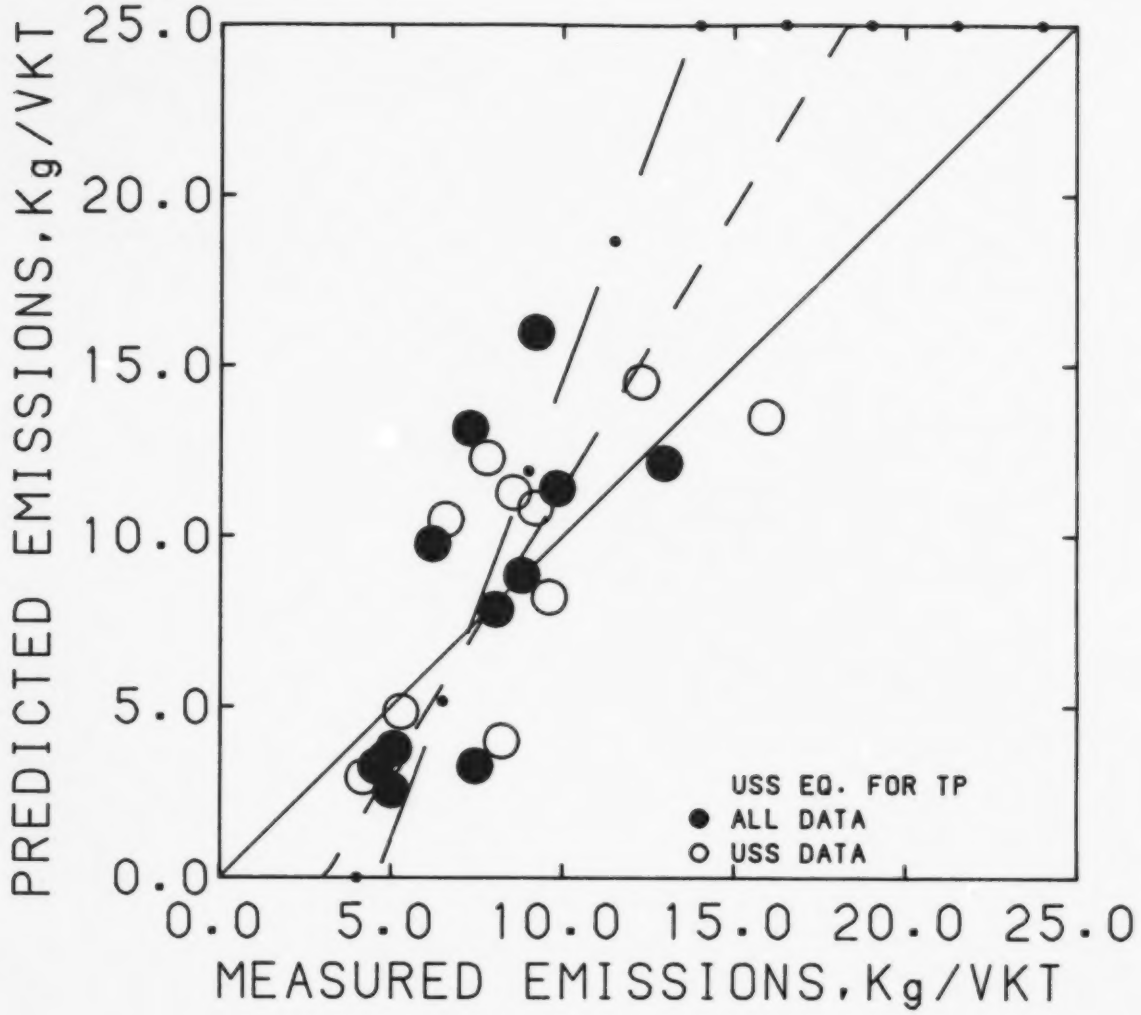

Figure 41. Scatter diagrams of: the test averaged TP emission factor measurements and that predicted by USS's equation (filled circles) along with the associated regression line (dotted line); and the values of TP emission factor both measured and predicted by USS (open circles) along with the associated regression line (broken line).

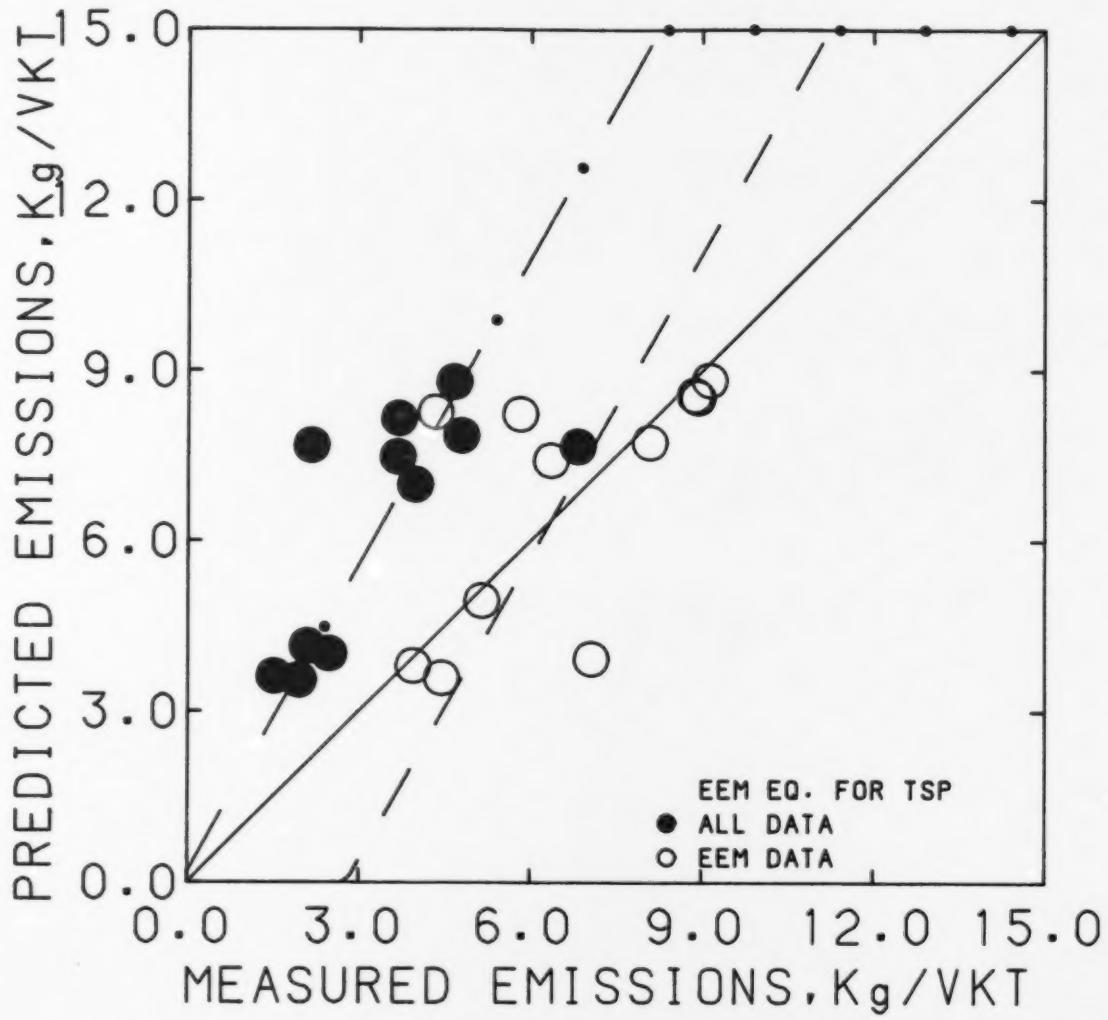

Figure 42. Scatter diagrams of: the test averaged TSP emission factor measurements and that predicted by EEM's equation (filled circles) along with the associated regression line (dotted line); and the values of TSP emission factor both measured and predicted by EEM (open circles) along with the associated regression line (broken line).

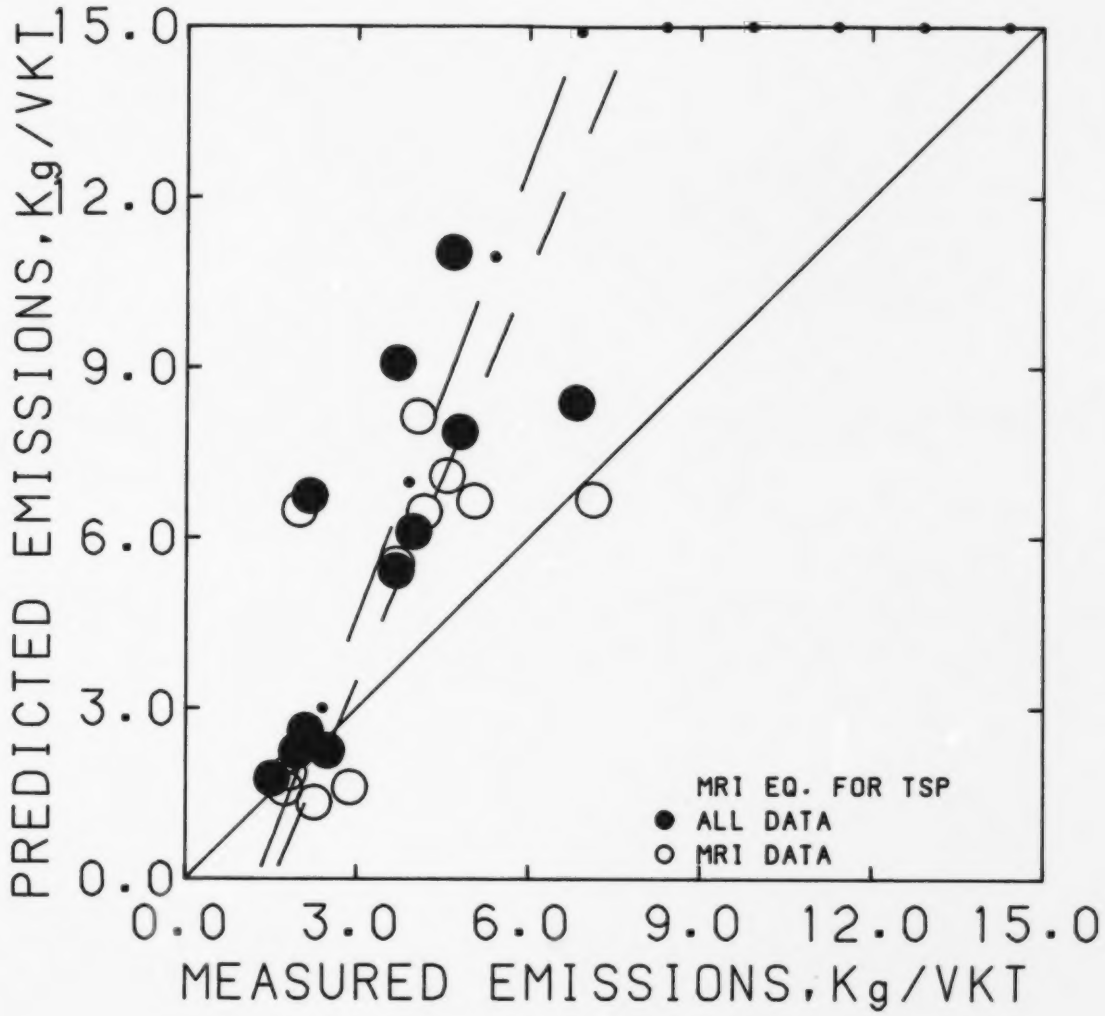

Figure 43. Scatter diagrams of: the test averaged TSP emission factor measurements and that predicted by MRI's equation (filled circles) along with the associated regression line (dotted line); and the values of TSP emission factor both measured and predicted by MRI (open circles) along with the associated regression line (broken line).

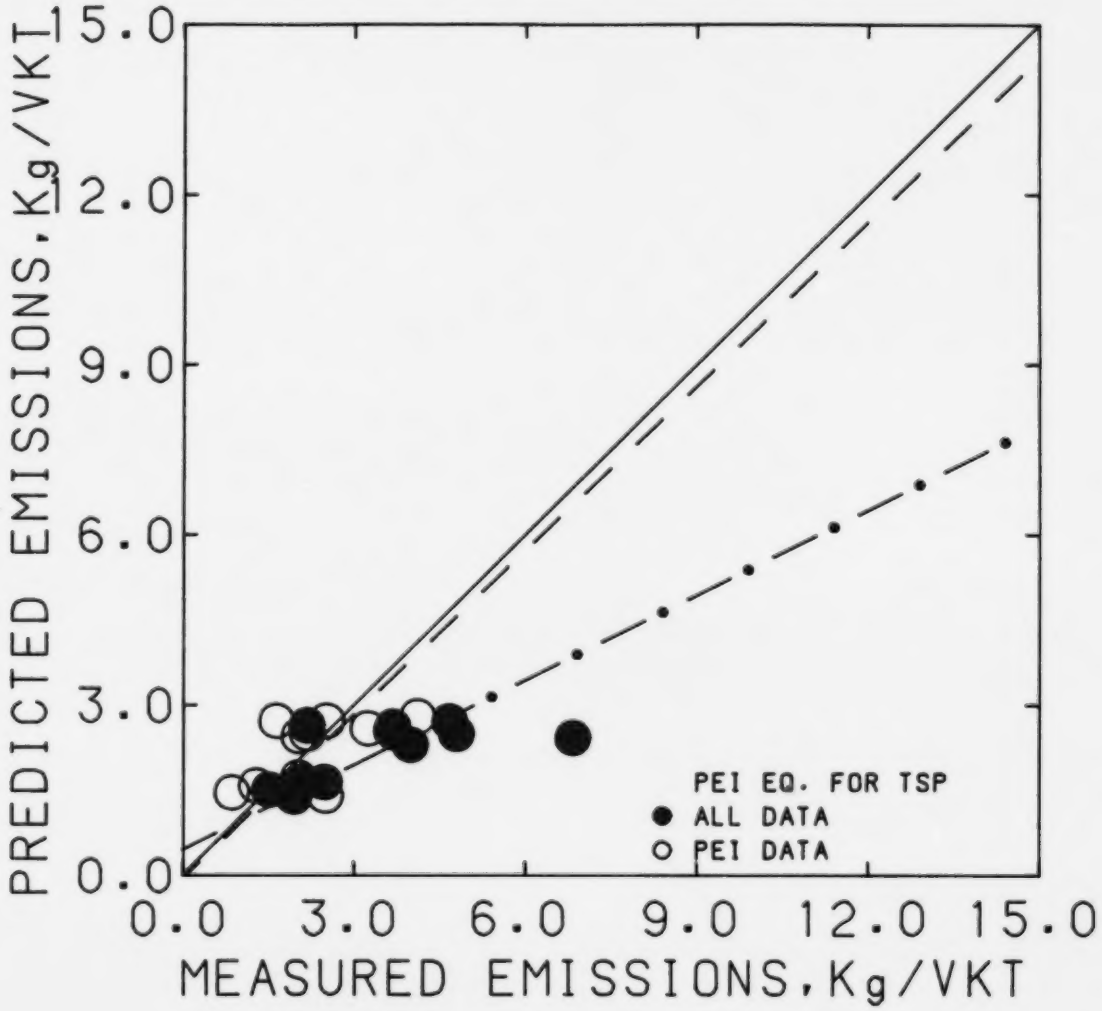

Figure 44. Scatter diagrams of: the test averaged TSP emission factor measurements and that predicted by PEI's equation (filled circles) along with the associated regression line (dotted line); and the values of TSP emission factor both measured and predicted by PEI (open circles) along with the associated regression line (broken line).

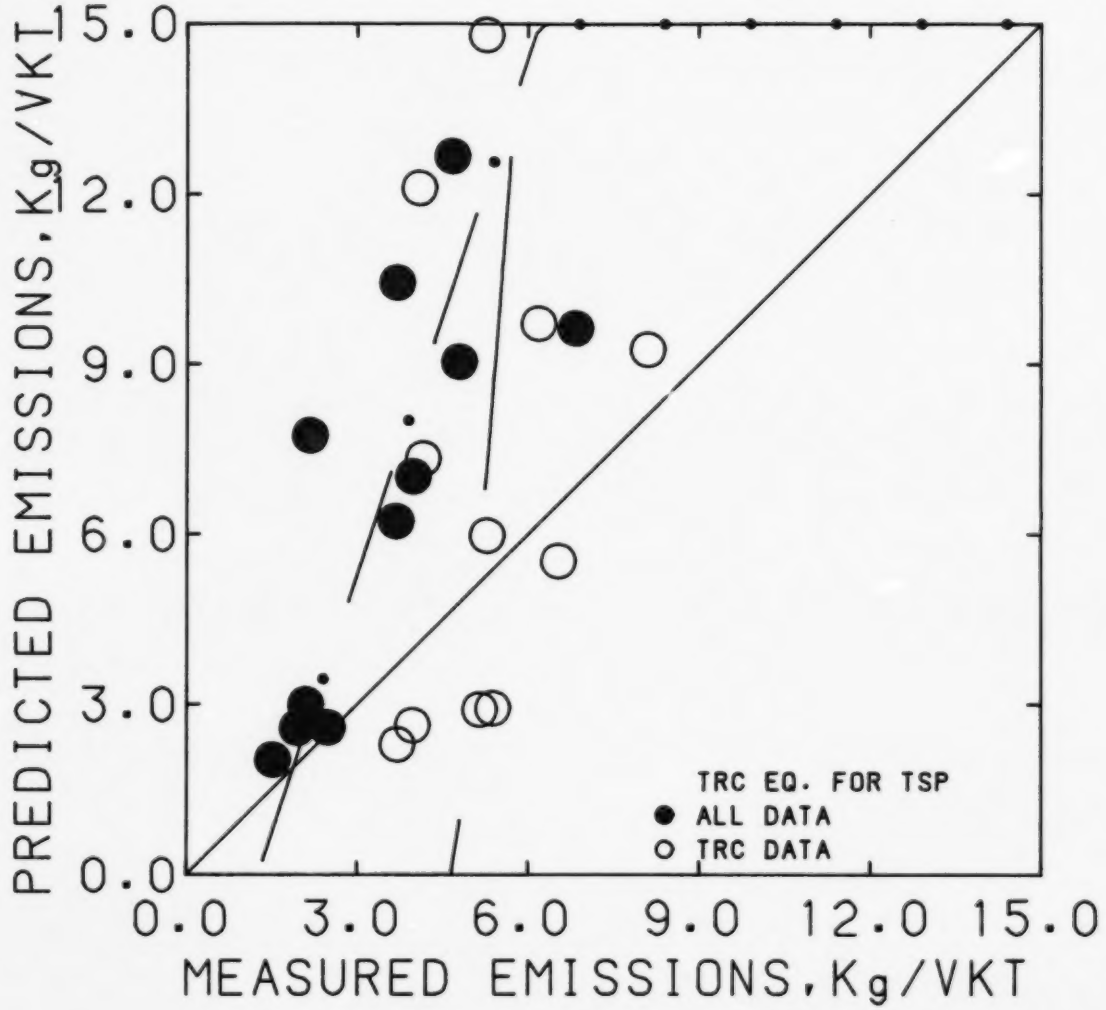

Figure 45. Scatter diagrams of: the test averaged TSP emission factor measurements and that predicted by TRC's equation (filled circles) along with the associated regression line (dotted line); and the values of TSP emission factor both measured and predicted by TRC (open circles) along with the associated regression line (broken line).

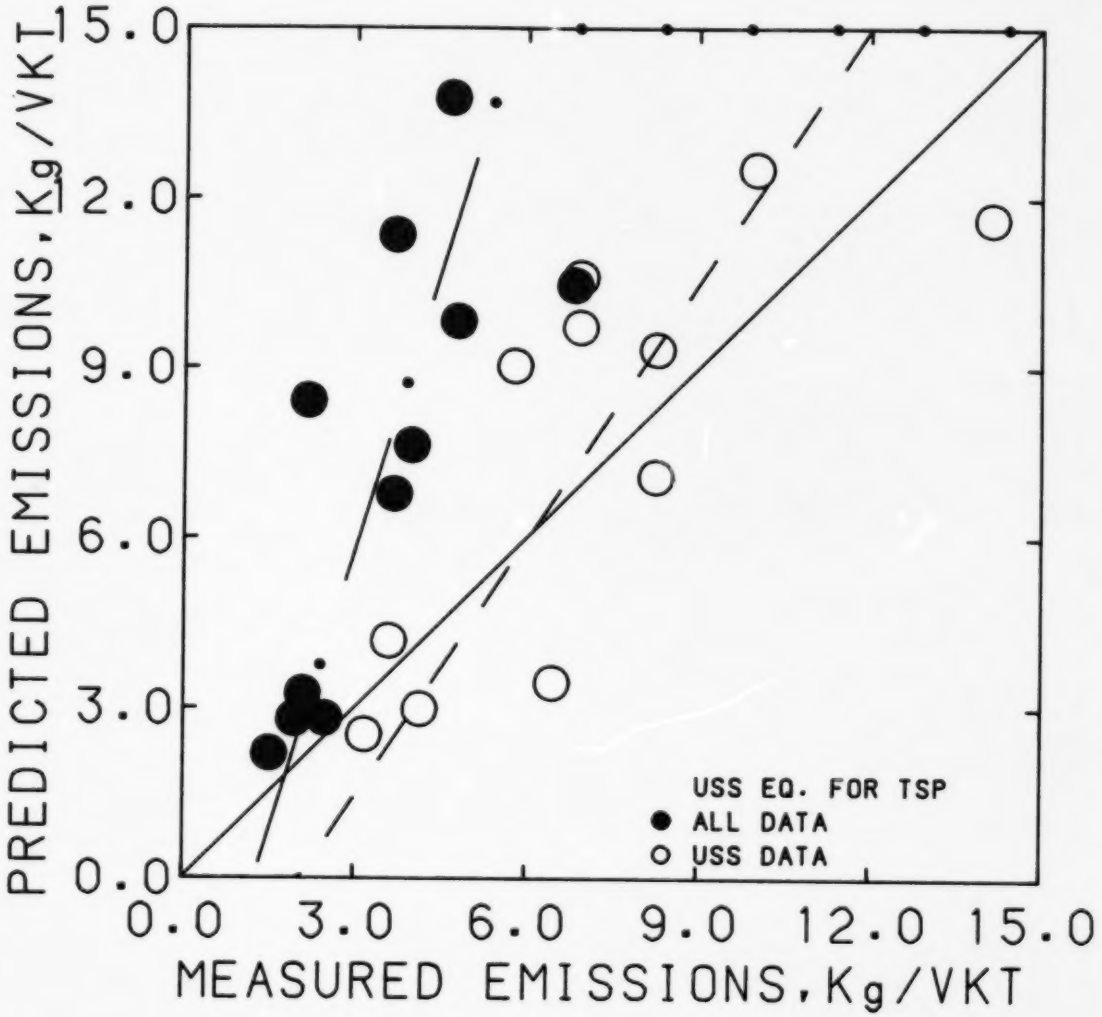

Figure 46. Scatter diagrams of: the test averaged TSP emission factor measurements and that predicted by USS's equation (filled circles) along with the associated regression line (dotted line); and the values of TSP emission factor both measured and predicted by USS (open circles) along with the associated regression line (broken line).

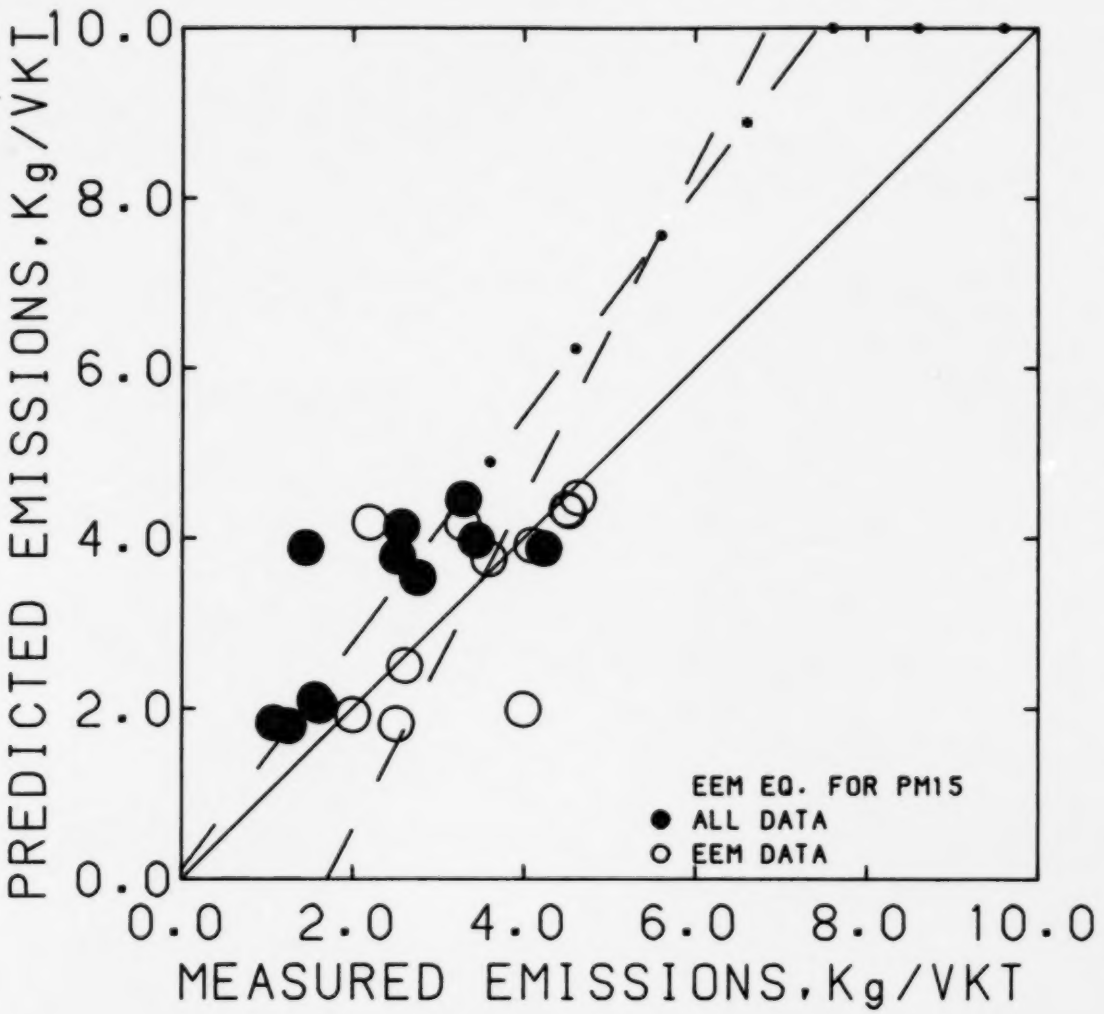

Figure 47. Scatter diagrams of: the test averaged PM_{15} emission factor measurements and that predicted by EEM's equation (filled circles) along with the associated regression line (dotted line); and the values of PM_{15} emission factor both measured and predicted by EEM (open circles) along with the associated regression line (broken line).

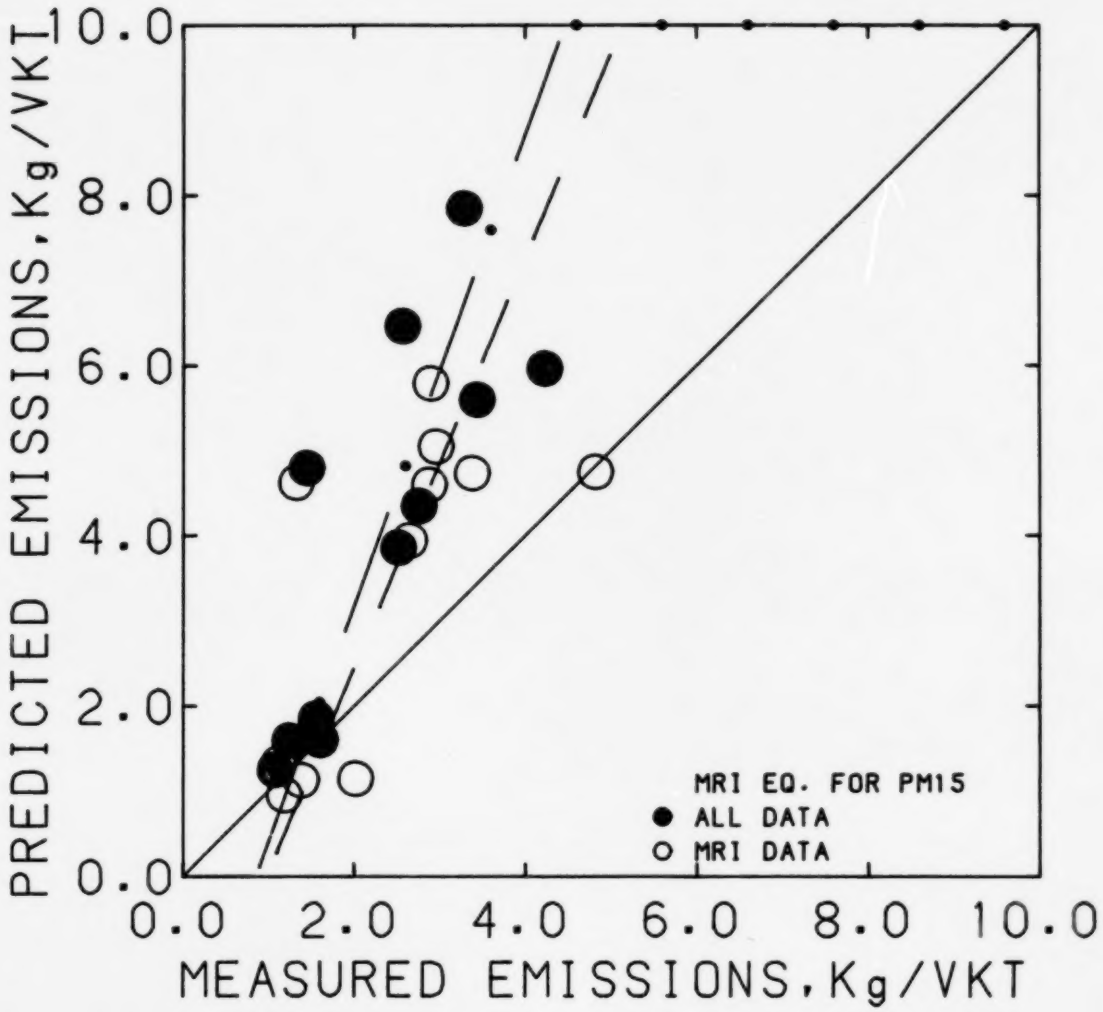

Figure 48. Scatter diagrams of: the test averaged PM_{15} emission factor measurements and that predicted by MRI's equation (filled circles) along with the associated regression line (dotted line); and the values of PM_{15} emission factor both measured and predicted by MRI (open circles) along with the associated regression line (broken line).

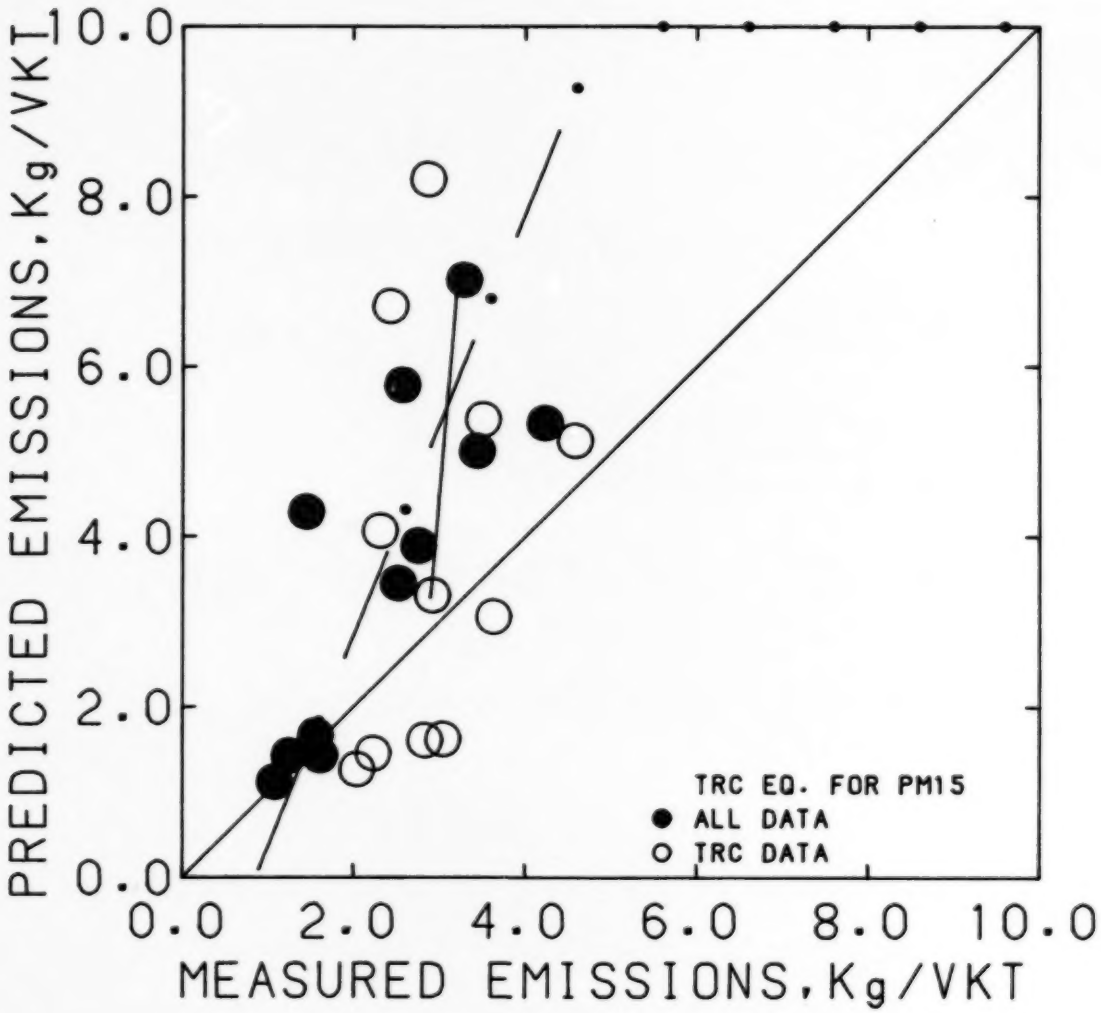

Figure 49. Scatter diagrams of: the test averaged PM_{15} emission factor measurements and that predicted by TRC's equation (filled circles) along with the associated regression line (dotted line); and the values of PM_{15} emission factor both measured and predicted by TRC (open circles) along with the associated regression line (broken line).

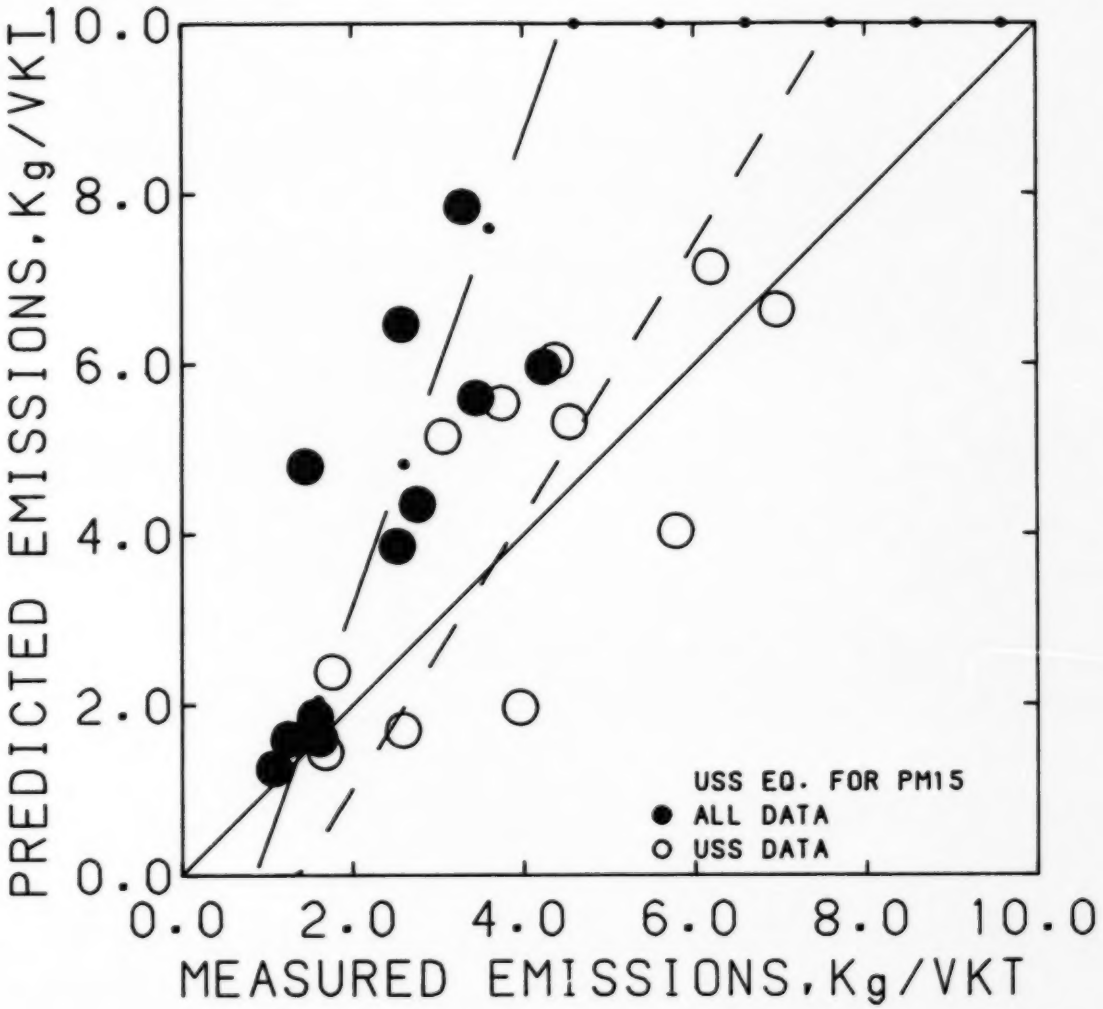

Figure 50. Scatter diagrams of: the test averaged PM_{15} emission factor measurements and that predicted by USS's equation (filled circles) along with the associated regression line (dotted line); and the values of PM_{15} emission factor both measured and predicted by USS (open circles) along with the associated regression line (broken line).

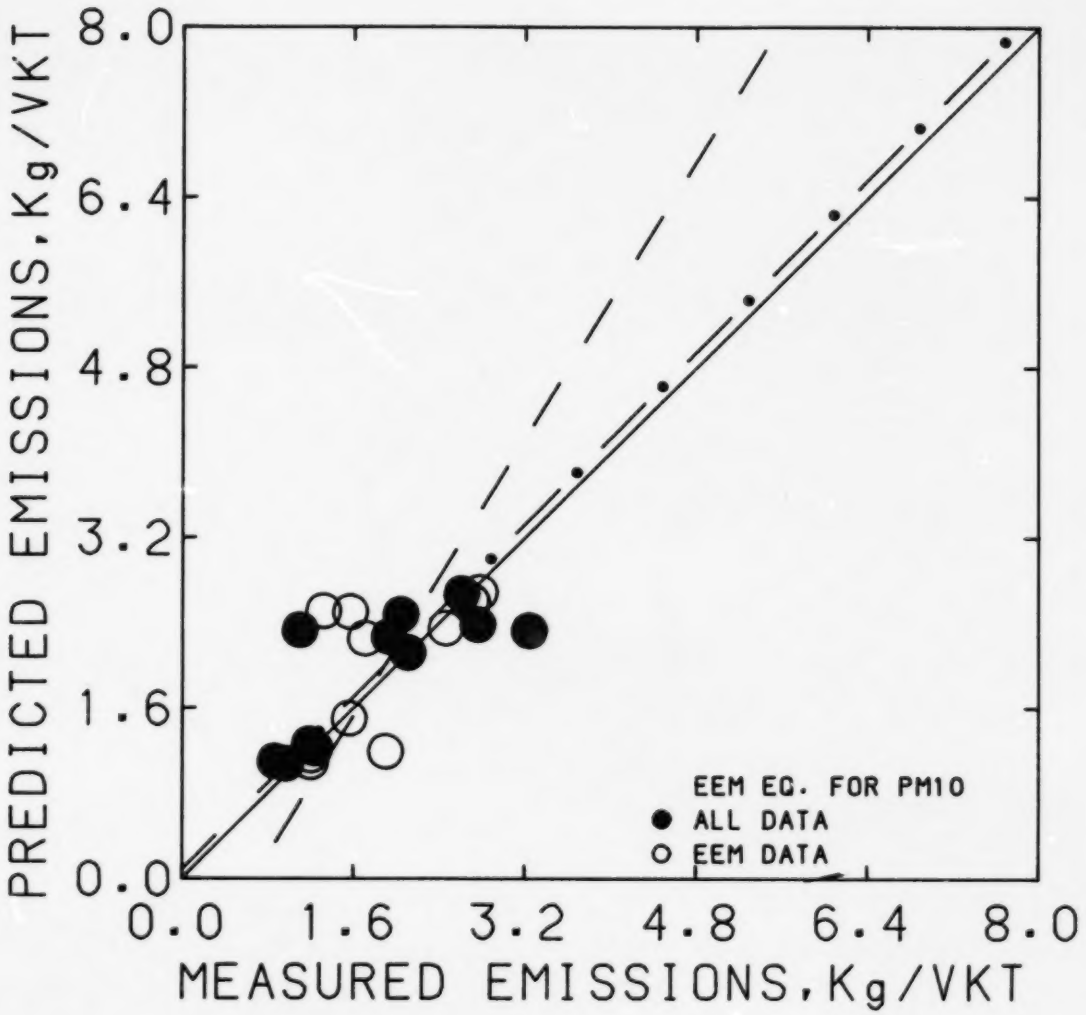

Figure 51. Scatter diagrams of: the test averaged PM_{10} emission factor measurements and that predicted by EEM's equation (filled circles) along with the associated regression line (dotted line); and the values of PM_{10} emission factor both measured and predicted by EEM (open circles) along with the associated reqression line (broken line).

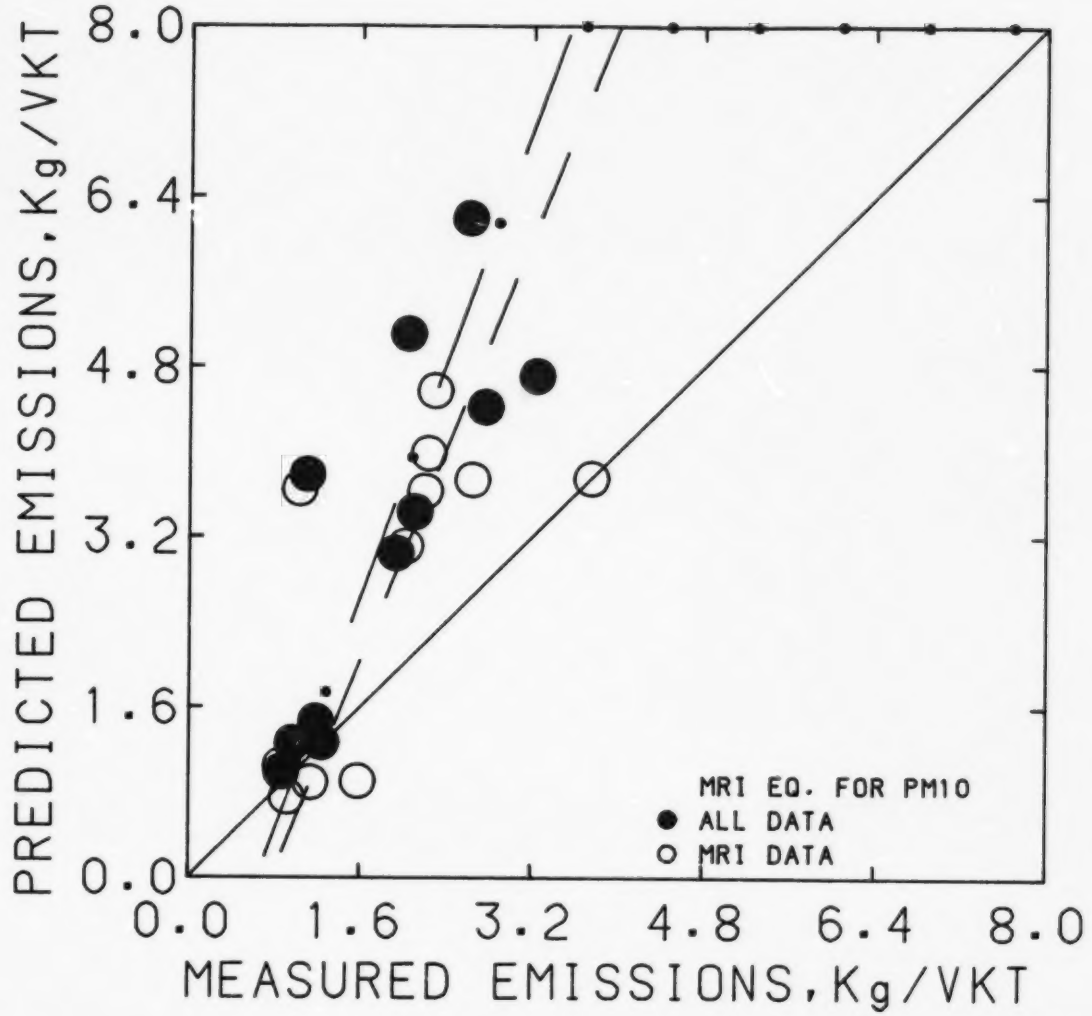

Figure 52. Scatter diagrams of: the test averaged PM_{10} emission factor measurements and that predicted by MRI's equation (filled circles) along with the associated regression line (dotted line); and the values of PM_{10} emission factor both measured and predicted by MRI (open circles) along with the associated regression line (broken line).

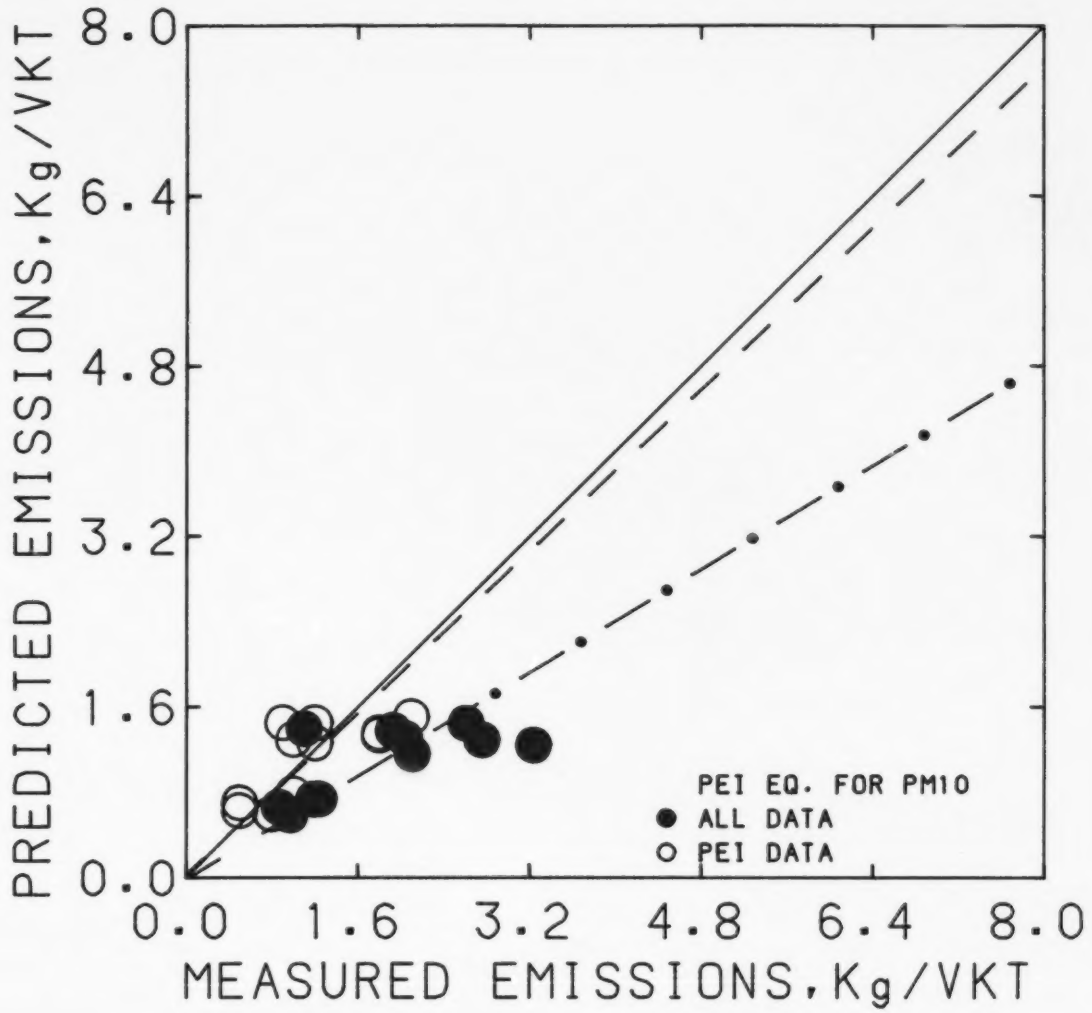

Figure 53. Scatter diagrams of: the test averaged PM_{10} emission factor measurements and that predicted by PEI's equation (filled circles) along with the associated regression line (dotted line); and the values of PM_{10} emission factor both measured and predicted by PEI (open circles) along with the associated regression line (broken line).

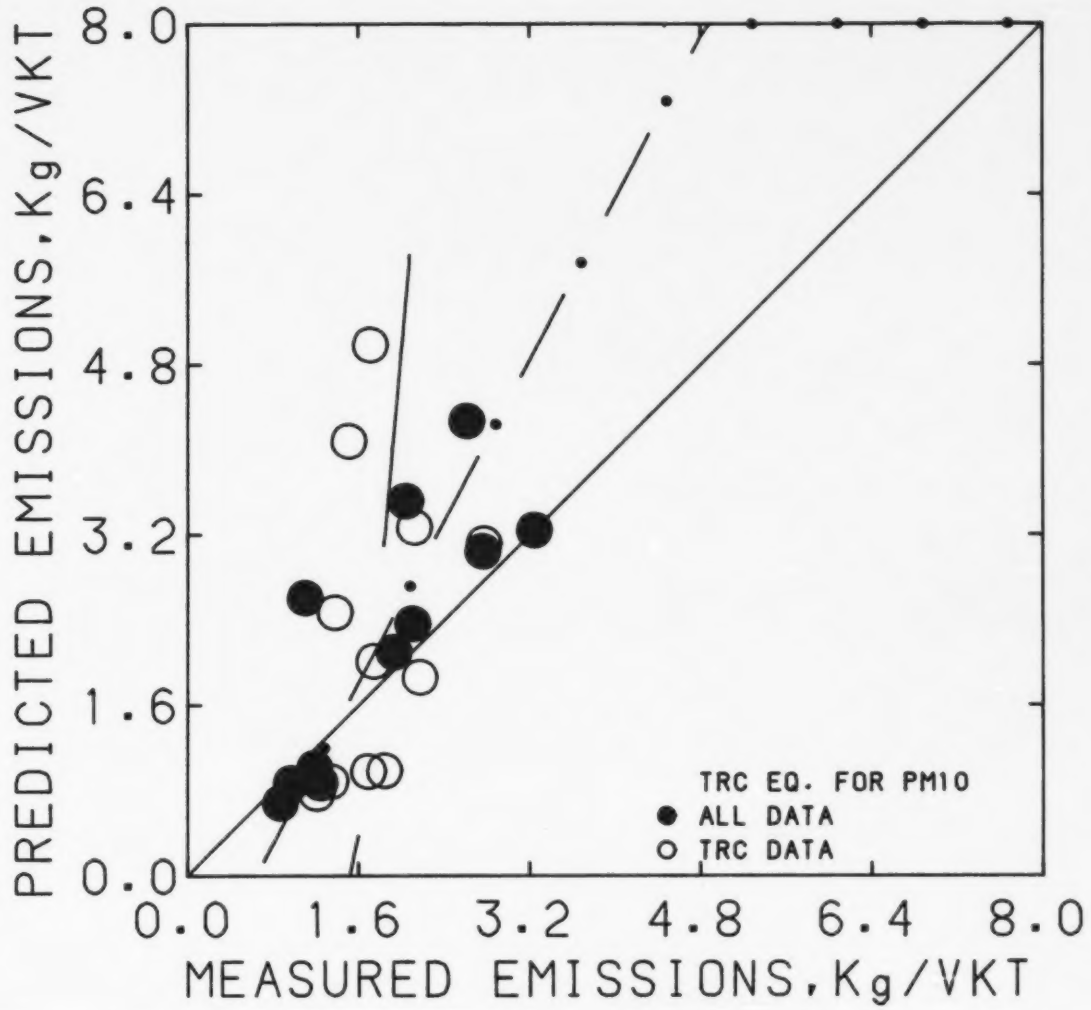

Figure 54. Scatter diagrams of: the test averaged PM_{10} emission factor measurements and that predicted by TRC's equation (filled circles) along with the associated regression line (dotted line); and the values of PM_{10} emission factor both measured and predicted by TRC (open circles) along with the associated regression line (broken line).

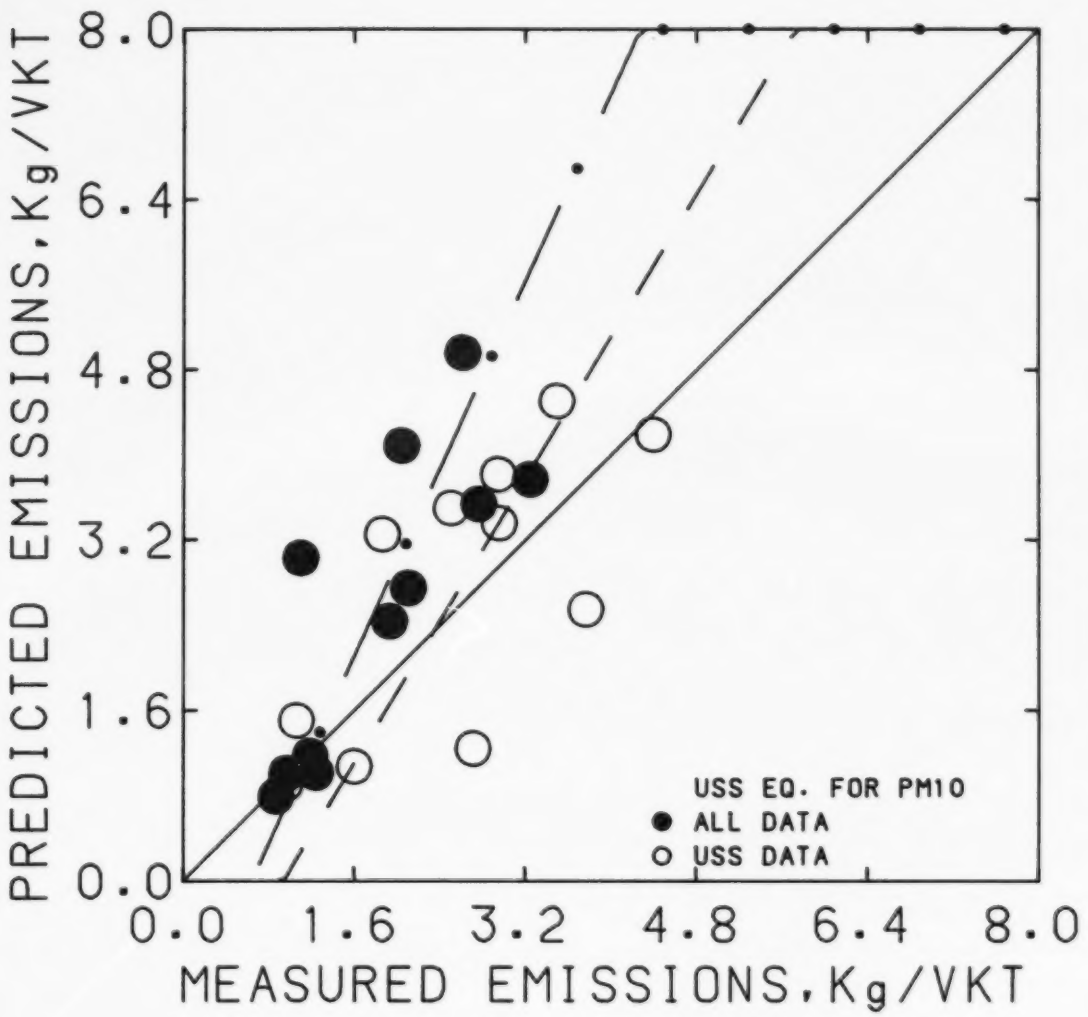

Figure 55. Scatter diagrams of: the test averaged PM_{10} emission factor measurements and that predicted by USS's equation (filled circles) along with the associated regression line (dotted line); and the values of PM_{10} emission factor both measured and predicted by USS (open circles) along with the associated regression line (broken line).

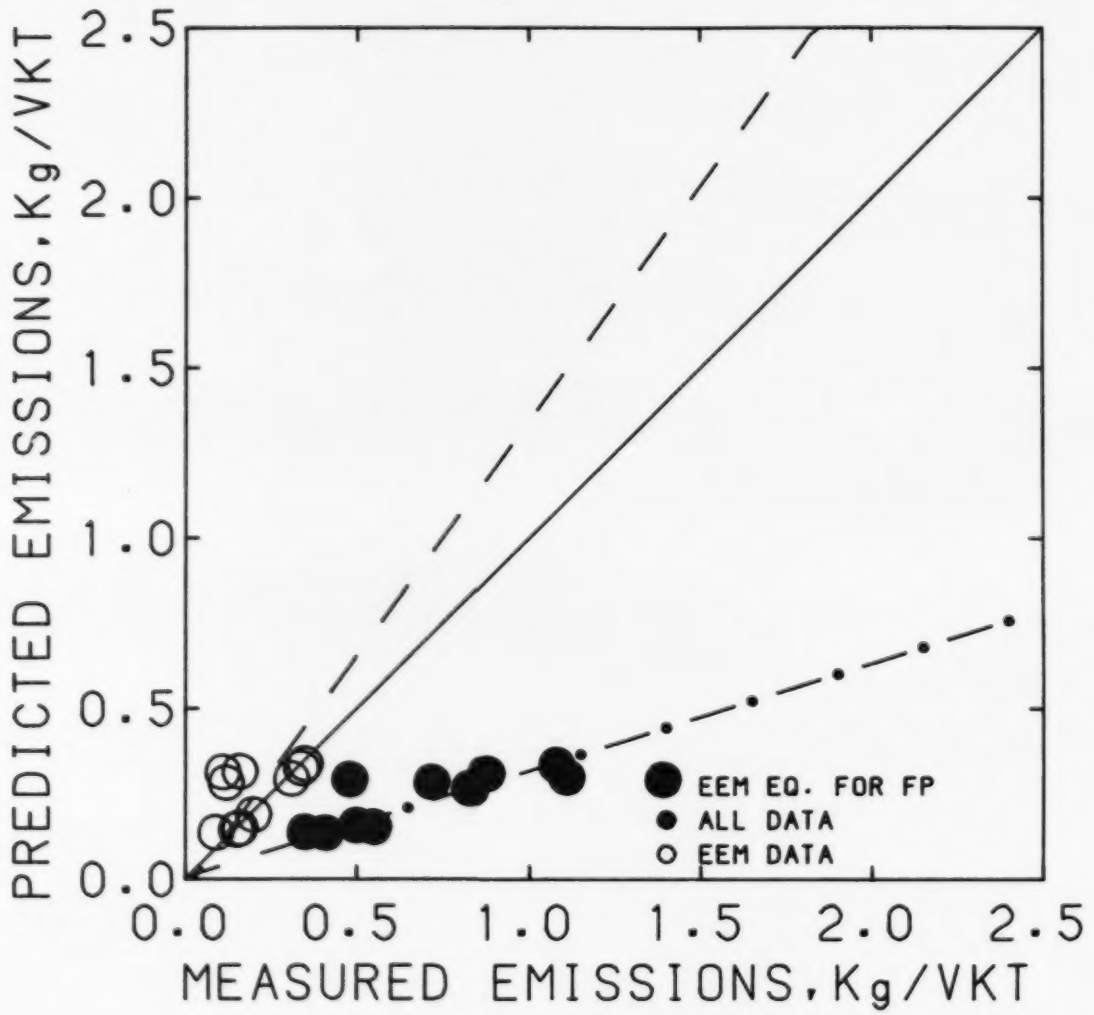

Figure 56. Scatter diagrams of: the test averaged FP emission factor measurements and that predicted by EEM's equation (filled circles) along with the associated regression line (dotted line); and the values of FP emission factor both measured and predicted by EEM (open circles) along with the associated regression line (broken line).

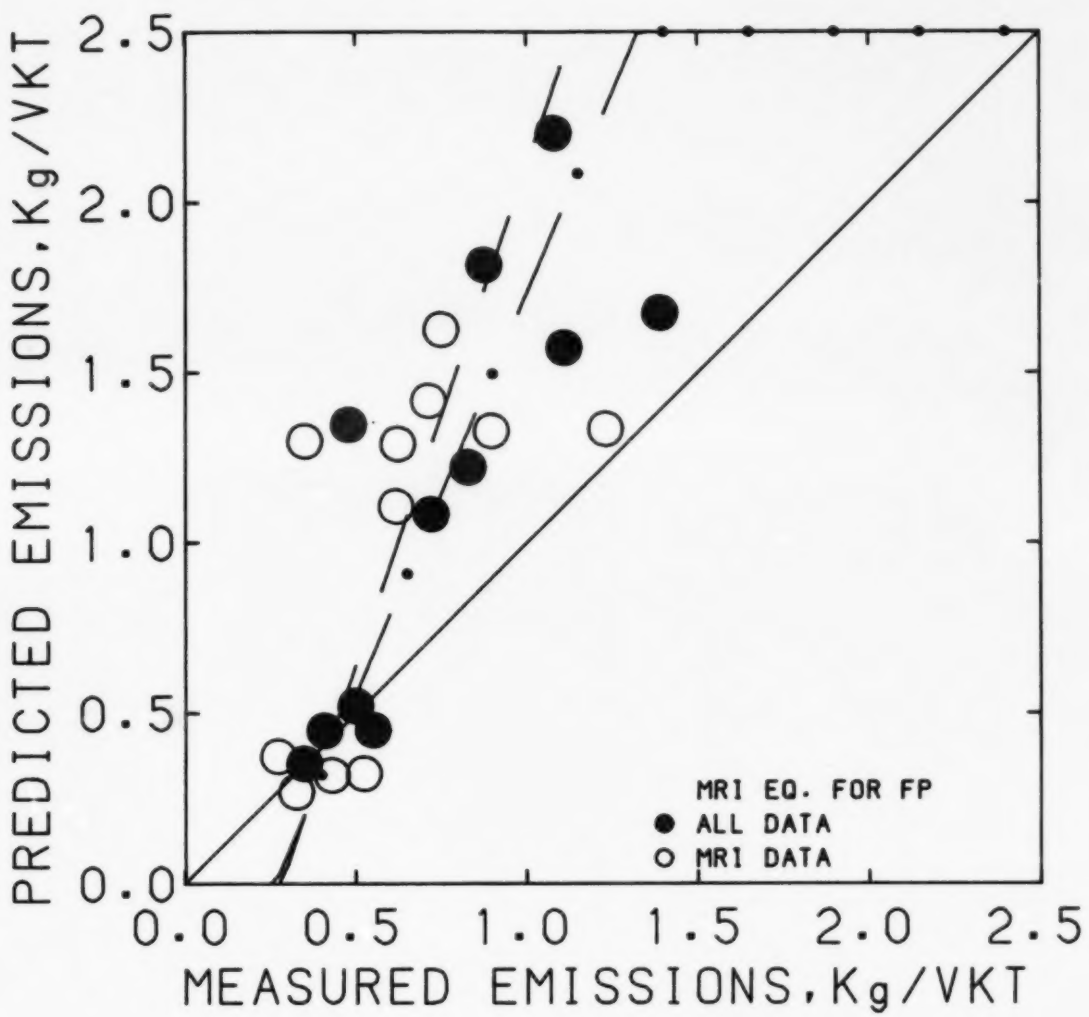

Figure 57. Scatter diagrams of: the test averaged FP emission factor measurements and that predicted by MRI's equation (filled circles) along with the associated regression line (dotted line); and the values of FP emission factor both measured and predicted by MRI (open circles) along with the associated regression line (broken line).

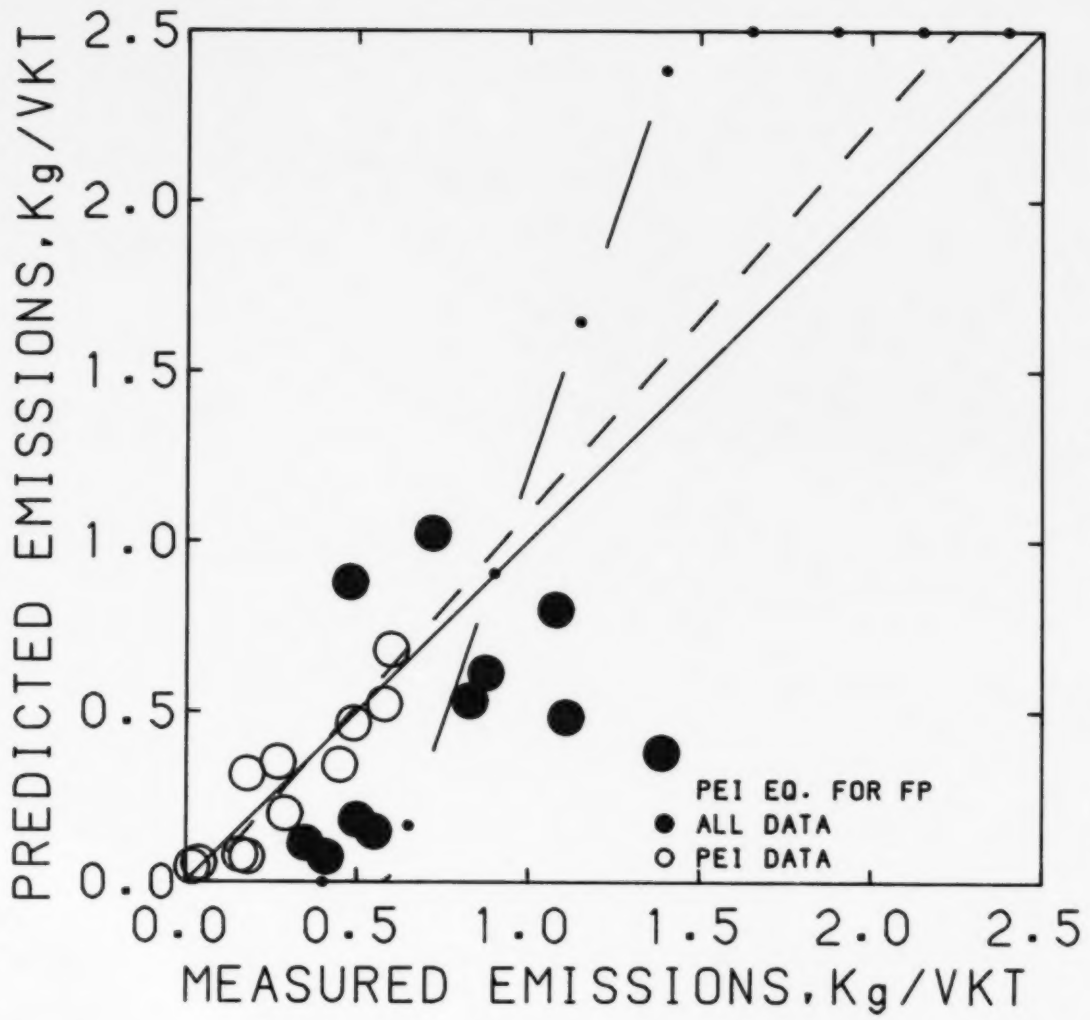

Figure 58. Scatter diagrams of: the test averaged FP emission factor measurements and that predicted by PEI's equation (filled circles) along with the associated regression line (dotted line); and the values of FP emission factor both measured and predicted by PEI (open circles) along with the associated regression line (broken line).

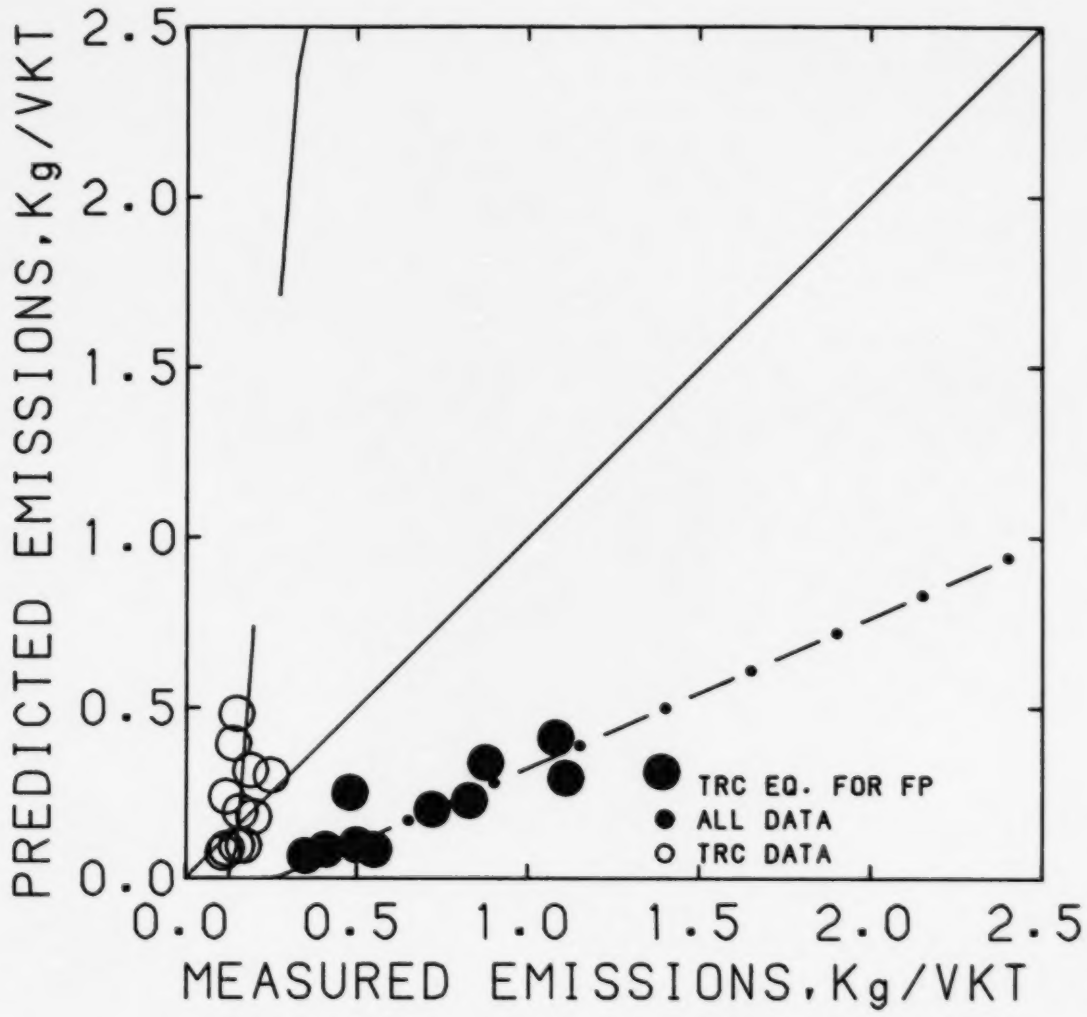

Figure 59. Scatter diagrams of: the test averaged FP emission factor measurements and that predicted by TRC's equation (filled circles) along with the associated regression line (dotted line); and the values of FP emission factor both measured and predicted by TRC (open circles) along with the associated regression line (broken line).

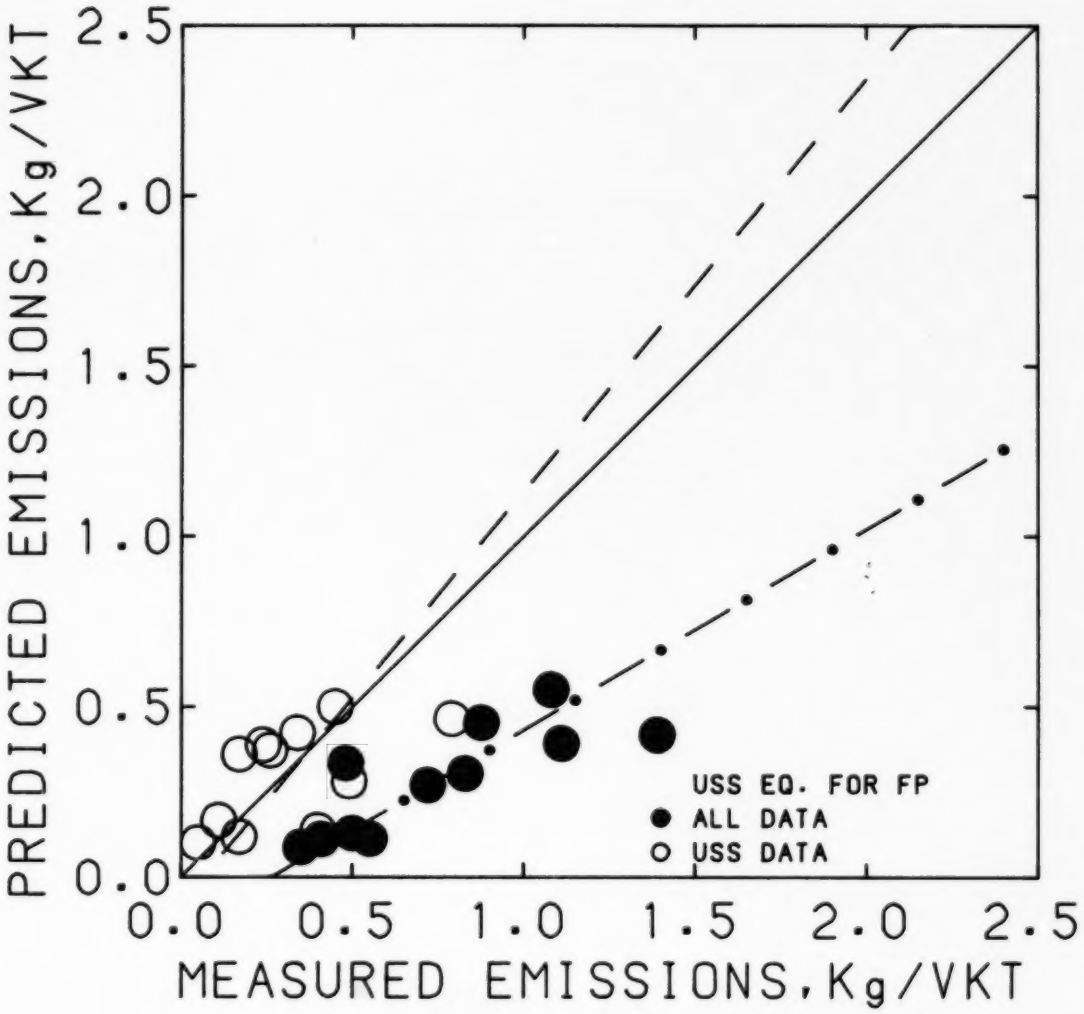

Figure 60. Scatter diagram of: the test averaged FP emission factor measurements and that predicted by USS's equation (filled circles) along with the associated regression line (dotted line); and the values of FP emission factor both measured and predicted by USS (open circles) along with the associated regression line (broken line).

REFERENCES

1. C. Cowherd and R.V. Hendriks, "Fugitive emissions from integrated iron and steel plants.. open dust sources." Paper 77-6.2, presented at the 70th Annual Meeting of the APCA, Toronto, Canada, June 1977.

2. J. Palmisano and D. Martin, "The use of nontraditional control strategies in the iron and steel industry: air bubbles, water bubbles, and multimedia based control strategies." Paper 84-39.1, presented at the 77th annual meeting of the APCA, San Francisco, California, June 1984.

3. C. Cowherd, K. Axetell, C.M. Guenther, and G. Jutze, "Development of emission factors for fugitive dust sources." EPA-450/3-74-037, U.S. Environmental Protection Agency, Research Triangle Park, North Carolina, June 1974. (NTIS PB 238262)

4. R.H. Knuth, "Calibration and field application of a Sierra model 235 cascade impactor." Am. Ind. Hyg. Assoc. J. 45(6): 393-398 (1984).

5. T. A. Cahill, R. A. Eldred, J. Barone, and L. Ashbaugh, "Ambient aerosol sampling with stacked filter units," FHWA-RD-78-178, Federal Highway Administration, Washington, D.C., February 1979, available NTIS, PB80-126147.

6. G.S. Casuccio, P.B. Janocko, R.J. Lee, J.F. Kelly, S.L. Dattner, and J.S. Mgebroff, "The use of computer controlled scanning electron microscopy in environmental studies." J. APCA, 33(10):937-943 (1983).

7. D.A. Lundgren, "An aerosol sampler for determination of particle concentration as a function of size and time", J. APCA, 17(4):225-259 (1967).

8. A.K. Rao, "Sampling and analysis of atmospheric aerosols", Particle Technology Laboratory Publication No. 269, University of Minnesota. 195 pp, (1975).

9. J.J. Wesolowski, A.E. Alcocer, and B.R. Appel, "The validation of the lundgren impactor", in "The Character and origins of smog aerosols", (9): 125-146 (1980).

10. R. Dennis, R.W. Cass, D.W. Cooper, R.R. Hall, V. Hampl, H.A. Klemm, J.E. Langley, and R.W. Steam, "Filtration model for coal fly ash with glass fabrics", EPA-600/7-77-084, U.S. Environmental Protection Agency, Research Triangle Park, NC, August 1977. (NTIS PB 276489)

11. T. E. Baxter, D. D. Lane, C. Cowherd, Jr., and F. Pendleton, "Calibration of a Cyclone for Monitoring Inhalable Particles", Journal of Environmental Engineering, Vol. 112, No. 3, June 1986, pg. 468-478.

12. L.R. Graf, "Calibration of cyclone for high volume sampler", letter to Sierra Instuments from Environmental Research Corporation, St. Paul, MN, May 7, 1976.

13. J.W. Johnson, G.I. Clinard, L.G. Felix, and J.D. McCain, "A computer-based cascade impactor data reduction system," EPA-600/7-78-042 (NTIS PB 285433), U.S. Environmental Protection Agency, Research Triangle Park, NC, 1978.

14. TRS-80 Cascade Impactor Data Reduction System, Denver Research Institute, P.O. Box 10127, Denver, CO 80208.

15. U.S. Environmental Protection Agency, "Compilation of air pollutant emission factors", Third Edition (Supplement No. 14), AP-42, May 1983.

APPENDIX

The following list includes all documents generated by other organizations as a result of this study.

PHASE I - CURRENT PROCEDURES

Martin, D. J., and P. A. Catizone, Critical Review of Open Source Particulate Emission Measurements, Catizone & Martin Associates, Inc.*, 63 McKee Street, East Hartford, CN, 06108, November 1983.

Simmons, L. L., C. L. Norton, and D. M. Horgan, Procedures Used For Open Dust Source Testing at United States Steel Corporation in Allegheny County and Current Procedures used by Energy & Environmental Management, Inc., Energy & Environmental Management, Inc., P.O. Box 71, Murrysville, PA, 15668, November 1983.

Discussion and Analysis of Vertical Profiler Samples Using Computer Controlled Scanning Electron Microscopy (CCSEM). Energy Technology Consultants, 4758 Old William Penn Highway, Murrysville, PA, 15668.

Chandler, M. W. and A. Roffman, EIA Procedures For The Experimental Evaluation Of Fugitive Emission Factors From Paved and Unpaved Roads. Energy Impact Associates, Inc., P.O. Box 1899, Pittsburgh, PA 15230, November 1983.

Muleski, G. E., C. Cowherd, Jr., and T. Cuscino, Jr., Current Procedures for Open Source Particulate Emission Measures. Midwest Research Institute, 425 Volker Boulevard, Kansas City, MO, 64100, December 1983.

Rosbury, K. D., and R. A. Zimmer, Critical Review of Open Source Particulate Emission Measurements-Current Procedures. Robert A. Zimmer, PEDCo Environmental, Inc.**, 14062 Denver West Parkway, Golden, CO, 80401, November 1983.

Brookman, E. T., Critical Review of Open Source Particulate Emission Measurements-Current Procedures, TRC Environmental Consultants, Inc., 800 Connecticut Blvd., East Hartford, CT, 06108, November 1983.

Eckle, T. F., and D. L. Trozzo, Critical Review Of Open Source Particulate Emission Measurements - Current Procedures. Operating Procedures for Road Emission Measurement With U.S. Steel Corporation Exposure Profiler, U.S. Steel Corporation, Environmental Affairs, Monroeville, PA, 15146, 1983.

Eckle, T. C., Verification of Road-Dust Emission Reduction at U.S. Steel Corporation Fairless Works, U.S. Steel Corporation, Environmental Affairs, Monroeville, PA 15146, 1983.

PHASE II - FIELD COMPARISON

Simmons, L. L., C. L. Norton, and D. M. Horgon, Critical Review Of Open Source Particulate Emission Measurements/Phase II - Field Tests, Field Data Analysis and Report. Energy & Environmental Management, Inc., P.O. Box 71, Murrysville, PA, 15668, July 1984

Muleski, G. E., Critical Review of Open Source Particulate Emission Measurements - Part II - Field Comparison. Midwest Research Institute, 425 Volker Blvd., Kansas City, MO, 64110, August 1984.

Rosbury, K. D. and R. A. Zimmer, Critical Review of Open Source Particulate Emission Measurements - TASK 2 - Field Data Analysis and Report. PEDCo Environmental, Inc.,** 14062 Denver West Parkway, Golden, CO, 80401, 1984.

Brookman, E. T., Critical Review of Open Source Particulate Emission Measurements PART II - Field Comparison, TRC Environmental Consultants, Inc., 800 Connecticut Blvd., East Hartford, CT, 06108, July 1984.

Eckle, T. F., Critical Review of Open Source Particulate Emission Measurements - PHASE II - Field Test. Predictive Emission Factor Equation Based on Exposure Profile Measurement of Emissions from an Unpaved Road, U.S. Steel Corporation, Environmental Affairs, Monroeville, PA, 15146, 1984.

* No longer in operation.
** Now PEI Associates, Inc., 11499 Chester Road, Cincinnati, OH, 45246.